TURUN YLIOPISTON JULKAISUJA
ANNALES UNIVERSITATIS TURKUENSIS

SARJA - SER. D OSA - TOM. 1097

MEDICA - ODONTOLOGICA

UNIDIRECTIONAL FIBER-REINFORCED COMPOSITE AS AN ORAL IMPLANT ABUTMENT MATERIAL

Experimental studies of E-glass fiber/ BisGMA-TEGDMA polymer *in vitro*

by

Aous Abdulhaq Abdulmajeed

TURUN YLIOPISTO
UNIVERSITY OF TURKU
Turku 2013

From the Department of Prosthetic Dentistry, Institute of Dentistry, Faculty of Medicine, Finnish Doctoral Program in Oral Sciences - FINDOS Turku, University of Turku, Turku, Finland.

Supervised by
Professor Timo Närhi
Department of Prosthetic Dentistry, Institute of Dentistry
University of Turku
Turku, Finland.

and

Professor Pekka Vallittu
Department of Biomaterials Science, Institute of Dentistry
University of Turku
Turku, Finland.

Reviewed by
Professor Pentti Tengvall
Department of Biomaterials, Sahlgrenska Academy
University of Gothenburg
Gothenburg, Sweden.

and

Professor Hannu Larjava
Division of Periodontics and Dental Hygiene, Faculty of Dentistry
University of British Columbia
Vancouver, Canada.

Dissertation opponent
Professor Ignace Naert
Department of Prosthetic Dentistry, School of Dentistry
Catholic University of Leuven
Leuven, Belgium.

ISBN 978-951-29-5607-4 (PRINT)
ISBN 978-951-29-5608-1 (PDF)
ISSN 0355-9483
Painosalama Oy – Turku, Finland 2013

“In the name of God, the Most Gracious, the Most Merciful”

To my Parents…

TABLE OF CONTENTS

ABSTRACT

Aous Abdulmajeed

Unidirectional fiber-reinforced composite as an oral implant abutment material: Experimental studies of E-glass fiber/BisGMA-TEGDMA polymer *in vitro*

Department of Prosthetic Dentistry, Institute of Dentistry, University of Turku, Turku, Finland 2013.

Fiber-reinforced composites (FRCs) are a new group of non-metallic biomaterials showing a growing popularity in many dental and medical applications. As an oral implant material, FRC is biocompatible in bone tissue environment. Soft tissue integration to FRC polymer material is unclear.

This series of *in vitro* studies aimed at evaluating unidirectional E-glass FRC polymer in terms of mechanical, chemical, and biological properties in an attempt to develop a new non-metallic oral implant abutment alternative.

Two different types of substrates were investigated: (a) Plain polymer (BisGMA 50%–TEGDMA 50%) and (b) Unidirectional FRC. The mechanical behavior of high fiber-density FRCs was assessed using a three-point bending test. Surface characterization was performed using scanning electron and spinning disk confocal microscopes. The surface wettability/energy was determined using sessile drop method. The blood response, including blood-clotting ability and platelet morphology was evaluated. Human gingival fibroblast cell responses - adhesion kinetics, adhesion strength, and proliferation activity - were studied in cell culture environment using routine test conditions. A novel tissue culture method was developed and used to evaluate porcine gingival tissue graft attachment and growth on the experimental composite implants.

The analysis of the mechanical properties showed that there is a direct proportionality in the relationship between E-glass fiber volume fraction and toughness, modulus of elasticity, and load bearing capacity; however, flexural strength did not show significant improvement when high fiber-density FRC is used. FRCs showed moderate hydrophilic properties owing to the presence of exposed glass fibers on the polymer surface. Blood-clotting time was shorter on FRC substrates than on plain polymer. The FRC substrates also showed higher platelet activation state than plain polymer substrates. Fibroblast cell adhesion strength and proliferation rate were highly pronounced on FRCs. A tissue culture study revealed that gingival epithelium and connective tissue established an immediate close contact with both plain polymer and FRC implants. However, FRC seemed to guide epithelial migration outwards from the tissue/implant interface.

Due to the anisotropic and hydrophilic nature of FRC, it can be concluded that this material enhances biological events related with soft tissue integration on oral implant surface.

Keywords: Soft tissue attachment, Dental materials, Fiber-reinforced composite, Implant abutment, Mechanical properties, Surface energy, Blood compatibility, Fibroblast, Tissue culture.

TIIVISTELMÄ

Aous Abdulmajeed

Yhdensuuntaisilla lasikuiduilla lujitettu komposiitti hammasimplantin abutmentin materiaalina: Kokeellisia tutkimuksia E-lasikuidulla vahvistetusta BisGMA-TEGDMA polymeeristä *in vitro*

Hammasproteesioppi, Hammaslääketieteen laitos, Turun yliopisto, Turku, Finland 2013.

Lasikuitulujitteiset muovit ovat suhteellisen uusi ryhmä metallittomia biomateriaaleja. Kiinnostus kuitulujitteisten muovien käyttöön implanttimateriaalina on kasvanut monissa hammaslääketieteellisissä ja lääketieteellisissä hoidoissa. Kuitulujitteisesta muovista valmistettu hammasimplantti on aiemmin todettu bioyhteensopivaksi luukudoksen kanssa. Materiaalista valmistettujen implanttien kiinnittymisestä pehmytkudoksiin ei kuitenkaan ole ollut tutkittua tietoa. Tämän väitöskirjatyön tarkoituksena oli selvittää yhdensuuntaisilla lasikuiduilla vahvistetun komposiitin soveltuvuus hammasimplanttien ienkudoksen läpäisevän abutmenttiosan materiaaliksi sen mekaanisten, kemiallisten ja biologisten ominaisuuksien valossa.

Työssä verrattiin kahta erilaista materiaalia: (a) Pelkkä polymeeri komposiitti (BisGMA 50%-TEGDMA 50%) ja (b) Lasikuitulujitteinen komposiitti. Korkean kuitupitoisuuden vaikutus komposiitin mekaanisiin ominaisuuksiin tutkittiin kolmipistetaivutusta käyttämällä. Materiaalien pintarakenne analysoitiin pyyhkäisyelektroni- ja konfokaalimikroskooppi tutkimuksilla. Komposiiteissa käytettyjen monomeerien konversioaste selvitettiin FTIR spektrometrilla. Materiaalien pintaenergia tutkittiin kosketuskulmamittausta käyttämällä. Materiaalien käyttäytymistä verikontaktissa selvitettiin tutkimalla materiaalin pinnan vaikutus hyytymän muodostumiseen sekä verihiutaleiden kiinnittymiseen ja morfologiaan. Ihmisen ikenen fibroblastien kiinnittymistä ja jakautumista komposiittien pinnoilla tutkittiin rutiinikäytössä olevilla soluviljelymalleilla. Väitöskirjatyössä kehitettiin lisäksi uusi kudosviljelymalli, jonka avulla seurattiin sian ienkudoksen kiinnittymistä kokeellisten komposiitti-implanttien pinnoille.

Mekaanisten ominaisuuksien analyysi osoitti, että E-lasikuitujen suhteellisella määrällä on suora yhteys komposiitin elastiseen modulukseen, sitkeyteen sekä kuormankanto kykyyn. Taivutuslujuus ei kuitenkaan lisääntynyt suorassa suhteessa suuria kuitutiheyksiä käytettäessä. Lasikuitulujitteisen komposiitin pinta osoittautui hydrofiiliseksi materiaalin pinnalla olevien lasikuitujen ansiosta. Veri hyytyi nopeammin ja verihiutaleet aktivoituivat paremmin kuitulujitteisen komposiitin pinnalla pelkkään polymeerin verrattuna. Fibroblastien todettiin kiinnittyvän ja jakautuvan selvästi paremmin kuitulujitteisen komposiitin pinnalla. Kudosviljelytyö osoitti, että ienkudoksen epiteeli ja sidekudos kiinnittyvät suoraan sekä kuitulujitteisen että pelkän komposiitin pinnalle. Kuitulujitteisten materiaalien paljastuneet lasikuidut kuitenkin ohjasivat ikenen epiteeliä kasvamaan iensiirteen ja implantin kontaktipinnasta pois päin.

Yhteenvetona voidaan todeta, että anisotrooppisten ja hydrofiilisten ominaisuuksiensa ansiosta kuitulujitteinen materiaali edesauttaa implantin pehmytkudosliitoksen muodostumiseen johtavia biologisia mekanismeja.

Avainsanat: Abutmentti, fibroblasti, hammashoidon materiaalit, kudosviljely, kuitulujitteinen komposiitti, mekaaninen lujuus, pehmytkudosliitos, pintaenergia, veri.

LIST OF ABBREVIATIONS

ANOVA	Analysis of variance
BisGMA	Bisphenol-A-glycidyl dimethacrylate
ºC	Degrees Celsius
CAD/CAM	Computer-aided design/Computer-aided manufacturing
d	Day
DC	Degree of conversion
FRC	Fiber-reinforced composite
FTIR	Fourier transform infrared spectrometry
GPa	Gigapascal
h	Hour
min	Minute
MPa	Megapascal
N	Newton
n	Number of specimens per group
s	Second
SEM	Scanning electron microscopy
sd	Standard deviation
TEGDMA	Triethyleneglycoldimethacrylate
Vol.%	Volume percentage
XRD	X-ray diffraction

LIST OF ORIGINAL PUBLICATIONS

This thesis is based on the following original articles, which are referred to in the text by the Roman numerals I–IV.

I. **Abdulmajeed AA**, Närhi TO, Vallittu PK, Lassila LV. The effect of high fiber fraction on some mechanical properties of unidirectional glass fiber-reinforced composite. Dental Materials. 2011;27:313–321.

II. **Abdulmajeed AA**, Lassila LV, Vallittu PK, Närhi TO. The effect of exposed glass fibers and particles of bioactive glass on the surface wettability of composite implants. International Journal of Biomaterials. 2011; Article ID 607971.

III. **Abdulmajeed AA**, Walboomers XF, Massera J, Kokkari AK, Vallittu PK, Närhi TO. Blood and fibroblast responses to thermoset BisGMA-TEGDMA/glass fiber-reinforced composite implants *in vitro*. Clinical Oral Implants Research. 2013;00:1–9.

IV. **Abdulmajeed AA**, Willberg J, Syrjänen S, Vallittu PK, Närhi TO. *In vitro* assessment of the soft tissue/implant interface using porcine gingival explants. *Submitted*.

1. INTRODUCTION

Over the last few decades, implant research has mainly focused on studying the osseous healing around oral implants. However, ever since osseointegration of oral implants became highly predictable, interest has shifted towards achieving a flawless esthetic outcome. Based on this, considerable attention has been employed to evaluate the ultrastructure architecture and healing of the peri-implant mucosa. The main functions of the soft tissue cuff surrounding implant necks are to inhibit access for bacteria and their products and to well preserve the underlying bone. Thus, the stability and quality of the soft tissue interface with implant abutments is of utmost importance for short-term and long-term prognosis of oral implants.

There is ongoing research to develop alternative implant materials that could deliver better esthetic and biomechanical matching to the properties of living tissues than titanium does. One potential material could be, fiber-reinforced composite (FRC) made of bisphenol-A-glycidyl dimethacrylate (BisGMA) and triethyleneglycoldimethacrylate (TEGDMA) light-polymerizable biopolymers reinforced by unidirectional silanized E-glass fiber rovings.

FRCs are strong materials characterized by low elastic modulus (Figure 1) (Cheal *et al*., 1992). The mechanical properties of unidirectional FRCs are not only superior to metals but also close to that of natural bone (Goldberg & Burstone, 1992). In many dental applications, the use of FRCs has increased (Freilich & Goldberg, 1997; Freilich *et al*., 1998; Duncan *et al*., 2000; Freudenthaler *et al*., 2001; Narva *et al*., 2001; Lassila *et al*., 2004; Wolff *et al*., 2010). Attempts to use FRC as implant material for oral, orthopedic, and craniofacial applications are in practice (Ballo *et al*., 2009; Mattila, 2009; Tuusa *et al*., 2007; Aitasalo *et al*., 2013). While the amount of scientific literature on using FRC as a surgical device is inadequate, however, their use in surgery is promising especially when combined with bioactive modifiers, such as bioactive glass (BAG).

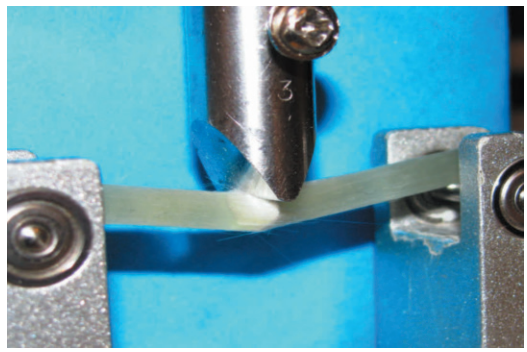

Figure 1 *Three-point bending test of fiber-reinforced composite (FRC) cylinder demonstrating high bending strength and toughness with delamination of individual fibers from the polymer matrix at the point of final failure (white region). The unidirectional E-glass fibers maintain the structural integrity of the FRC cylinder after failure.*

The practicality of using FRC as an oral implant material is investigated (Figure 2) (Ballo, 2008). A series of studies concluded that, with critical attention to the surgical technique and technical design of FRC, it can be successfully applied as a bone-anchoring device with a bone response comparable to titanium implants.

Figure 2 *Example of one-piece design of threaded unidirectional E-glass fiber-reinforced composite implant.*

Besides the good mechanical properties of FRC that ensures an enduring function under complex oral conditions, FRC as an implant abutment material is fairly simple to grind and adjust intraorally without overheating the underlying bone tissue (Figure 3).

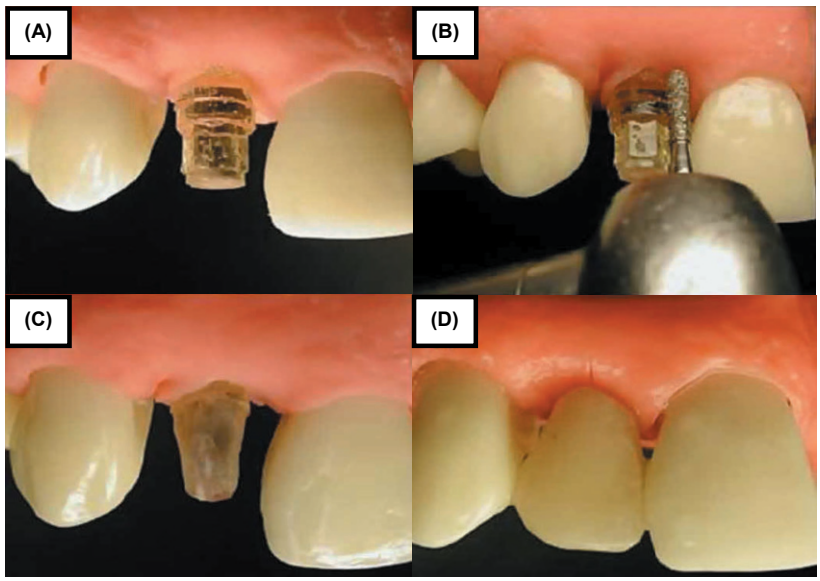

Figure 3 *Clinical simulating illustration of placement and preparation of abutment portion of fiber-reinforced composite implant (Ballo, 2008).*

However, there is no information available about the peri-implant soft tissue response to FRC material, hence **the aim of this project is to focus on the use of FRC as an implant abutment material, mainly from the soft tissue perspective.**

2. REVIEW OF LITERATURE

2.1. Anatomical structure of the soft tissue/tooth interface

The soft tissue around natural dentition is termed gingiva. The interface portion between the gingiva and the tooth consists of two different zones: epithelial zone and connective tissue zone. The epithelial zone extends from the gingival crest to the most apical end of the junctional epithelium, where the connective tissue zone begins. The latter extends to the alveolar bone crest, where the periodontal ligament starts (Figure 4). Stereological analysis of clinically healthy gingival units showed that soft tissue surrounding teeth comprises 4% of junctional epithelium, 27% of oral epithelium, and 69% of connective tissue (Schroeder *et al.*, 1973).

The epithelial zone can be, in turn, divided into two different epithelial zones: the oral sulcular epithelium and the junctional epithelium. The junctional epithelium is unique as it has two distinct basal laminas: the external basal lamina that attaches the junctional epithelium to the underlying connective tissue and the internal basal lamina that attaches the junctional epithelium to the tooth surface (Cate & Nanci, 2008). The external basal lamina shows the typical structures and components of a true basement membrane. The internal basal lamina differs essentially from a true basement membrane in its biochemical composition, i.e., lack of proteins such as collagen type IV and VII, laminin 111, laminin 511, and perlecan (Hormia *et al.*, 1998). The junctional epithelium possesses several protective roles: (1) It inhibits bacterial adhesion on the outer epithelial surface via rapid cell division and exfoliation, and there is increasing evidence that several specific antimicrobial and chemotactic substances exist in the junctional epithelium and contribute to the regulation of the innate immune defense; (2) Its unique external and internal basal laminas serve as barriers against infective agents; and (3) Its wide intercellular spaces create a passageway for transmigrating polymorphonuclear leukocytes and gingival crevicular fluid. This is considered as the most important defense mechanism at the dento-gingival junction (Loe & Karring, 1969; Schiott & Loe, 1970; Page *et al.*, 1997; Dale, 2002; Pöllänen *et al.*, 2003).

The connective tissue (i.e., lamina propria) zone can also be divided into two different compartments: the connective tissue supporting the epithelium, and the connective tissue actually interfacing the tooth surface (generally the cementum). The connective tissue is constituted by a ground substance in which a combination of collagen fibers (60%), fibroblasts (5%), and blood vessels and nerves (35%) can be found (Schiott & Loe, 1970). The ground substance is composed of water, proteoglycans, glycoproteins (e.g., fibronectin that is involved in adhesion and migration of cells), glycosaminoglycans, and serum-derived proteins.

Just above the crestal bone, the collagen fibers are found in the lamina propria of the gingiva and form a dense network of collagen fiber bundles that is called supragingival fiber apparatus (Cate & Nanci, 2008). These fibers can be distinguished in different

groups, depending on their origin, orientation, and termination. The most numerous fibers are the dento-gingival fibers, extending from the cementum to the lamina propria of the free and attached gingiva. These fibers are oriented perpendicularly to the surface of the tooth. Alveolo-gingival, circular, dento-periosteal, and transseptal fibers form the other groups (Cate & Nanci, 2008). The supragingival fiber apparatus connects the gingiva to alveolar bone and root cementum as well as providing a dense framework that accounts for the rigidity and biomechanical resistance of the gingiva. The collagen fibers are mainly of collagen type I and III. Collagen type I is the most dominant and represents mainly dense fibers, whereas collagen type III is related to loose connective tissue, subepithelially and around blood vessels (Chavrier *et al.*, 1984). Fibroblasts are the most common cells in the connective tissue that are responsible for the synthesis of fibers and other components of the ground substance, it thus play a key role in maintaining tissue integrity. The connective tissue also contains macrophages, mast cells, polymorphonuclear leukocytes, lymphocytes, plasma cells, and endothelial cells that play essential roles in the inflammatory and immune defense systems (Schroeder & Listgarten, 1997). Lamina propria of the gingiva is highly vascularized and the terminal blood vessels create two networks: the dentogingival plexus alongside the junctional epithelium and the subepithelial plexus beneath the oral epithelium (Egelberg, 1966).

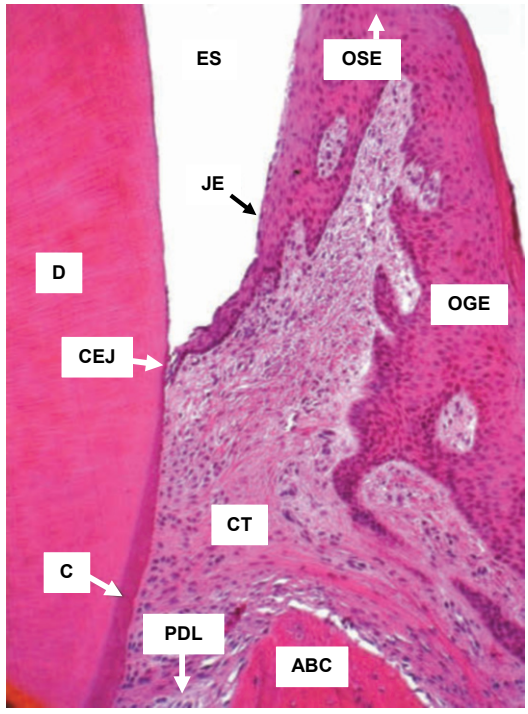

Figure 4 *Light microscopic view of the human dentogingival junction. D, dentin; CEJ, cemento-enamel junction; C, cementum; ES, enamel space; JE, junctional epithelium; CT, gingival connective tissue; PDL, periodontal ligament; ABC, alveolar bone crest; OSE, oral sulcular epithelium; OGE, oral gingival epithelium. (Source: LIGHT-MICROSCOPIC HISTOLOGY ATLAS. Authors: Clermont Y, Lalli M, Bencsath-Makkai Z. URL:* http://audilab.bmed.mcgill.ca/HA/html/oc_27_E.html *accessed 19:45, 03.5.2013).*

2.2. Anatomical structure of the soft tissue/implant interface

The soft tissue around oral implants is termed peri-implant mucosa. The interface portion between the mucosa and the implant consists of one epithelial and one connective tissue component. The peri-implant mucosa surrounding oral implants, specifically the epithelial component, shares many structural, ultrastructural, and functional features with the corresponding gingival tissue (Berglundh *et al.*, 1991; Buser *et al.*, 1992; Abrahamsson *et al.*, 1996; Berglundh & Lindhe, 1996; Abrahamsson *et al.*, 1998; Hermann *et al.*, 2000; Schierano *et al.*, 2002; Siar *et al.*, 2003; Rompen *et al.*, 2006). Many studies reported that the peri-implant epithelium is about 2 mm long compared to the corresponding 1 mm long junctional epithelium around teeth (Myshin and Wiens, 2005; Rompen *et al.*, 2006). The peri-implant epithelium displays slower cell proliferation with no evidence of true adhesion to the abutment surface (Fujiseki *et al.*, 2003; Larjava *et al*., 2011). However, the most remarkable difference from the natural dentition lies in the structure of the underlying connective tissue. First, owing to the absence of cementum layer, most fibers in the connective tissue are relatively directed parallel to the implant surface with no insertion into the implant (Listgarten & Lai, 1975; Berglundh *et al.*, 1991; Listgarten *et al.*, 1991; Buser *et al.*, 1992; Abrahamsson *et al.*, 1998). While the dento-gingival fibers are directed perpendicular/oblique to the tooth surface with firm insertion into the cementum (Figure 5), thus they serve as a barrier against epithelial downgrowth and impede bacterial invasion (Gargiulo *et al.*, 1961a; Stern, 1981). Second, the peri-implant connective tissue is characterized by predominance of collagen fibers (>85%) with few fibroblasts (7–8%) and vascular structures (2–3%) (i.e., scar-like connective tissue) (Buser *et al.*, 1992; Berglundh *et al.*, 1994; Abrahamsson *et al.*, 1996; Moon *et al.*, 1999; Schupbach & Glauser, 2007). As a consequence, the defensive mechanism against bacteria around oral implants is considerably impaired in comparison to natural dentition.

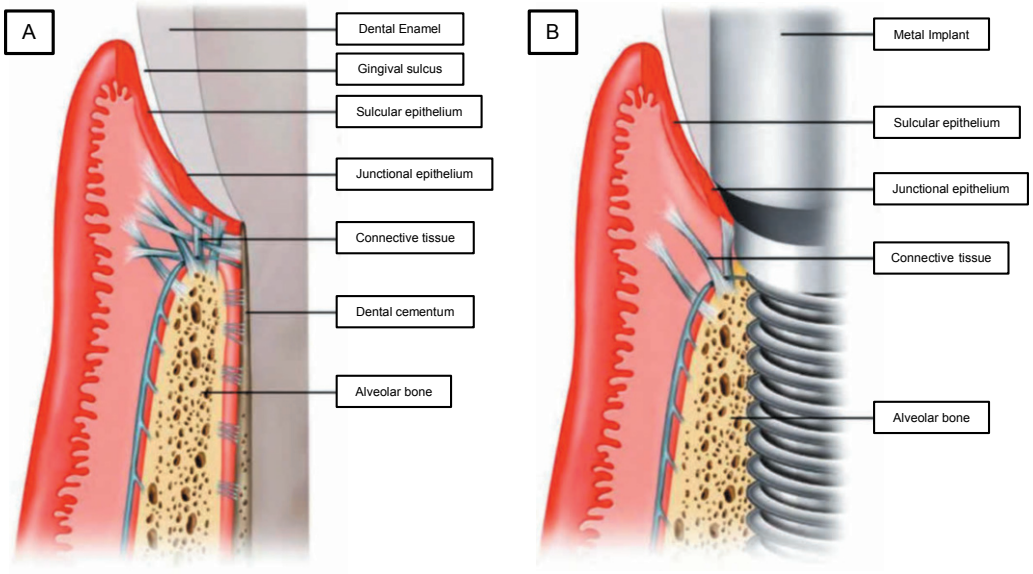

Figure 5 *Difference between tooth- and implant-soft tissue interfaces. (Source: Rose LF. (2004) Periodontics: Medicine, Surgery and Implants. Elsevier. 26;1114–1116).*

A. Biological attachment to a natural tooth. Connective tissue fibers insert into the root apical to the junctional epithelium.

B. Biological attachment to an oral implant. There is no insertion of connective tissue fibers into the implant surface.

2.3. Biological width

The biological width is a term frequently used to describe the vertical dimension of soft tissue facing the tooth surface coronal to the alveolar bone crest. Gargiulo *et al*. stated that the biologic width (i.e., sulcus depth, junctional epithelium, and connective tissue attachment) is a physiological and stable dimension that is dependent on the location of alveolar bone crest (Gargiulo *et al*., 1961b).

Cochran *et al*. measured and compared the biological width around titanium implants with those around natural teeth and concluded the following (Cochran *et al.*, 1997; Gargiulo *et al.*, 1961b); sulcus depth (0.16 mm vs. 0.69 mm), junctional epithelium (0.97 mm vs. 1.88 mm), connective tissue attachment (1.07 mm vs. 1.05 mm), and biological width (2.04 mm vs. 3.08 mm) for natural teeth and oral implants, respectively. The notion of biological width sets a basis for successful soft tissue integration to oral implants. The biological width around implants is constant and close to 3 mm irrespective of the implant system used and the original mucosal thickness (Abrahamsson *et al.*, 1996). These peri-implant soft tissue dimensions are mandatory to prevent alveolar bone loss and allow stable soft tissue cuff formation (Berglundh & Lindhe, 1996).

2.4. Oral implant abutment materials

Many different materials are used in fabrication of the transmucosal component of oral implants. Theoretically, abutments could be fabricated from any material - metal, ceramic, polymer, or composite. A review by Rompen *et al*. concluded that titanium abutments are the most biocompatible material towards soft tissue in long-term clinical studies, and ceramic materials like zirconia and aluminum oxide show interesting clinical results. However, materials like resins and composites are not recommended up to now, while dental porcelain or gold should be avoided (Rompen *et al.*, 2006). Still, these conclusions are questionable as no clinical trials were included in the analyses, and the recommendations are based on *in vitro* and animal studies (Linkevicius & Apse, 2008).

Currently, three different compositions are commercially available: titanium (metal); alumina (ceramic); and zirconia (ceramic). Nevertheless, fiber-reinforced composite (polymer) will be introduced, in this thesis, as a potential abutment material.

2.4.1. Titanium

Over the last decades, commercially pure titanium (cp-Ti) or titanium alloys are the biomaterials of choice in implant dentistry (i.e., gold standard), due to their excellent biocompatibility in living tissues, adequate mechanical properties, and corrosion resistance. However, titanium abutments do show some potential drawbacks. Increasing esthetic demands justified the search for other materials with better optical properties. Titanium can also introduce artifacts in modern imaging examinations (e.g., MRI and CT) (Eggers *et al.*, 2005; Kamel *et al.*, 2003). Furthermore, titanium abutments cannot be prepared in the oral cavity once they are connected to the implants. More recently, there is concern regarding the potential hypersensitivity towards titanium implants, occurred in a limited number of patients. The presence of titanium nanoparticles may be the cause (Sicilia *et al.*, 2008; Javed *et al.*, 2011a; Siddiqi *et al.*, 2011).

2.4.2. Alumina

Demands for highly esthetic restorations led to the introduction of tooth-colored ceramic abutments made of densely sintered aluminum oxide (Al_3O_2) (Prestipino & Ingber, 1993a; Prestipino & Ingber, 1993b). Clinical studies show stable peri-implant mucosa around alumina abutments (Andersson *et al.*, 2001; Andersson *et al.*, 2003; Henriksson & Jemt, 2003), consisting of junctional epithelium and connective tissue similar to the peri-implant mucosa around titanium abutments. Apart from the fact that alumina abutments perform well biologically as well as esthetically, they possess a fracture risk during both laboratory work and after abutment connection.

2.4.3. Zirconia

Due to the shortcoming in the mechanical properties of alumina abutments, zirconia was introduced as a potential abutment material and it has replaced alumina as the

ceramic abutment material of choice. Zirconia implant abutments are fabricated from yttria-stabilized tetragonal zirconia polycrystals (Y-TZP) (Blue *et al.*, 2003). Zirconia abutments possess many advantages in addition to its esthetic properties such as mechanical strength and reliability due to its unique stress-induced transformation mechanism (Scott, 1975), biocompatibility in hard and soft tissues (Hisbergues *et al.*, 2009), low bacterial colonization potential (Scarano *et al.*, 2004; do Nascimento *et al.*, 2013), and it also allows CAD/CAM fabrication process. However, long-term clinical evaluations of zirconia implants are still needed.

2.4.4. Fiber-reinforced composite (FRC)

FRCs are a new group of non-metallic dental biomaterials that was first used clinically in the early 1960s as a denture base reinforcement (Smith, 1961). However, the use of FRCs in dentistry had its breakthrough in late 1990's when the novel approach of the "so-called" polymer preimpregnation of glass fibers was introduced (Vallittu, 1999a). This time delay was due to the incomplete developed processing technologies of FRC with highly viscous dental resin systems. The main rationale for using FRC in dentistry is its mechanical properties (Table 1) that can be optimized to be equal of those of dentine or bone (Goldberg & Burstone, 1992; Vallittu, 1998b; Ballo *et al.*, 2008a).

Table 1 *Comparison of mechanical properties of different materials with unidirectional fiber-reinforced composite (FRC), representative values only (Black & Hastings, 1998; Lassila et al., 2005).*

Property/Materials	Strength (MPa)	Young's modulus (GPa)
Ti-alloy	965 (tensile)	116
Alumina	300 (tensile)	380
Zirconia	820 (tensile)	220
FRC	700–1200 (flexural)	20–40
Cortical bone (longitudinal direction)	133 (tensile)	17.7
Cortical bone (transverse direction)	52 (tensile)	12.8
Cancellous bone	7.4 (tensile)	0.4
Dentin	39.3 (tensile)	11

FRC materials consist of fibers (such as E-glass) embedded in a polymer matrix (such as BisGMA-TEGDMA). The fibers and the polymer matrix maintain their chemical and physical identities and the new material (e.g., FRC) has a combination of desirable properties unachievable by either of the constituents acting alone. The fibers are usually the main load-carrying elements, while the matrix functions are: (1) Transferring stresses between fibers; (2) Holding fibers together in the composite structure; (3) Protecting fibers' surface from mechanical abrasion; and (4) Providing a barrier against an adverse environment (Hull, 1996; Mallick, 1997).

The reinforcing fibers can be continuously: Unidirectional (rovings); Bidirectional (weaves); or Randomly oriented (mat). These fibers can also be short, randomly oriented fibers. Among different high performance fibers, glass fibers appear to be the fibers of choice in dental applications owing to the good esthetic properties and firm adhesion of silanized glass fibers to the resin matrix (Vallittu, 1994; Matinlinna *et al.*, 2004). Glass fibers vary according to their composition; the most commonly used fiber is E-glass (electrical glass) that is considered as a chemically stable and durable glass within a pH range of 4–11 (Norström *et al.*, 2003), in addition to its low cost and high production rates. Several articles have revealed the relationship between the quantity of fibers in the polymer matrix and the improvements in the transverse, flexural, and impact strength of FRCs (Vallittu & Narva, 1997; Isaac, 1999; Vallittu, 1999a; Behr *et al.*, 2000). By increasing the quantity of fibers, the flexural strength and modulus of elasticity increases linearly (Furtos *et al*., 2012). In a polymer matrix, this quantity should be expressed in volume not weight percentage. A formula exists for transforming fiber weight percentage into volume percentage (Vallittu & Narva, 1997).

It is noteworthy that fibers are mechanically more efficient in achieving a stiff and durable composite than particulate fillers, and that with the aid of fibers; the load-bearing capacity of the material can be increased. Unidirectional FRC has relative stiffness and strength comparable to metal when loading alongside the fibers, but with much less weight. Due to the anisotropic nature of unidirectional FRC, the material has different physical properties in different directions, thus FRC devices should be carefully designed.

Effective wetting of fibers by the resin matrix, also called resin impregnation, is essential for their effective use (Vallittu, 1995a; Vallittu, 1998b). Optimal reinforcement and transfer of stresses from the polymer matrix to the reinforcing fibers can be achieved through thorough resin impregnation. Fibers are difficult to impregnate with high-viscosity resin systems (Vallittu, 1995a; Vallittu, 1995b). If a proper degree of impregnation is not reached due to the high viscosity and/or polymerization shrinkage of the resin, water sorption will increase through voids leading to decreased mechanical properties of FRC (Miettinen & Vallittu, 1997). Additionally, voids of poorly impregnated fibers serve as oxygen reservoirs, which can inhibit the radical polymerization of the polymer matrix (Vallittu, 1999a). This further decreases the strength of the FRC and increases the residual monomer content that can leach out and cause adverse reactions to the oral mucosa (Hensten-Pettersen, 1998).

Two types of resin can be used in FRCs: cross-linked or linear. A cross-linking polymer (thermoset polymer) refers to multifunctional or dimethacrylate resins, while a linear polymer (thermoplastic polymer) refers to monofunctional methacrylate resins (Mallick, 2008).

In FRCs, the "so-called" semi-interpenetrating polymer network (semi-IPN) structure, the matrix is multiphase in nature consisting of a cross-linking polymer and a linear polymer mixed together with a photo-initiator (Vallittu, 2009). FRC with cross-linked polymer matrix has higher modulus of elasticity than FRC with linear or semi-IPN polymer matrix (Lassila *et al.*, 2002; Lassila *et al.*, 2004; Bouillaguet *et al.*, 2006).

Nevertheless, linear and semi-IPN polymer matrices demonstrate higher toughness than cross-linked polymer matrix. FRC with semi-IPN polymer matrix is considered advantageous over the cross-linked dimethacrylate or epoxy-type of polymer matrices in terms of handling properties and adhesion of root canal posts and dental restorations to resin-luting cements (Le Bell *et al.*, 2004).

Setting reactions in the resin matrix are either cross-linking reactions or polymerization reactions. The cross-linking reaction is the formation of a cross-link, where chains are bonded together either by a direct connection or an intermediary ion, atom, molecule, or chain. This develops a three dimensionally strongly cross-linked system (Darvell, 2006b). The polymerization reaction is the formation of a polymer by sequential addition of monomeric units. Typical polymerization reactions are condensation and addition (including free-radical addition polymerization) polymerizations (Darvell, 2006a). In the case of photopolymerization of FRCs, the exposure time, polymerization temperature, and light intensity influences the flexural properties and the degree of monomer conversion (Loza-Herrer MA, 1998a; Loza-Herrer MA, 1998b).

Of thermosets, the bisphenol-A-glycidyl dimethacrylate (BisGMA) is extensively used as a dental base monomer since early 1960s (Bowen, 1963). For use in dental composites, BisGMA is a very viscous monomer (Davy *et al.*, 1998) and a diluent monomer of triethyleneglycoldimethacrylate (TEGDMA) is commonly added for thinning the resin to obtain applicable handling characteristics. In the BisGMA-TEGDMA dental resin systems (Figure 6), BisGMA functions to improve the resin's reactivity and decrease the volumetric shrinkage induced by photopolymerization, while TEGDMA functions to increase the vinyl double bond conversion (Antonucci & Stansbury, 1997; Reed *et al.*, 1997).

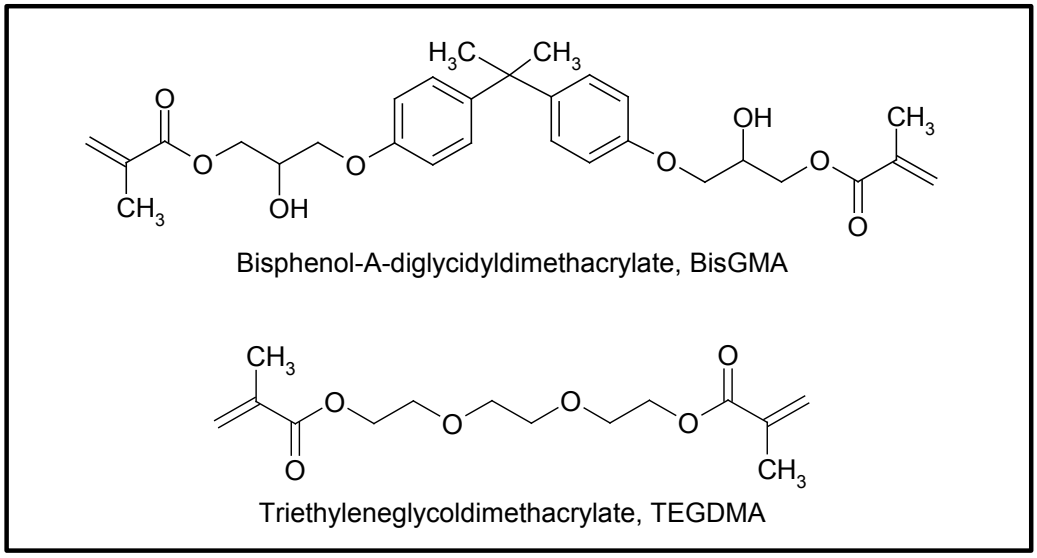

Figure 6 *The chemical structure of BisGMA and TEGDMA monomers used in fiber-reinforced composite fabrication.*

The use of FRC has rapidly increased in many dental disciplines and applications such as removable and fixed prosthodontics (Narva *et al.*, 2001; Vallittu, 1997a; Vallittu, 1999b; Freilich *et al.*, 1998; Wolff *et al.*, 2010), periodontal splints (Freilich & Goldberg, 1997), root canal posts (Lassila *et al.*, 2004; Mannocci *et al.*, 2005), and orthodontic treatment (Freudenthaler *et al.*, 2001). Furthermore, attempts recently created to use FRC as implant material in orthopedic and craniofacial surgeries (Zhao *et al*., 2009; Mattila, 2009; Travan *et al.*, 2010; Tuusa *et al.*, 2007; Tuusa *et al.*, 2008). Although the amount of scientific literature on using FRC material as a surgical device is limited, it shows potential for use in surgery especially when combined with bioactive modifiers, such as bioactive glass.

Among the dental applications of FRCs, one novel application is the implementation of FRC as an oral implant material. In a series of studies conducted, FRC exhibits sufficient mechanical properties under loading conditions and biocompatibility in a bone environment (Ballo, 2008). The main goal behind those studies was to introduce an implant material, which possess the ability to tailor its modulus of elasticity to values close to that of bone tissues, since the mismatch in Young's modulus between implant material and bone tissues (e.g., in poor bone conditions) and the related stress shielding and overloading could result in failure of implant treatment (Lemons, 1998; Ramakrishna *et al*., 2001). However, there is no information on how this material can behave on the soft tissue level as an implant abutment. The transmucosal component is considered as a challenging part of the oral implant that must be carefully designed, since optimal mechanical properties are required due to the lack of support from the surrounding bone tissue. However, it should be simultaneously capable of allowing epithelial and connective tissue attachment and minimizing bacterial colonization.

2.5. Influence of material's characteristics on soft tissue integration

The creation of a stable and healthy soft tissue seal around oral abutments that shelters the underlying tissues from the intraoral environment depends mainly upon the adhesion, proliferation, and colonization of epithelial and fibroblastic cells. Abutment surface characteristics, among which surface chemistry, surface roughness, and surface energy are key controlling determinants (Linkevicius & Apse, 2008; van Brakel *et al.*, 2011; Teughels *et al.*, 2006; Bürgers *et al.*, 2010; Al-Ahmad *et al.*, 2010; Grossner-Schreiber *et al.*, 2001; Abrahamsson *et al.*, 2002; Quirynen *et al*., 1994; Hamdan *et al.*, 2006).

2.5.1. Surface Chemistry

There is clear data from human and experimental animal studies research that all commercially available abutment materials show desirable biocompatibility (Degidi *et al.*, 2006; Vigolo *et al.*, 2006; Linkevicius & Apse, 2008).

Linkevicius *et al*. published a systematic review on the influence of abutment material on peri-implant tissue quality (Linkevicius *et al*., 2008). A meta-analysis could not be

performed due to differences in the experimental designs. The authors proposed that there is no evidence that titanium abutments better maintain stable peri-implant tissues than zirconium oxide, aluminum oxide, and gold materials. However, despite the distinguished record of titanium abutments (Lekholm *et al.*, 2006), there is an obvious trend towards non-metallic implant materials motivated by patients and implant-manufacturing companies.

2.5.2. Surface roughness

The surface roughness (i.e., topography) of a biomaterial plays a significant role in failure or success upon placement in a biological environment (Kasemo, 2002). In the case of oral implants, the establishment of a decent bone and soft tissue integration is mandatory (Ellingsen, 2003). The implant/tissue integration is complicated by the fact that various types of tissues interface with the implant surface (i.e., epithelium, connective tissue, and bone). For the bone/implant contact region, initial bone formation is necessary to allow early loading and favorable conditions for bone remodeling and long-term stability (Cochran, 1999). On the other hand, it is crucial that the epithelium and connective tissue quickly create a seal that surrounds the neck of the oral implant to prevent bacterial invasion (Quirynen *et al.*, 2002; Larjava *et al*., 2011) and downgrowth of the overlaying epithelium (Chehroudi *et al.*, 1988). One approach to address this issue is to develop an implant surface with different surface topographies (Scacchi, 2000), since certain cell types show a preference for rough or smooth topography (Brunette, 2001). Fibroblasts prefer smooth surfaces, whereas osteoblasts favor rougher surfaces (Brunette, 2001; Ponsonnet *et al.*, 2002; Wirth *et al.*, 2005; Kunzler *et al.*, 2007). Nevertheless, recent published reports showed histologic evidence of intimate connective tissue attachment to laser-microgrooved abutment surfaces (Nevins *et al.*, 2010 & 2012).

R_a and S_a are the most commonly used surface parameters in oral implant literature. R_a is the two-dimensional counterpart of the three-dimensional descriptor S_a. R_a and S_a are defined as the arithmetic mean of the absolute departures from a mean plane (Wennerberg, 1996). A certain threshold roughness (i.e., R_a around 0.2 μm) is necessary to form a stable soft tissue cuff around titanium abutments and that any increase in R_a value above 0.2 μm will expedite early plaque formation (Bollen *et al.*, 1996). Nevertheless, it is hypothesized that the impact of surface roughness on contact angles obtained from polymer surfaces disappear if the R_a value is below 0.1 μm (Busscher *et al.*, 1984).

2.5.3. Surface wettability

Measurement of the wettability of a material, expressed by the contact angle (θ_C) in the presence of the different liquids, is a predictive index of cytocompatibility (Kasemo, 1983; Mekayarajjananonth & Winkler, 1999). Contact angle techniques evolved from the method first described by Young in 1805 (Baier *et al.*, 1968). If a small amount of liquid is placed on a solid surface and it does not spread, a drop is formed. The angle of intersection of a line tangent to the liquid and the surface of the solid that it contacts is the contact angle

(Figure 7). This angle is characteristic of the substances in the system because of the surface tension of the liquid and the surface energy of the solid, modified by certain properties such as roughness. Stated another way, a high contact angle indicates poor wettability, while a low contact angle indicates good wettability (Winkler *et al.*, 1975).

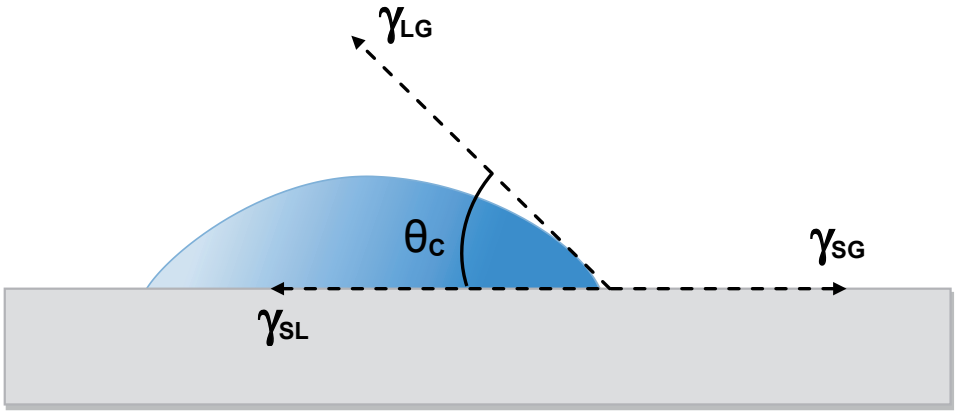

Figure 7 *An illustration of the sessile drop technique with a liquid droplet partially wetting a solid substrate: θ_C = Equilibrium contact angle; γSG= Interfacial tension between the solid and gas; γSL= Interfacial tension between the solid and liquid; and γLG= Interfacial tension between the liquid and gas.*

Surface free energy (SFE) is important for wettability (Baier *at al.*, 1968). SFE is the energy at the surface of a solid, which is greater than its interior energy. The outer atoms are unequally attracted to each other. Therefore, the unsaturated bonds generate surface energies (Anusavice, 1996). SFE of a given surface can be calculated from the contact angles measurements obtained using a range of liquids (Combe *et al.*, 2004). When a liquid is placed on a higher-energy surface, the contact angle will be lower as compared with a lower-energy surface (Baier *et al.*, 1968).

Considerable attention is devoted to increasing wettability and higher surface energy, since both characteristics enhance the interactions between biologic environments and implant surfaces (Baier *et al.*, 1984; Eriksson *et al.*, 2004; Kennedy *et al.*, 2006). Hallab *et al.* revealed that the SFE was a major surface determinant of cell adhesion and proliferation, and that the SFE components of different materials investigated are more useful than surface roughness for directing cell adhesion and colonization (Hallab *et al.*, 2001). Schakenraad *et al.* concluded that the SFE of a polymer surface is obviously the most governing factor influencing cellular attachment even if a protein layer has covered the polymer surface (Schakenraad *et al.*, 1988). Furthermore, in a fairly recent study, soft and hard tissue integration appeared to be mainly influenced by surface hydrophilicity rather than microtopography (Schwarz *et al.*, 2007). In spite of that, surface roughness could interrupt the relationships between cell proliferation and SFE (Ponsonnet *et al.*, 2003).

2.6. Wound healing at soft tissue/implant interface

The wound healing-process around oral abutments utilizes the same principles as any other soft tissue wound healing, whereby complex biological interactions on a cellular and biomechanical level occur to the oral mucosa alongside the newly inserted abutment, resulting in the formation of peri-implant soft tissue. However, recent studies comparing wound healing around clinically healthy teeth and oral implant abutments suggest that peri-implant soft tissue healing differs from periodontal tissue healing. The peri-implant soft tissue healing represents a higher pro-inflammatory state (Nowzari *et al*., 2008 & 2012; Emecen-Huja *et al.*, 2013).

Immediately upon implantation, a blood clot separates the gingival soft tissue mucosa from the transmucosal component of oral implant. The blood clot is then infiltrated by inflammatory cells (primarily polymorphonuclear cells) and substituted by a dense fibrin mesh. At day 4, the initial soft tissue seal is formed by a fibrin layer (Berglundh *et al.*, 2007). Fibroblasts occupy the fibrin network and synthesize collagen fibers. Throughout this process, the fibrin mesh is gradually interchanged by a fibrous connective tissue (Berglundh *et al.*, 2007). Two weeks after implant installation, a newly formed connective tissue that is rich in fibroblasts and vascular units comes into close contact with the abutment surface. Within a few days of the healing process, epithelial cells from the surrounding wound margins begin migration towards the abutment surface, 1 to 2 weeks later proliferation of the epithelial cells take place followed by flattening of the cells alongside the surface, which leads to the formation of junctional epithelium (Berglundh *et al.*, 2007). Maturation and remodeling of the peri-implant soft tissue occurs between 6 to 12 weeks after implant installation, and it is mostly characterized by organization and alignment of collagen fibers, besides formation of a mature epithelial barrier (Berglundh *et al.*, 2007). From the clinical perspective, remodeling of the peri-implant soft tissue is of great importance as the quality of the regenerated tissue is determined at this stage.

2.7. Implant failure

Failure of implant treatment can be classified as early or late. Early failure occurs soon after implant installation whereby osseointegration is never achieved. Late failure occurs in a successfully integrated implant some time after implant installation. The etiology of late failure could be biomechanical overload or marginal disease/infection. However, an analysis of the clinical trials of the ITI system shows that a low percentage of failures are caused by occlusal overload (Albrektsson & Isidor, 1994). Thus, the main reason of late failures could be related to peri-implant infections (Paquette *et al.*, 2006). During the 6th European Workshop on Periodontology in 2008, it was proposed that the term ‘‘peri-implant disease’’ is a ‘‘collective term for inflammatory reactions in the tissues surrounding an implant’’ and that peri-implant mucositis will be used to describe ‘‘the presence of inflammation in the mucosa at an implant with no signs of loss of supporting bone’’ (Zitzmann & Berglundh, 2008). Additionally, it was proposed that the term

periimplantitis is "an inflammatory process around an implant, characterized by soft tissue inflammation and loss of supporting bone" (Zitzmann & Berglundh, 2008).

The formation of a biofilm around oral implants plays a significant role in the initiation and progression of peri-implant diseases, similarly to natural teeth (Mombelli & Lang, 1998). It is generally accepted that peri-implantitis is an extension of peri-implant mucositis (Lang & Berglundh, 2011). Studies show that peri-implantitis and periodontitis have many features in common. Peri-implantitis and periodontitis show great similarities in the bacterial composition of the associated biofilm (Agerbaek *et al*., 2006; Heitz-Mayfield & Lang, 2010; Dahlén *et al*., 2012). Inflammatory cells, with B-lymphocytes and plasma cells being the most dominating cell types, infiltrate the connective tissue adjacent to the pocket epithelium. Similar cytokines such as interleukin (IL)-1, IL-6, IL-8, IL-12, and tumor necrosis factor (TNF)-alpha have been found between peri-implantitis and periodontitis (Duarte *et al*., 2009; Javed *et al.*, 2011b). Despite sharing similarities with periodontitis in both bacterial initiators and key immune components, peri-implantitis differs in the severity of inflammatory signs and the rate of disease progression. Outcomes of human and animal studies on undisturbed plaque biofilm formation on implants and teeth demonstrated more advanced inflammatory cell infiltration in the peri-implant mucosa (Ericsson *et al.*, 1992; Zitzmann *et al*., 2004; Berglundh *et al*., 2011). Clinical and radiographic features of peri-implantitis show more pronounced tissue destruction, which approaches the crestal bone (Lindhe *et al*., 1992). The increased susceptibility for peri-implant bone loss could be related to the absence of collagen fiber insertions (Schou *et al.*, 1993). Additionally, inflammation and bone loss around oral implants could occur due to the poor peri-implant epithelial attachment, thereby allowing for apical migration of plaque (Larjava *et al*., 2011). Therefore, the establishment of quick and firm epithelium and connective attachment around oral implant abutments is mandatory.

Furthermore, repeated removals of implant abutments until the final restoration is placed, in addition to the fact that lab-made custom abutments have non-standardized surface chemistry and topography, represent major challenges for soft tissue/abutment integration during the restorative phase of treatment. However, it seems with the current treatment modalities that the soft tissue attachment to implant abutments is not adequate enough to prevent peri-implant infections. Hence, further research is necessary to develop implant surfaces for better soft tissue attachment during the healing process.

3. AIMS OF THE THESIS

The research presented in this thesis was based on the working hypothesis that unidirectional E-glass fiber-reinforced composite exhibits appropriate mechanical properties and maintains biocompatibility in a soft tissue environment to be used in the fabrication of oral implant abutments.

Accordingly, the following specific aims were set to:

1. Determine the effect of E-glass fiber volume on some mechanical properties of high fiber-density FRCs (Study I).
2. Assess the effect of exposed E-glass fibers on the surface wettability behavior of FRCs (Study II).
3. Evaluate blood response, including blood-clotting ability and platelet adhesion morphology on FRCs *in vitro* (Study III).
4. Study the adhesion and proliferation of human gingival fibroblasts on FRCs *in vitro* (Study III).
5. Examine gingival tissue attachment and growth to FRCs *in vitro* (Study IV).

4. MATERIALS AND METHODS

4.1. Fabrication of the substrates investigated

The materials used for the fabrication of experimental substrates are listed in Table 2. The substrates investigated in the present studies had almost similar polymerization condition, however, substrates of different shapes were fabricated to fulfill each experiment requirements.

Table 2 *Materials used in the experimental studies.*

Product	Description	Manufacturer	Composition	Study
Stick Resin	Light curing resin	Stick Tech, Turku, Finland (Lot # 54031672)	BisGMA-* TEGDMA** (50–50%)	I, II, III, and IV
E-glass* fiber**	Unidirectional fiber	Ahlstrom, Karhula, Finland (Lot # 11372313)	55% SiO_2, 15% Al_2O_3, 22% CaO, 6% B_2O_3, 0.5% MgO, and > 1.0% Fe + Na + K	I, II, III, and IV
Filler	0.7 μm filler	Esschem, Linwood, Pennsylvania (Lot # 625-29)	Barium-aluminium-boro-silicate glass 5% silane	I

* BisGMA, bisphenol A glycidyl dimethacrylate
** TEGDMA, triethylene glycol dimethacrylate
*** E-glass, electrical glass

4.1.1. Polymerization condition

The substrates were photopolymerized for 2 min per side (Elipar S10, 3M Espe, Seefeld, Germany). The irradiance was 950 mW/cm^2, as measured using curing radiometer. Consequently, the polymerization was pursued for 25 min in a light curing oven (LicuLite, Dentsply De Trey GmbH, Dreieich, Germany), whereby the temperature was elevated to 90°C. In order to optimize the degree of monomer conversion (DC%), the substrates were post-polymerized for 24 hours (h) in hot-air oven at 120°C (studies II, III, and IV). Additionally, the substrates in study III were immersed for 3 days (d) in distilled water to release any residual monomers, thereby enhancing the biocompatibility of the polymer matrix (Ballo *et al.*, 2008). The substrates were conditioned for 2 d at room temperature before use.

4.1.2. Shape of the experimental substrate

4.1.2.1. Preparation of cylindrical-shaped substrates for mechanical testing (Study I)

Five groups of unidirectional FRC with different fractions of glass fiber vol% were prepared; two additional groups were prepared by adding silanized barium-silicate glass particulate fillers (size 0.7 μm) with two different percentages 5% and 10%, respectively. The different groups investigated in this study are listed in Table 3.

Table 3 *Groups of substrates used in the investigation according to their fiber content.*

Groups	Amount of glass fiber
Group A	7 bundles
Group B	7.5 bundles
Group C	8 bundles
Group D	8.5 bundles
Group E	9 bundles
Group F	8 bundles + 5% fillers
Group G	8 bundles + 10% fillers

The unidirectional E-glass fibers were preimpregnated with light-polymerizable BisGMA-TEGDMA (50–50%) polymer and incubated for 48 h in an incubator at 37°C before polymerization (D 06062, Modell 600, Memmert GmbH + Co. KG, Schwabach, Deutschland). Cylindrical substrates (n=12) were fabricated for each group by pulling the fiber bundles through a special cylindrical mold with an opening diameter of 4.2 mm (Figure 8); each bundle consists of about 4,000 continuous unidirectional silanized E-glass fibers (diameter approx. 15 µm).

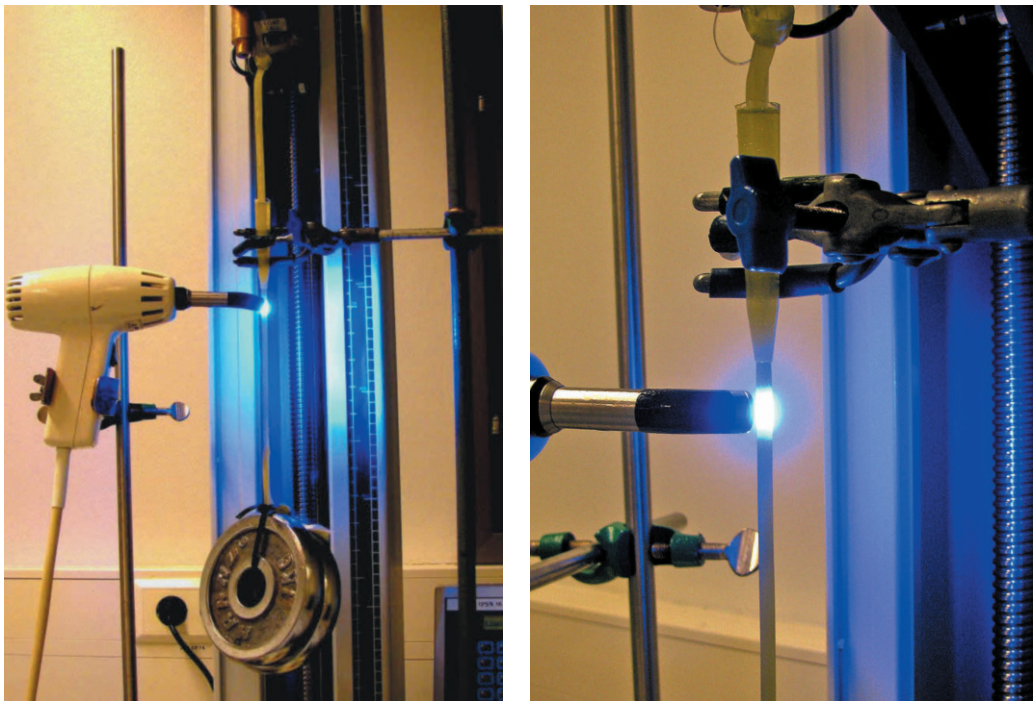

Figure 8 *Fabrication of the unidirectional E-glass fiber-reinforced composite substrates.*

After polymerization, the cylindrical substrates were ground from the endings using wet silicon carbide grinding paper (FEPA #1200). The size of each substrate was verified by

measuring its diameter from three different random areas. The substrates had average diameter of 4.0 mm (Figure 9). This dimension was chosen, as it resembles the average diameter of oral implants (i.e., its load-bearing capacity should exceed average maximum occlusal forces within the physiological strain limit of bone) (Lum & Osier, 1992).

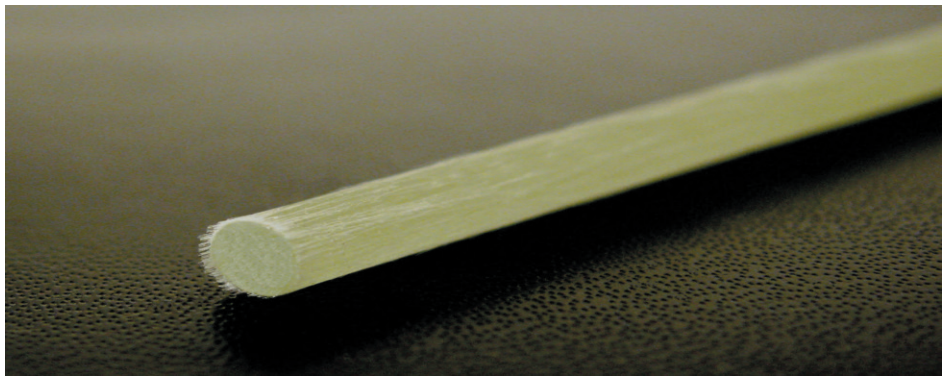

Figure 9 *Unidirectional E-glass fiber-reinforced composite substrate.*

4.1.2.2. Preparation of square-shaped substrates for surface wettability evaluations (Study II)

Two different groups of substrates were prepared (10x10x6 mm, n=10 per group); the first group was composed of plain polymer as a control group, and the second group was composed of unidirectional FRCs of various fiber orientations (i.e., transverse and in-plane directions) (Figure 10). For both groups, two different sets were prepared by using various polymerization methods (photopolymerized and post-polymerized of increased temperature).

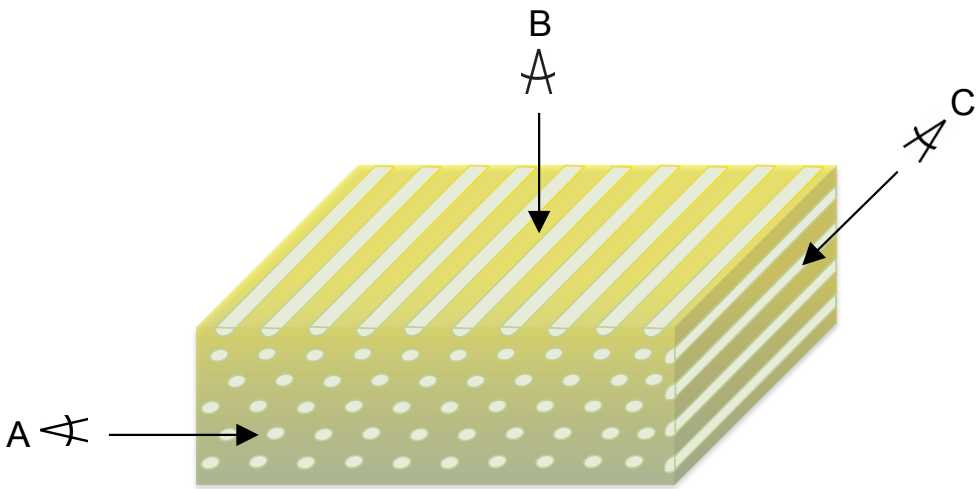

Figure 10 *Schematic and simplified picture of unidirectional E-glass fiber-reinforced composite substrate showing fibers in different orientation planes: (A) Fibers running transversely; (B) Fibers running in-plane (perpendicular); and (C) Fibers running in-plane (parallel).*

The unidirectional E-glass fibers were preimpregnated with BisGMA-TEGDMA (50–50%) polymer in molds and incubated for 48 h in an incubator at 37°C. After polymerization, the surfaces of the substrates were ground using wet silicon carbide grinding paper (FEPA #180–2400) and polishing cloths with a 0.1 µm AP-D suspension. This polishing procedure, besides exposing the glass fibers, ensures producing smooth surfaces in order to disregard the influence of surface roughness on contact angle measurements. The substrates were ultrasonically cleaned for 10 min in both ethanol and distilled water to eliminate possibly embedded grinding material.

4.1.2.3. Preparation of square-shaped substrates for blood response and cell culture experiments (Study III)

Two different groups of substrates were prepared (10x10x2 mm). The first group was composed of plain polymer as a control group and the second group was composed of unidirectional FRCs of in-plane direction (Figure 10). For the FRC group, the unidirectional E-glass fibers were preimpregnated with BisGMA-TEGDMA (50–50%) polymer in molds and incubated for 24 h in an incubator at 37°C. After polymerization, the surfaces of the substrates were ground using wet silicon carbide grinding paper (FEPA #180–2400), thereby exposing the glass-fibers on the substrate surfaces. The substrates were ultrasonically cleaned for 10 min in both ethanol and distilled water to eliminate possibly embedded grinding material and then autoclaved for 20 min at 121°C before use.

4.1.2.4. Preparation of cylindrical-shaped substrates for gingival tissue culture experiment (Study IV)

Two different implants were prepared (length 10 mm, diameter 2 mm, n=4 per time-point). The first implant was composed of plain polymer as a control implant and the second implant was composed of unidirectional FRCs of in-plane direction (Figure 11).

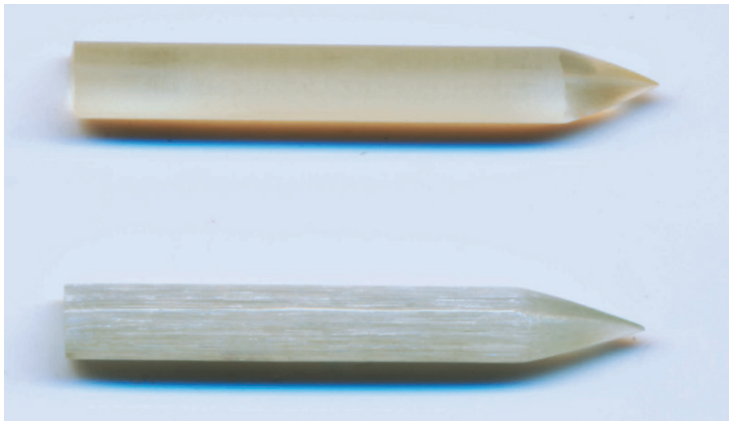

Figure 11 *Cylindrical-shaped plain polymer and unidirectional E-glass fiber-reinforced composite implants.*

For the FRC group, the unidirectional E-glass fibers were preimpregnated with BisGMA-TEGDMA (50–50%) polymer and incubated for 24 h at room temperature. A specially designed device was used to prepare the pre-tensioned FRC poles (Figure 12). The impregnated fiber bundles were first attached to the upper hook above the gutter and then to the lower weight holder, where a 10.3 kg weight was added to create pre-tension. Subsequently, the nozzle that was attached to a certain holder was pulled through the bundles at a speed of 4 mm/s. Polymerization of the FRC pole was performed by LED lamps positioned circularly in the nozzle holder around the rovings. After polymerization, the surfaces of the substrates were manually ground using wet silicon carbide grinding paper (FEPA #180–2400), thereby, exposing the E-glass fibers on the substrate surfaces. The substrates were ultrasonically cleaned for 10 min in both ethanol and distilled water to eliminate possibly embedded grinding material and then autoclaved for 20 min at 121°C before use.

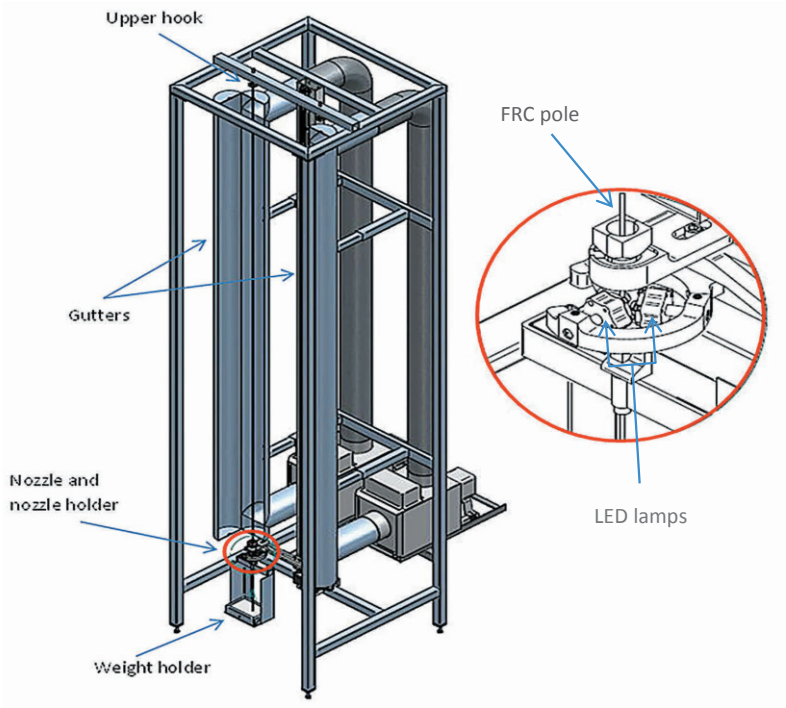

Figure 12 *Unidirectional fiber-reinforced composite pole manufacturing device. The illustration was adapted with permission from Pasi Saarenmaa.*

4.2. Mechanical testing of high density FRC (I)

4.2.1. Three-point bending test

The three-point bending test was used to evaluate some of the mechanical properties of unidirectional FRCs adapted to ISO 10477:92 standards (crosshead speed 5.0 mm/

min). All substrates investigated were examined with a material testing machine (model LRX, Lloyd Instruments Ltd., Fareham, England) and the stress-strain curves were documented using a PC-computer program (Nexygen, Lloyd Instruments Ltd., Fareham, England). Following mechanical testing, the substrates were visually inspected with a light-microscope in an effort to distinguish the origin of fracture and the mode of failure.

4.2.2. Fiber volume percentage calculations

The fiber content of the substrates expressed as a volume percentage (vol.%) was measured using the combustion analysis with a burnout furnace (Radiance Multi-stage msc, Jelrus International, Hicksville, New York). The substrates were dried for 2 d in a desiccator at room temperature, and then weighed to an accuracy of 0.001 mg prior to combustion. In order to combust the polymer matrix, the temperature was elevated 12°C per minute until the temperature reached 700°C. The substrates were maintained for 1 h at 700 ± 25°C and then reweighed again. The fiber volume (V_f) was calculated using the following equation (Vallittu & Narva, 1997):

$$V_f(\%) = \frac{W_f/r_f}{W_f/r_f + W_r/r_r} \times 100,$$

where W_f is the weight proportion of E-glass, r_f (=2.54 g/cm^3) is the density of E-glass, W_r is the weight proportion of resin, and r_r is the density of resin, which was calculated from the unreinforced test substrates.

In order to confirm the measurements given by the combustion process, the fiber content was also measured using the gravimetric analysis based on Archimedes' principle in accordance with the following equation:

$$V_f(\%) = \frac{r_s - r_r}{r_f - r_r} \times 100,$$

where r_s is the density of the substrate, r_r and r_f are as defined above.

4.3. Scanning electron microscopy (I and III)

The surfaces of the substrates were characterized using field-emission scanning electron microscopy (FE-SEM) (Leo Gemini 1530; Zeiss, Oberkochen, Germany). Approximately 20 nm of carbon layer was applied to the substrates using a sputter coater (Temcarb TB500, Emscope Laboratories Ltd., Ashford, United Kingdom). In study I, the cross-section surfaces of substrates were visually examined with FE-SEM to observe the distribution of the fiber contents. In study III, the surface topography of the substrates in addition to the morphological characteristics platelets were observed with FE-SEM.

4.4. Roughness and imaging characterization (II and III)

A spinning disk confocal microscope with a white light source (COM, NanoFocus µSurf, Oberhausen, Germany) was used to determine R_a and S_a surface parameters. The R_a/S_a values according to DIN EN ISO 4287 were measured at 100x magnification. In calculation of the R_a/S_a values a Gaussian filter (ISO 11562) was used. At 100x magnification, the vertical resolution of the lens is 2 nm and the numerical aperture 0.8–0.95 for a measurement area of 160–158 µm. For the measurements done with the 100x lens, the cutoff wavelength of 80 µm was used. At least five readings per substrate were made at different random areas. The mean value was calculated and quantitatively expressed as a numerical value (in micrometers).

4.5. FTIR spectroscopy (III)

The DC% was determined using a Fourier transform infrared (FTIR) spectrometer (Spectrum One, Perkin Elmer, Beaconsfield Bucks, United Kingdom) with attenuated total reflectance (ATR) accessory. First, the spectrum of the unpolymerized resin was measured on the ATR tray. The post-polymerized substrate was scanned for its FTIR spectrum; the upper surface of the substrate was slightly pushed against the ATR to ensure firm contact with the substrate. The FTIR spectra were recorded with 16 scans at a resolution of 4 cm^{-1}. The DC% was calculated from the aliphatic C=C peak at 1638 cm^{-1} and normalized against the aromatic C=C peak at 1608 cm^{-1} in accordance with the following formula:

$$DC\% = \left[1 - \frac{C_{aliphatic} / C_{aromatic}}{U_{aliphatic} / U_{aromatic}} \right] \times 100$$

Where:
$C_{aliphatic}$ absorption peak at 1638 cm^{-1} of the cured substrate
$C_{aromtic}$ absorption peak at 1608 cm^{-1} of the cured substrate
$U_{aliphatic}$ absorption peak at 1638 cm^{-1} of the uncured substrate
$U_{aromatic}$ absorption peak at 1608 cm^{-1} of the uncured substrate

The fraction of remaining double bonds for each spectrum was determined by standard baseline techniques using the comparison of maximum heights of aliphatic and reference peaks for calculations.

4.6. X-ray Diffraction analysis (III)

The phase composition of the substrates after quenching was identified using an X-ray diffraction analyzer (XRD; X'Pert PRO MPD, Philips, Eindhoven, Netherlands) with Cu Kα radiation (λ= 1.5418Å). The scans were performed from 2θ = 0 to 60° with a step size of 0.02°.

4.7. Surface wettability (II)

4.7.1. Contact angle measurements

Equilibrium contact angles (θ_C) were measured using sessile drop method (described in detail elsewhere, de Jong *et al.*, 1982) with a contact angle meter (KSVCAM100 KSV, Instruments LTD, Helsinki, Finland). A drop was placed on the substrate's surface and imaged for 20 s by collecting one image per 2 s. Determination of contact angle was based on the Young-Laplace equation, yielding the contact angles on both sides of the droplet and their mean values. Three liquids were used as a probe for the calculations of surface free energy (SFE) (Table 3). The result was the mean of at least 10 drops on each substrate. For the FRC surfaces, the contact angles were measured in two directions with respect to fiber orientation (i.e., parallel and perpendicular to the camera's axis).

Table 3 *Test liquids and their surface tension components (Costanzo et al., 1990).*

Liquid	Source	Surface tension (mN/m)			
		γ^{TOT}	γ^{D}	γ^{+}	γ^{-}
Distilled water, ultrapure water Milli-Q	Produced in-house	72.8	21.8	25.5	25.5
Diiodomethane > 99% purity	Sigma-Aldrich, St. Louis, USA (Lot # S82251)	50.8	50.8	0	0
Formamide, pro analysis	Merck, Darmstadt, Germany (Lot # 1.09684.2500)	58	39	2.28	39.6

4.7.2. Surface free energy calculations

The SFE was calculated using two theoretical approaches: Owens-Wendt (OW) and Van-Oss (VO). The OW approach gives the long-range dispersion (Lifshitz-van der Waals) (γ^{D}) and the short-range polar (hydrogen bonding) (γ^{P}) components of SFE (Owens & Wendt, 1969). The VO approach brings the dispersive (γ^{LW}) and the polar acid-base (γ^{AB}) components, the latter is divided into two parts, acidic (γ^{+}) and basic (γ^{-}) (Van Oss *et al.*, 1998) in accordance with the following equations:

$$1+\cos\theta = 2(\gamma_s^d)^{1/2}((\gamma_L^d)^{1/2}/\gamma_L) + 2(\gamma_s^p)^{1/2}((\gamma_L^p)^{1/2}/\gamma_L)$$

$$(1+\cos\theta)\gamma_L = 2\left[(\gamma_s^{LW}\gamma_L^{LW})^{1/2} + (\gamma_L^-\gamma_s^+)^{1/2} + (\gamma_s^-\gamma_L^+)^{1/2}\right]$$

where γ_s is the SFE of the surface, γ_L the SFE of the liquid and $\gamma_s^{ab}=(\gamma_s^-\gamma_L^+)^{1/2}$.

For both approaches, the spreading pressure was not taken into account. This pressure contributes to SFE and has to be considered if the SFE is higher than 60 mJ/m^2 (Busscher, 1992). In the current work, SFE values were lower than this limit and therefore the spreading pressure was disregarded.

4.8. Blood response (III)

4.8.1. Blood-clotting

The thrombogenicity of the plain polymer and FRC substrates was evaluated using a whole blood kinetic clotting time method, as previously described (Imai & Nose, 1972; Huang *et al.*, 2003). Fresh human whole blood was drawn from a healthy adult female volunteer, who had not taken any medication affecting platelets function, by venipuncture into vacutainer tubes. The first 3 ml of the drawn blood was discarded to avoid contamination by tissue thromboplastin caused by needle puncture. Briefly, a 100 µl volume of blood was carefully added to the surface of the substrates (n=4), which were placed into 12-well plates. All substrates were incubated at room temperature for 10, 20, 30, 40, 50, and 60 min. At the end of each time-point, the substrates were incubated for 5 min with 3 ml of ultrapure water. Each well was sampled in triplicate (200 µl each) and transferred to a 96-well plate. The red blood cells that were not trapped in a thrombus were lysed with the addition of ultrapure water, thereby releasing hemoglobin into the water for subsequent measurement. The concentration of hemoglobin in solution was assessed by measuring the absorbance at 570 nm using ELISA plate reader. The size of the clot is inversely proportional to the absorbance value. Blood-clotting on the surfaces at all time-points investigated was also observed using a digital camera (Canon SX210 IS, Tokyo, Japan).

4.8.2. Platelets adhesion and morphology

A platelet adhesion test was used to evaluate the adhesion behavior and activation of the platelets on the substrates. Fresh human whole blood was drawn, from the same volunteer of blood-clotting experiment, and anticoagulated with 0.109 M solution of sodium citrate at a dilution ratio of 9:1 (blood/sodium citrate solution). Then platelet-rich plasma (PRP) was obtained by centrifuging anticoagulated blood at 1500 rpm for 15 min at room temperature. After that, 100 µl of PRP was carefully added to the surface of the substrates (n=5) and incubated for 1 h at 37°C. Subsequently, the substrates were rinsed thoroughly three times with phosphate buffered saline (PBS) and fixed for 2 h with 2.5% glutaraldehyde. Then, all substrates were successively dehydrated at increasing alcohol concentrations. FE-SEM Images at different magnifications were collected for each substrate to observe platelet morphologies.

4.9. Cell culture experiments (III)

4.9.1. Cell cultures

Fibroblasts initiated from healthy human gingival biopsy samples were maintained in DMEM supplemented with 10% fetal bovine serum and 100 U/µg penicillin-streptomycin (Gibco BRL, Life Technologies, Paisley, UK) and incubated at 37°C in a 5% CO_2 environment. Semi-confluent cultures were trypsinized, and the cells were counted and

resuspended in complete culture medium. Culture medium was changed three times a week.

4.9.2. Adhesion kinetics

Fibroblasts were plated at a density of 25,000 cells/cm^2 on the substrates investigated (n=5). After 1, 3, 6, and 24 h of incubation, the substrates were washed three times with PBS to remove nonadherent cells. The substrates were placed into TE-buffer (10 mmol/L Tris-HCl, 1 mmol/L EDTA, pH 7.5) and stored at –70°C. Quantitative DNA measurements were then used to determine the amount of adhered cells. Briefly, the thawed substrates were sonicated on an ice-water-bath for 10 min to release genomic DNA. Intercalating dye (PicoGreen® dsDNA quantitation kit, Molecular Probes Europe, Leiden, The Netherlands) was added to the substrates, and fluorescence was measured using excitation and emission wavelengths of 490 nm and 535 nm, respectively (Victor™ 1420 multilabel counter, Wallac, Turku, Finland). Amounts of DNA were read from a λ-phage dsDNA standard curve.

4.9.3. Adhesion strength

Fibroblasts were plated at a density of 12,500 cells/cm^2 on the substrates investigated (n=6) and allowed to adhere for 6 h. The strength of attachment was evaluated using serial trypsinizations with 1:10 diluted enzymes in PBS (0.005% Trypsin, 0.05 mM EDTA; Gibco, Invitrogen) (Meretoja *et al.*, 2010). Substrates were washed three times with PBS to remove nonadherent cells and placed to sterile culture plates with enzyme solution. Plates were incubated on a rotary shaker (Max Q 2000; Barnstead International, Dubuque, Iowa), with an orbital speed of 140 rpm at room temperature for a total of 20 min, with enzyme replacement after 1, 5, and 10 min. Each time, the solution with detached cells was transferred to cryotubes, Triton X-100 detergent was added to a final concentration of 0.1% and tubes were frozen at –70°C. To determine the total amount of adherent cells, washed culture substrates were trypsinized with undiluted enzyme at 37°C for 5 min, followed by vigorous pipetting. Finally, detergent was added to the cell suspension and cells were frozen at –70°C. Amounts of DNA in each detachment substrate were measured, as explained previously, and normalized in relation to the total adhesion substrates.

4.9.4. Cell proliferation

Proliferation of cultured cells was determined using AlamarBlue™ assay (BioSource International, Camarillo, California) in colorimetric format. Fibroblasts were plated at a density of 12,500 cells/cm^2 on the substrates investigated and cultured for up to 7 d. The substrates (n=6) were withdrawn from the culture, at predetermined times, and placed into sterile culture plates containing fresh culture medium with 10% assay reagent. After 3 h of incubation, the absorbance values were read at 570 nm and 595 nm using ELISA plate reader (Multiskan MS, Labsystems, Helsinki, Finland). Measured absorbances were used to calculate the reduction of assay reagent, and the cell proliferation rate

was normalized in respect to the proliferation rate of the plain polymer control at the first time-point, which was arbitrarily set to 100%. A linear relationship between the cell number and absorbance readings was established using tissue culture polystyrene substrates.

4.9.5. Confocal fluorescence microscopy

Culture substrates were washed twice with PBS and cells fixed for 20 min with 3% paraformaldehyde at room temperature. Fixed cells were permeabilized with 0.1% Triton X-100 and nonspecific binding was blocked with 5% bovine serum albumin and 2.5% fetal bovine serum. Actin cytoskeleton was stained with tetramethylrhodamine isothiocyanate (TRITC)-conjugated Phalloidin (FAK100, Millipore, Billerica, Massachusetts). Cells were imaged using a confocal microscope equipped with Argon-Krypton laser (Zeiss LSM 510 Meta; Carl Zeiss, Oberkochen, Germany).

4.10. Tissue culture model (IV)

4.10.1. Implantation and tissue culture

The gingival explants were obtained from freshly slaughtered pigs. Approximately 3 h after slaughter, 8 mm punch explants (i.e., full thickness buccal and lingual attached marginal gingival tissues) were dissected from the mandibles of 4 pigs using a biopsy punch (Stiefel® Biopsy Punch; Stiefel Laboratorium GmbH, Offenbach am Main, Germany). Each experimental implant was inserted into the center of the explant and through a sterile Millipore HA membrane (pore size 0.45 μm, Millipore Corporation, Bedford, Massachusetts) that was placed underneath the explant. Thereafter, the tissue/implant specimens were placed individually in a 6-well culture plate at the air/fluid interface supported by a stainless steel grid (i.e., rafted tissue culture model) (Figure 13). Each well was filled with 6 ml of medium consisting of Eagle's minimum essential medium (EMEM M-2279) (Sigma-Aldrich Chemie GmbH, Steinheim, Germany) supplemented with (10% fetal bovine serum (FBS), 100 U/μg penicillin, streptomycin 100 μg/ml, and 200mM L-glutamine) (Gibco BRL, Life Technologies, Paisley, UK). The culture plates were incubated at 37°C in a 5% CO_2 environment. The culture medium was changed every 24 h. Specimens were harvested after 4, 10, and 14 d in culture for the preparation of undecalcified samples. For the control material, two gingival explants were fixed for 1 h in 10% buffered formalin immediately after taking biopsies for the preparation of routine histological samples. Gingival explants with no implants were also cultured to serve as baseline controls for general tissue morphology.

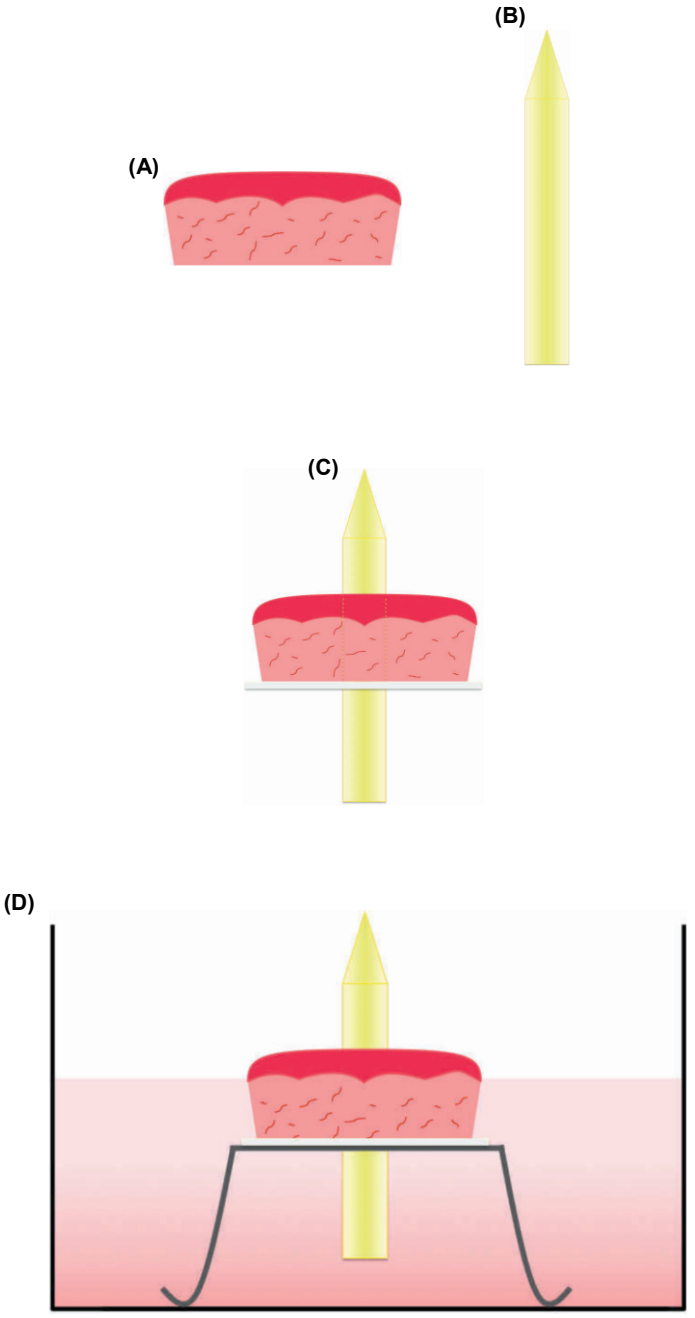

Figure 13 *Schematic view of the rafted tissue culture model: (A) Porcine gingival explant; (B) Experimental implant material; (C) Implant piercing through the center of 8 mm explant and polycarbonate membrane; and (D) Tissue/implant specimen suspended in the culture medium at the air/liquid interface by a metal mesh.*

4.10.2. Histological and light microscopy analyses

At the end of each incubation period, the specimens (i.e., gingival explants attached to the implants) were fixed in 10% buffered formalin for 1 d at room temperature, then dehydrated in an ascending ethanol series and embedded in Technovit 7200 VLC resin (Heraeus Kulzer, Wehrheim, Germany). Undecalcified sections (20 μm) were prepared by the cutting-grinding technique, and stained (Van Gieson or hematoxylin and eosin) for light microscopic analysis. The stained sections were analyzed under an Aristoplan photomicroscope (Leitz, Wetzlar, Germany) and the images were taken using a Leica DFC 320 digital camera (Leica Microsystems AG, Wetzlar, Germany) with Leica Application Suite version 4.1.0.

4.11. Statistical analysis

Statistical analysis was performed with Statistical Package for the Social Sciences software (SPSS. Inc, Chicago, Illinois). The distribution of data was normal, which was determined by the Kolmogorov-Smirnov test. Therefore, parametric tests were used for testing the statistically significant differences. Differences were considered significant at 95% confidence level.

In study I, the data were analyzed using one-way analysis of variance (ANOVA) followed by Scheffe post hoc test. The independent variable was fiber vol% fraction, and dependent variables were modulus of elasticity, toughness, strength, and load bearing capacity. In study II, the data were analyzed using one-way ANOVA followed by Tukey's *post-hoc* test. The independent variable was the contact angle, and dependent variables were fiber orientation and type of polymerization. In study III, the data were analyzed using two-tailed *t* test and one-way ANOVA followed by Tukey's *post-hoc* test. The independent variable was time, and dependent variables were optical density, amount of DNA, cell attachment, and cell activity.

5. RESULTS

5.1. Mechanical test (I)

5.1.1. Fiber volume percentage

The fiber vol.% fraction of the substrates investigated using combustion and gravimetric analyses is shown in Table 4.

Table 4 *The fiber vol.% fraction of high fiber-density unidirectional fiber-reinforced composite substrates.*

Groups	Fraction of glass fiber, vol.%	
	Combustion analysis	Gravimetric analysis
Group A (7 bundles)	49.0%	51.7%
Group B (7.5 bundles)	52.8%	53.4%
Group C (8 bundles)	55.8%	56.2%
Group D (8.5 bundles)	57.0%	58.2%
Group E (9 bundles)	60.3%	61.7%
Group F (8 bundles + 5% fillers)	52.6%	53.6%
Group G (8 bundles + 10% fillers)	56.5%	57.4%

The SEM observations showed that the glass fibers in group A substrates (i.e., 51.7 fiber vol.% fraction) were not evenly distributed within the matrix. While in group E substrates (i.e., 61.7 fiber vol.% fraction), the fibers were more evenly distributed throughout the cross-section (Figure 14).

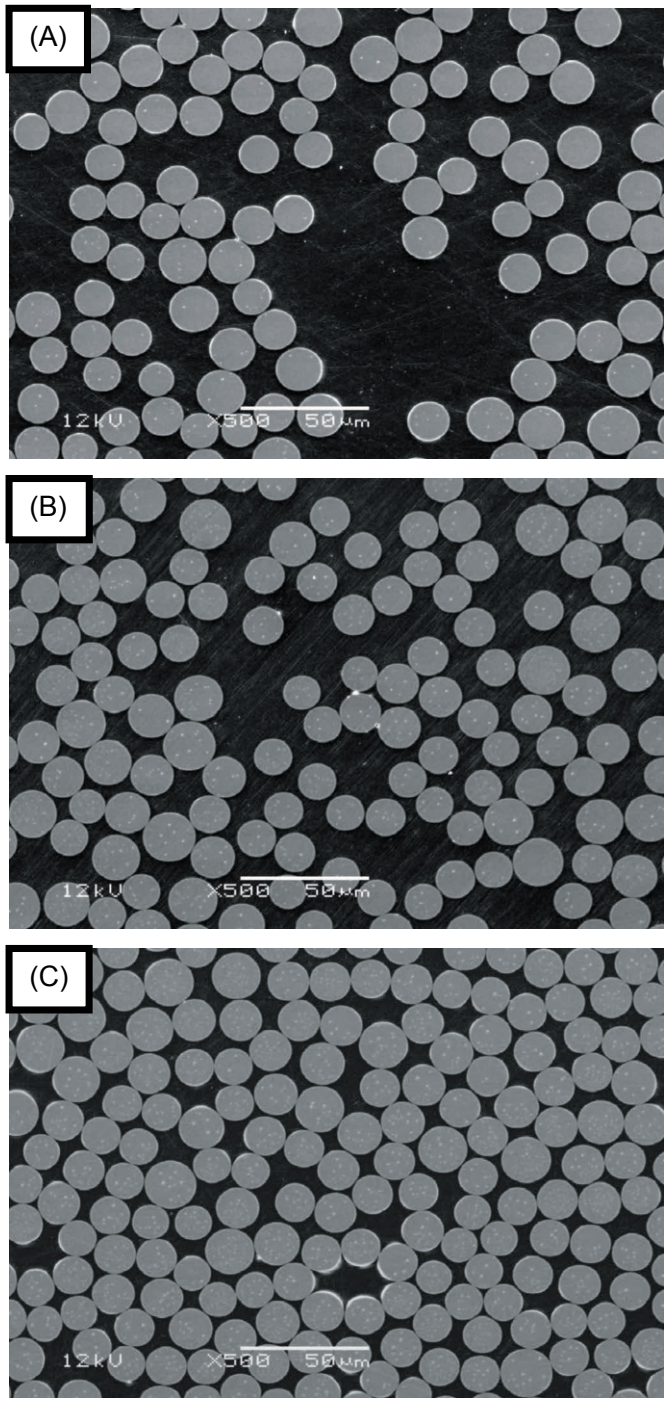

Figure 14 *Scanning electron micrographs illustrating the cross-section of unidirectional E-glass fiber-reinforced composite substrates with increasing fiber vol.% fraction: (A) Group A (51.7 fiber vol.% fraction, 7 bundles E-glass fibers); (B) Group C (56.2 fiber vol.% fraction, 8 bundles E-glass fibers); and (C) Group E (61.7 fiber vol.% fraction, 9 bundles E-glass fibers). Adopted from original publication I.*

5.1.2. Three-point bending test

An increase in the vol.% fraction of glass fibers from 51.7% to 61.7% resulted in: 27% increase ($p<0.001$) in the modulus of elasticity (Figure 15); 34% increase ($p<0.05$) in the toughness (Figure 16); and 15% increase ($p<0.001$) in the load bearing capacity (Figure 17). There was only an 8% increase ($p>0.05$) in the strength, which was insignificant (Figure 18). The addition of particulate fillers to FRC substrates showed no enhancements in the mechanical properties.

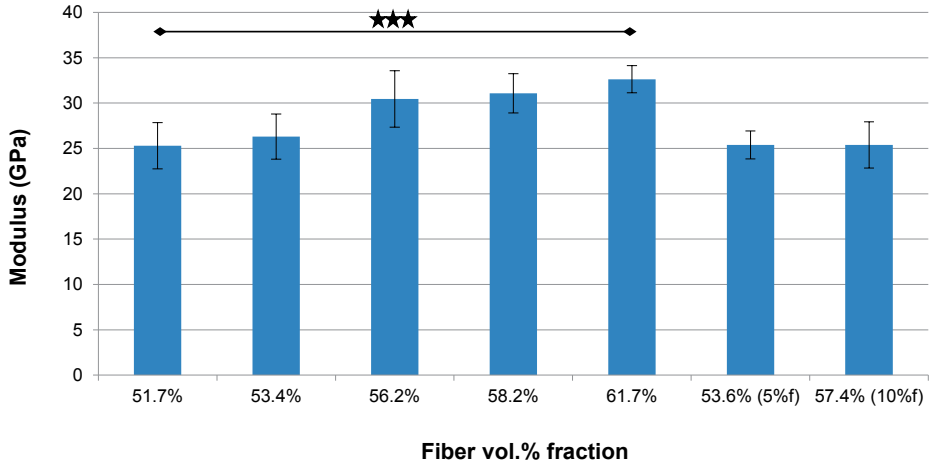

Figure 15 *Mean mechanical modulus and standard deviation of unidirectional E-glass fiber-reinforced composites with increasing fiber vol.% fraction (n=12). Groups with x%f in parenthesis contain particulate fillers. Significant difference (***$p<0.001$) among the groups. Adopted from original publication I.*

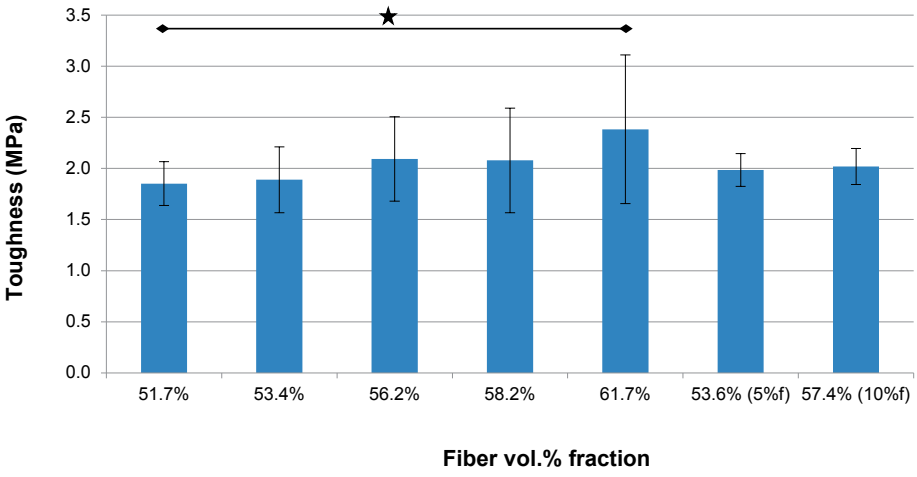

Figure 16 *Mean mechanical toughness and standard deviation of unidirectional E-glass fiber-reinforced composites with increasing fiber vol.% fraction (n=12). Groups with x%f in parenthesis contain particulate fillers. Significant difference (*$p<0.05$) among the groups. Adopted from original publication I.*

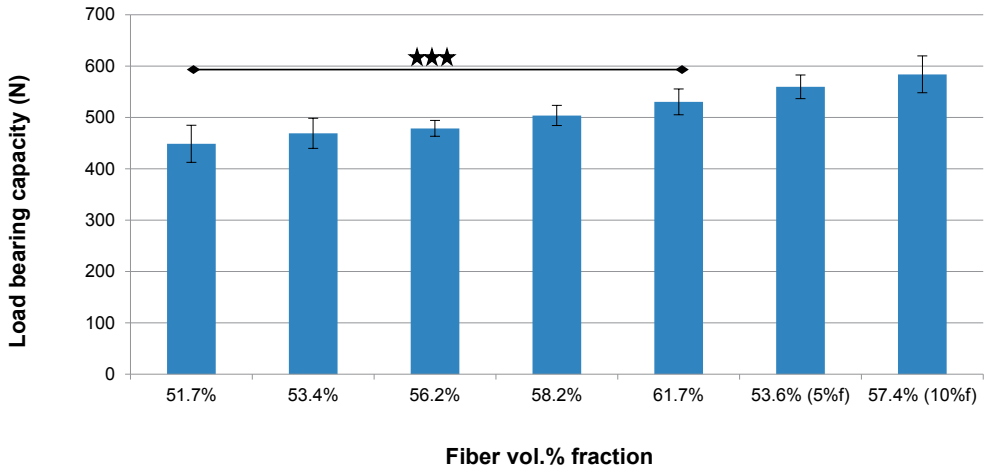

Figure 17 *Mean mechanical load bearing capacity and standard deviation of unidirectional E-glass fiber-reinforced composites with increasing fiber vol.% fraction (n=12). Groups with x%f in parenthesis contain particulate fillers. Significant difference (***p<0.001) among the groups. Adopted from original publication I.*

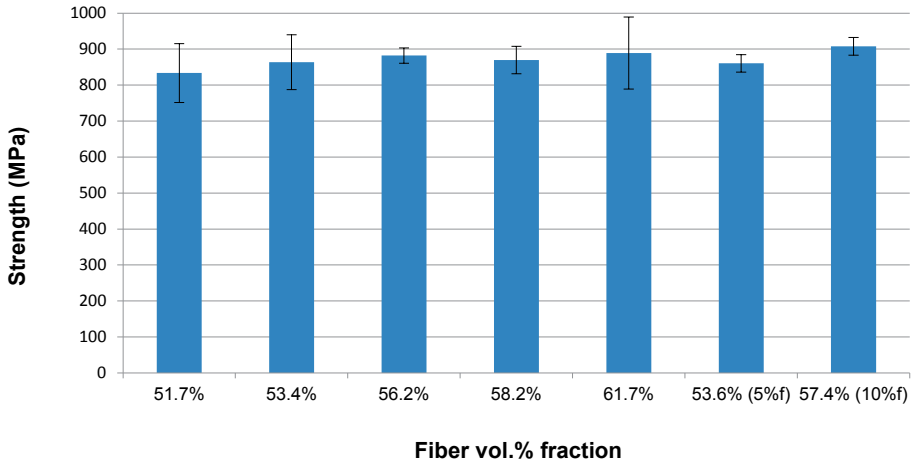

Figure 18 *Mean mechanical strength and standard deviation of unidirectional E-glass fiber-reinforced composites with increasing fiber vol.% fraction (n=12). Groups with x%f in parenthesis contain particulate fillers. Adopted from original publication I.*

The light microscopy analysis of FRCs after mechanical testing demonstrated that; the initial fracture pattern is characterized by a typical longitudinal matrix splitting in the vertical plane, while the final failure showed some visible signs of matrix transverse splitting (Figure 19 a and b).

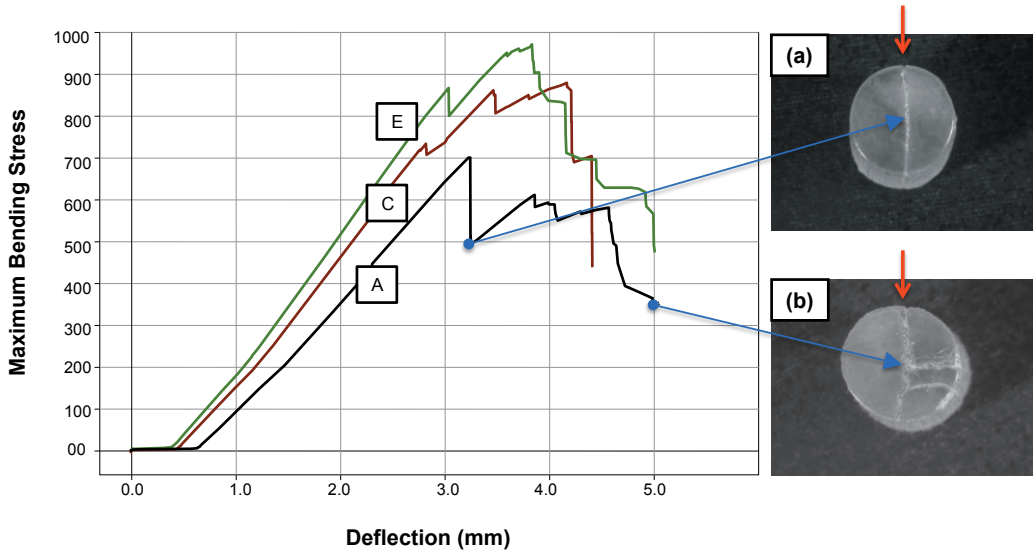

Figure 19 *Fracture modes or damage accumulation in stress-deflection curve for unidirectional E-glass fiber-reinforced composites (FRCs): A (i.e., 7 bundles); C (i.e., 8 bundles); and E (i.e., 9 bundles). Cross-section microphotographs of FRC substrate revealing typical fracture patterns: (a) initial fracture and (b) final fracture. Red arrows indicate direction of loading force. Adopted from original publication I.*

5.2. Roughness and imaging characterization (II and III)

In study II, the R_a values of the substrates investigated are presented in Table 5. All surfaces showed R_a of less than 0.1 µm. The confocal profiler 3D observations of the substrates after smooth polishing are displayed in Figure 20.

Table 5 *Mean values and standard deviations (SD) of surface roughness measurements.*

Groups	Mean roughness (R_a), µm (SD)	
	Photo polymerized	Post-polymerized by heat
FRC with in-plane oriented fibers	0.061 (0.013)	0.037 (0.008)
FRC with transversely oriented fibers	0.024 (0.003)	0.018 (0.004)
Plain polymer: BisGMA-TEGDMA (50%–50%)	0.006 (0.001)	0.008 (0.001)

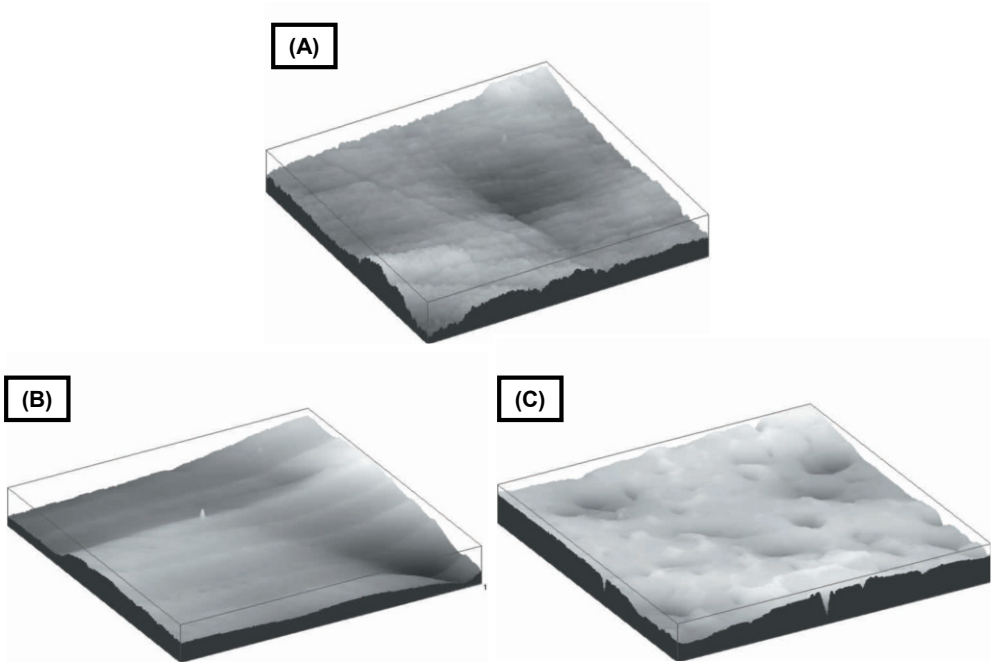

Figure 20 *Confocal profiler 3D images of the substrates investigated: (A) Plain polymer; (B) FRC with in-plane oriented fibers; and (C) FRC with transversely oriented fibers. Adopted from original publication II.*

In study III, the R_a/S_a for plain polymer and FRC substrates were (0.03 ± 0.009 μm)/(0.04 ± 0.003 μm) and (0.05 ± 0.02 μm)/(0.06 ± 0.015 μm), respectively. The difference in the surface roughness parameters between the substrates types was considered insignificant ($p>0.05$). The FE-SEM surface topographical observations are demonstrated in Figure 21. The surfaces displayed smooth characteristics with some grinding and polishing grooves spread over the surface.

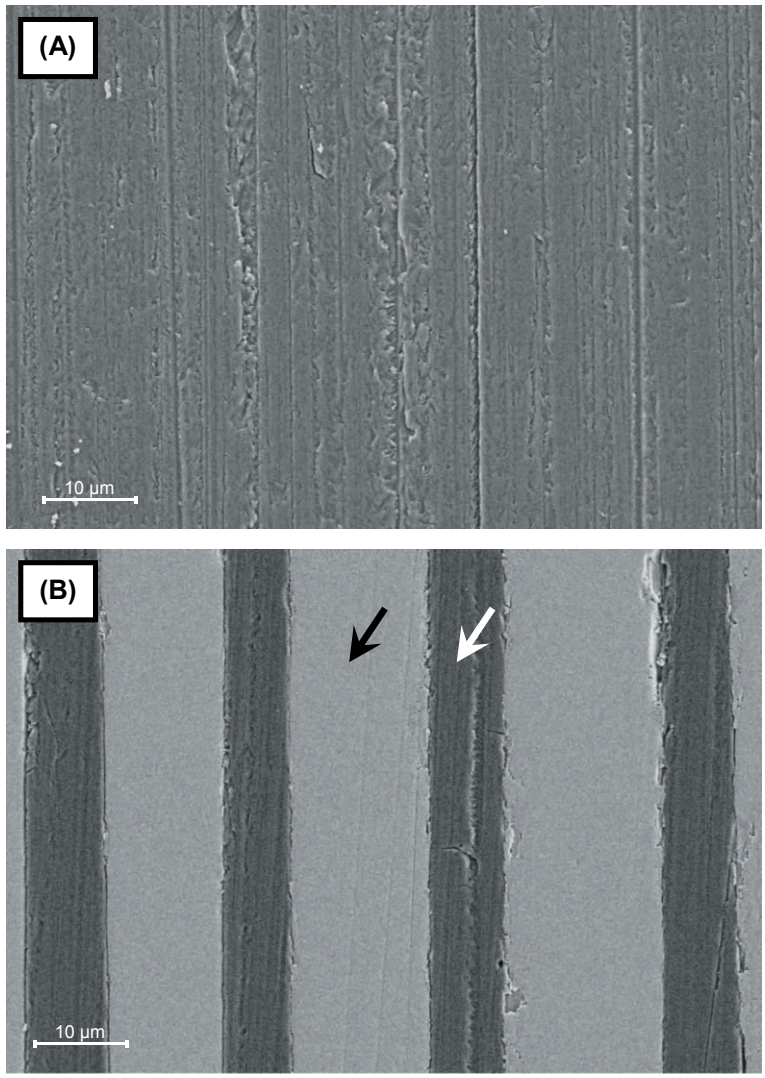

Figure 21 *Scanning electron micrographs of the substrates investigated: (A) Plain polymer and (B) fiber-reinforced composite. The black arrow in (B) indicates E-glass fiber and the white arrow in (B) indicates polymer matrix. Adopted from original publication III.*

5.3. X-ray Diffraction analysis (III)

The XRD of the substrates are displayed in Figure 22. The results exhibited only broad bands that are characteristic of an amorphous state (i.e., there was no sign of crystallization). Both spectra showed a peak centered at 44.6°, related to the aluminum sample holder.

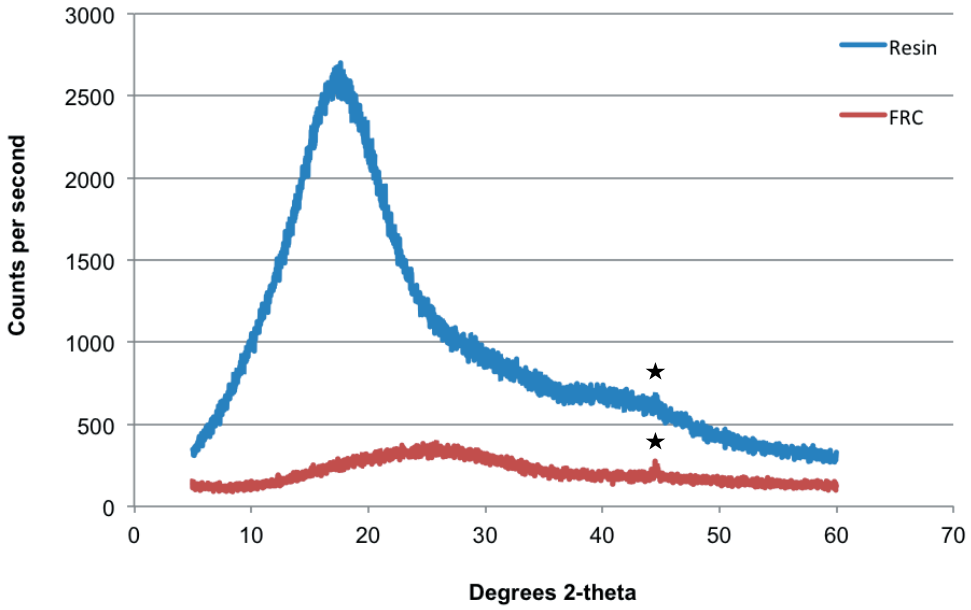

Figure 22 *XRD spectra of the plain polymer and fiber-reinforced composite substrates. The peaks marked by asterisks are attributed to the aluminum sample holder. Adopted from original publication III.*

5.4. Surface wettability (II)

5.4.1. Contact angle measurements

FRCs are hydrophilic materials that exhibit good wettability characteristics. Table 6 shows the equilibrium contact angles values obtained from the surfaces investigated after mechanical polishing to obtain a minimum roughness.

Table 6 *Mean values and standard deviations (SD) of contact angle measurements.*

Groups	Contact angle, degrees (SD)					
	Photo polymerized			Post-polymerized by heat		
	Water	Diiodomethane	Formamide	Water	Diiodomethane	Formamide
FRC with in-plane oriented fibers (perpendicular view)	60.0 (1.4)	45.9 (0.6)	41.0 (1.3)	50.0 (1.0)	44.9 (1.0)	43.4 (0.8)
FRC with in-plane oriented fibers (parallel view)	69.0 (1.3)	48.0 (0.9)	51.0 (1.2)	65.8 (1.1)	47.1 (0.6)	49.3 (0.9)
FRC with transversely oriented fibers	54.3 (0.9)	44.6 (0.5)	39.4 (0.3)	52.0 (1.5)	43.2 (0.7)	39.8 (0.8)
Plain polymer: BisGMA-TEGDMA (50%–50%)	70.2 (1.0)	39.8 (0.6)	49.8 (1.4)	65.6 (1.4)	36.7 (0.6)	47.9 (0.5)

The contact angle values varied on the same FRC surface according to the alignment of E-glass fibers (Figure 23).

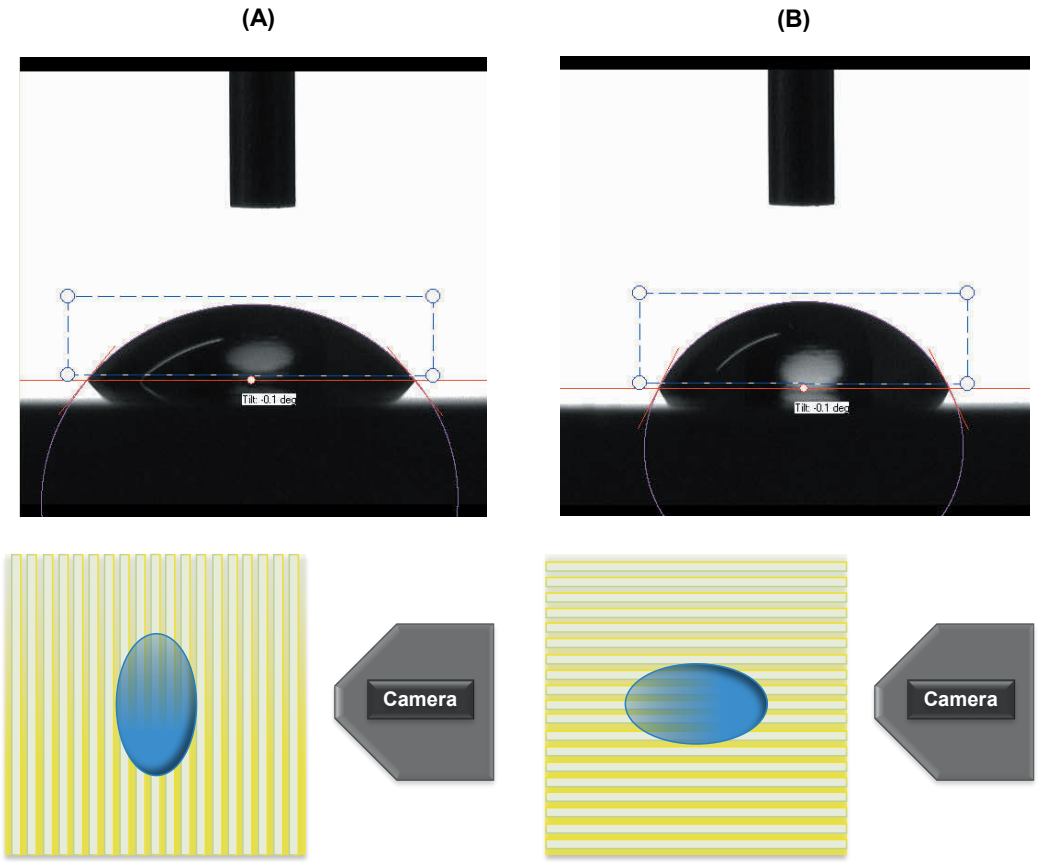

Figure 23 *Water contact angle measurements on fiber-reinforced composites: (A) Fibers running in-plane (perpendicular) to the camera axis and (B) Fibers running in-plane (parallel) to the camera axis.*

5.4.2. Surface free energy calculations

FRCs had better SFE components than plain polymer substrates. For the FRC materials (Figure 24), the surface with transverse distribution of fibers showed higher polar (γ^P) and total SFE (γ^{TOT}) components than the surface with in-plane distribution of fibers ($p<0.001$).

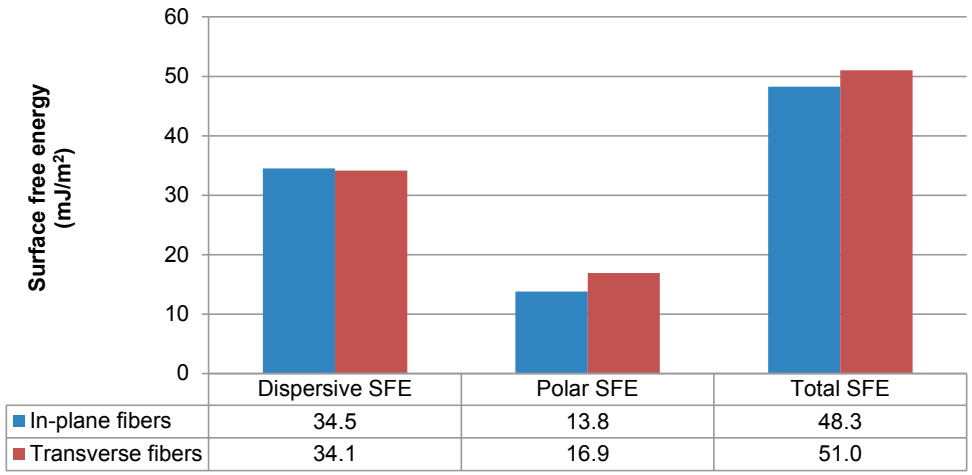

Figure 24 *Dispersive (γ^D), polar (γ^P), and total (γ^{TOT}) components of surface free energy for fiber-reinforced composites calculated using the Owens-Wendt approach. Adopted from original publication II.*

Furthermore, the SFE calculations demonstrated different values on the same FRC surface according to E-glass fibres alignment (Figure 25).

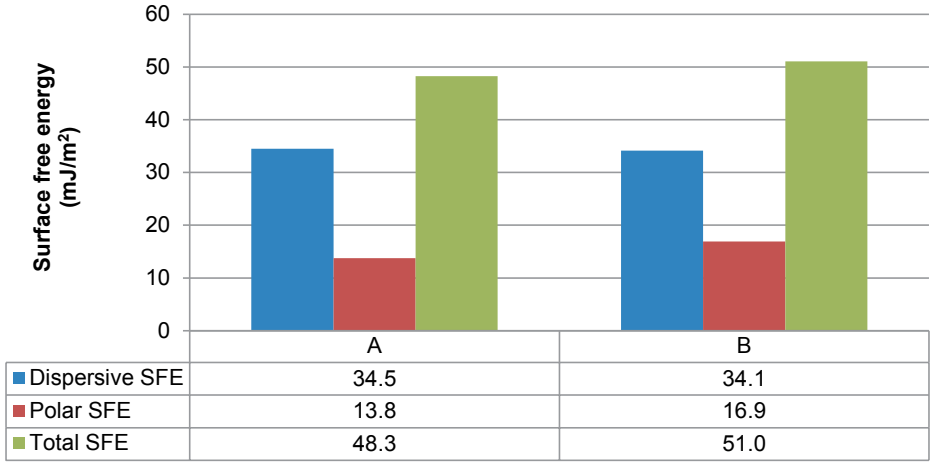

Figure 25 *Dispersive (γ^D), polar (γ^P), and total (γ^{TOT}) components of surface free energy for fiber-reinforced composites calculated using the Owens-Wendt approach: (A) Fibers running in-plane (perpendicular) to the camera axis and (B) Fibers running in-plane (parallel) to the camera axis. Adopted from original publication II.*

Post-polymerization by heat enhanced the SFE components of the substrates ($p<0.001$). The DC% of the polymer phase of the composite materials was 89.1% ± 0.5%. The impact of the polymerization method on different components of SFE is shown in Figure 26.

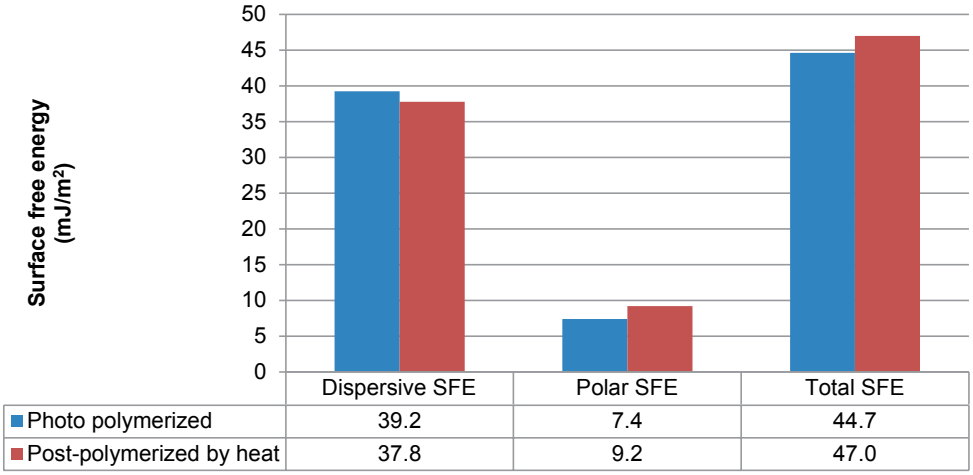

	Dispersive SFE	Polar SFE	Total SFE
Photo polymerized	39.2	7.4	44.7
Post-polymerized by heat	37.8	9.2	47.0

Figure 26 *Dispersive (γ^D), polar (γ^P), and total (γ^{TOT}) components of surface free energy for plain polymer substrates with different polymerization methods calculated using the Owens-Wendt approach. Adopted from original publication II.*

5.5. Blood response (III)

5.5.1. Blood-clotting

Figure 27 displays the blood-clotting profiles for plain polymer and FRC substrates. The total clotting time for FRC substrate was approximately 30 min compared to 50 min for plain polymer substrate, indicating faster blood-clotting ability of the former ($p<0.001$). Figure 28 displays the digital photographs of plain polymer and FRC substrates after 10–60 min of contact-time with blood.

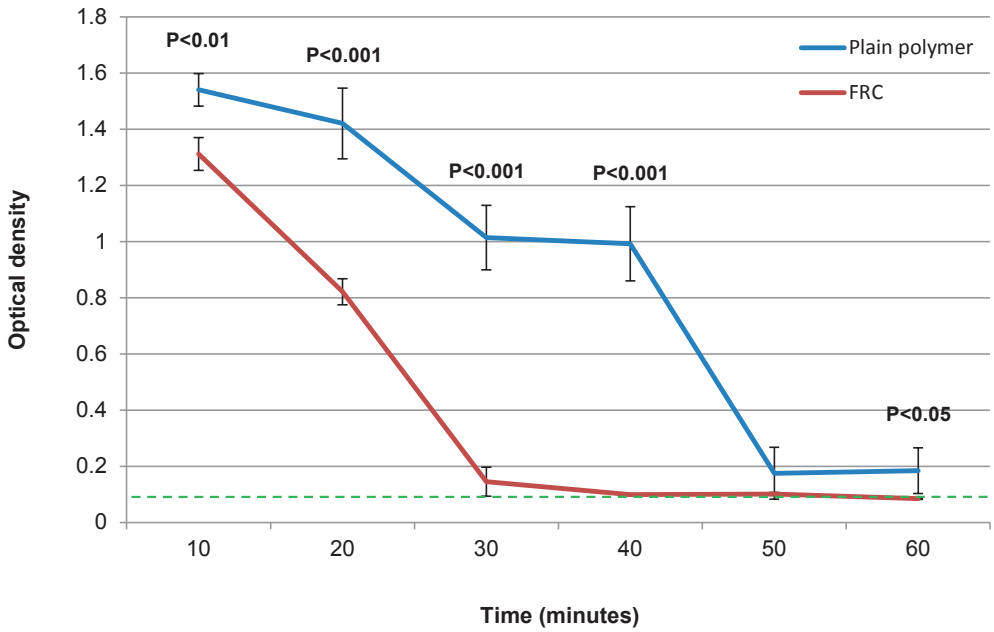

Figure 27 *Blood-clotting profiles for plain polymer and fiber-reinforced composite surfaces, showing the optical density versus time. Blood is considered completely clotted at an absorbance of 0.1. Data are presented as mean ± standard deviation (n=4). Significant differences between the substrate types at same time-point are indicated.*

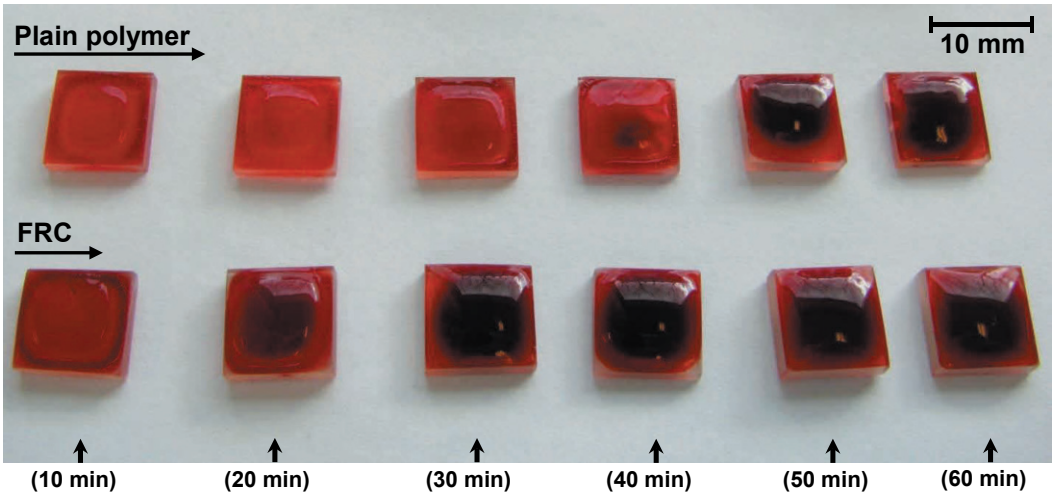

Figure 28 *A digital photograph of plain polymer and fiber-reinforced composite (FRC) substrates after 10, 20, 30, 40, 50, and 60 min of blood/surface contact. Significant blood clot formation is shown on FRC substrates. Adopted from original publication III.*

5.5.2. Platelets adhesion and morphology

Figure 29 displays the platelets morphology after 1 h adhesion period. The platelets attached to both substrate types. Nevertheless, platelets activation and aggregation were more pronounced, qualitatively, on FRC substrates than on plain polymer substrates.

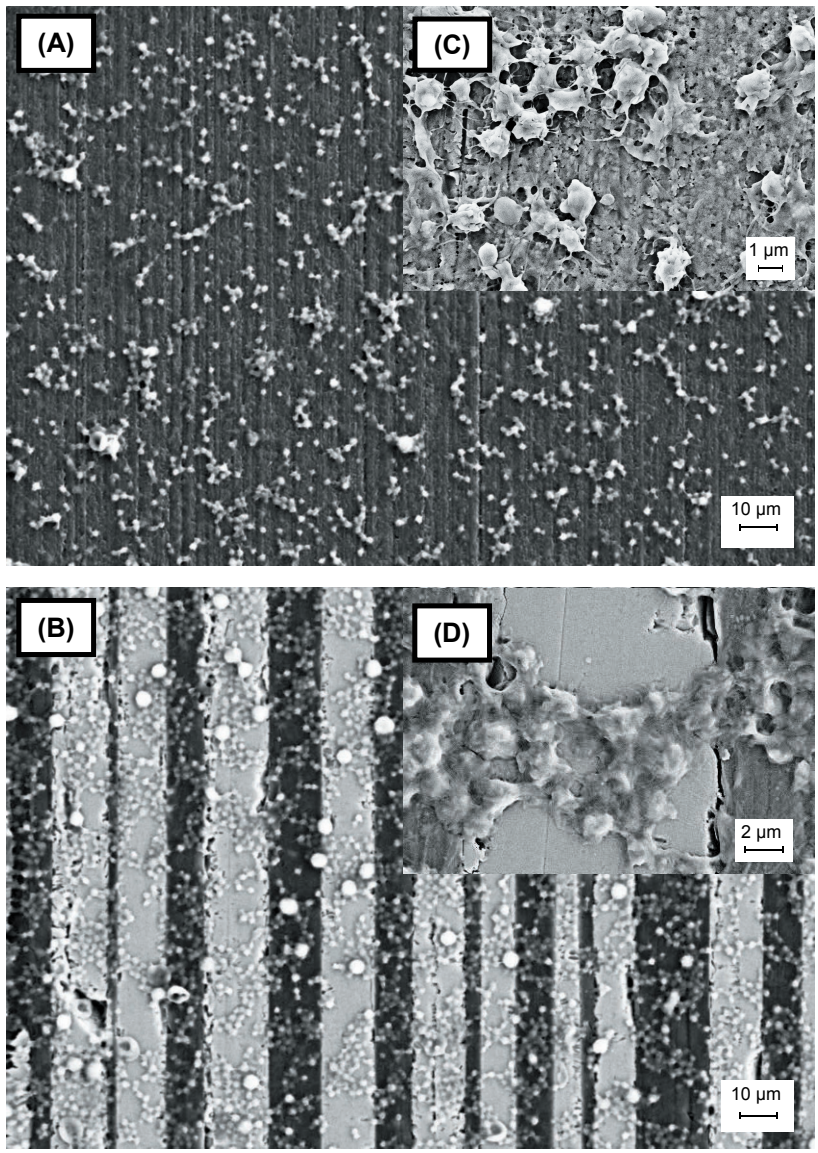

Figure 29 *Scanning electron micrographs of platelets morphology after 1 h adhesion period on the substrates investigated: (A) Plain polymer and (B) fiber-reinforced composite. Inner images (C and D) are the high magnification of (A and B), respectively. Adopted from original publication III.*

5.6. Cell culture experiments (III)

5.6.1. Adhesion kinetics (III)

Incubation times from 1 to 24 h were used to evaluate the amount of adhered human gingival fibroblasts on plain polymer and FRC substrates (Figure 30). Significant differences at 1, 6, and 24 h time-points were observed between the substrate types ($p<0.01$, $p<0.01$, and $p<0.001$, respectively). Furthermore, the amount of adhered cells increased significantly on the FRC substrates throughout the experiment ($p<0.01$, $p<0.001$, and $p<0.001$, respectively), whereas the only significant increase ($p<0.001$) for plain polymer substrates was seen by 24 h.

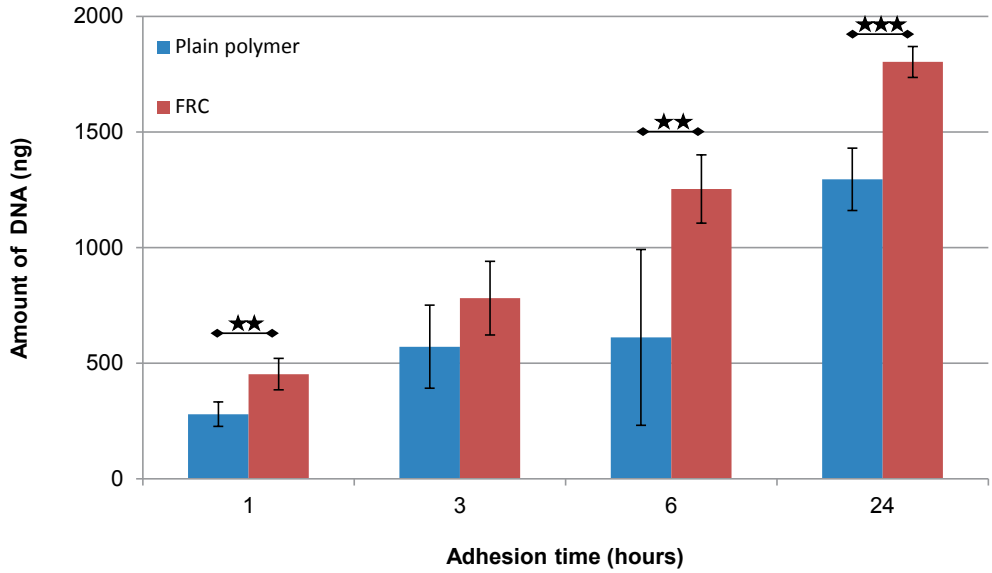

Figure 30 *The amount of DNA released from the plain polymer and fiber-reinforced composite (FRC) surfaces from 1 to 24 h of fibroblasts adhesion. Data are presented as mean ± standard deviation (n=5). Significant differences (**p<0.01 and ***p<0.001) between the substrate types at same time-point. On FRC substrates the amount of DNA increased significantly between all time-points (p<0.01, p<0.001, and p<0.001, respectively), while on plain polymer substrates the amount of DNA only increased significantly from 6 to 24 h (p<0.001).*

5.6.2. Adhesion strength (III)

The strength of human gingival fibroblasts attachment was assessed after 6 h of adhesion on plain polymer and FRC substrates. Fibroblasts cell detachment was relatively easier from the plain polymer substrates following agitation and gentle trypsinization at room temperature. The detachment curve revealed that, in 20 min, the cumulative cell detachment on plain polymer substrates was 70% ± 5% (Figure 31), comparing to 59% ± 5% on FRC substrates, indicating stronger cell adhesion on the latter ($p<0.01$).

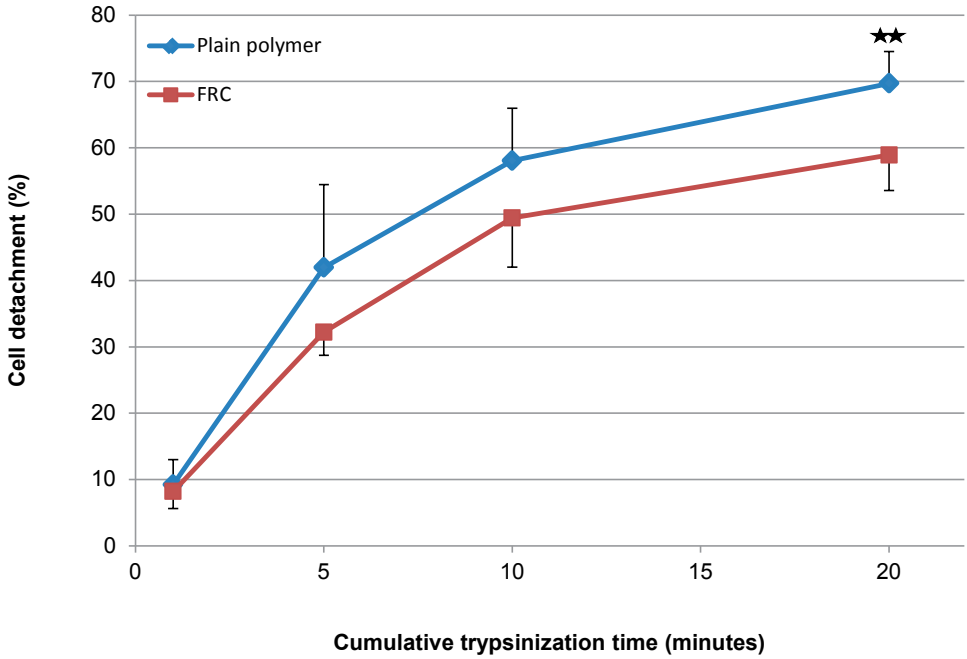

Figure 31 *The cumulative amounts of fibroblasts detached from the plain polymer and fiber-reinforced composite substrates after 1 to 20 min of serial trypsinization. Data are presented as mean ± standard deviation (n=6), and normalized to the total amount of attached cells after 6 h of adhesion. Significant difference (**p<0.01) between the substrate types at same time-point.*

5.6.3. Cell proliferation (III)

Human gingival fibroblasts were cultured for 7 d on plain polymer and FRC substrates (Figure 32). Both substrate types showed similar amount of cell adhesion, approximately equal to 50% seeding efficiency (data not shown). Fibroblasts cell proliferation rate was significantly higher on FRC than on plain polymer substrates ($p<0.01$ to $p<0.001$) from day 3 onwards. Throughout the culture period, both substrate types showed significant increases ($p<0.001$) in cell proliferation rates, except for the plain polymer substrates from 1 d to 3 d, where the increase in proliferation rate was statistically insignificant.

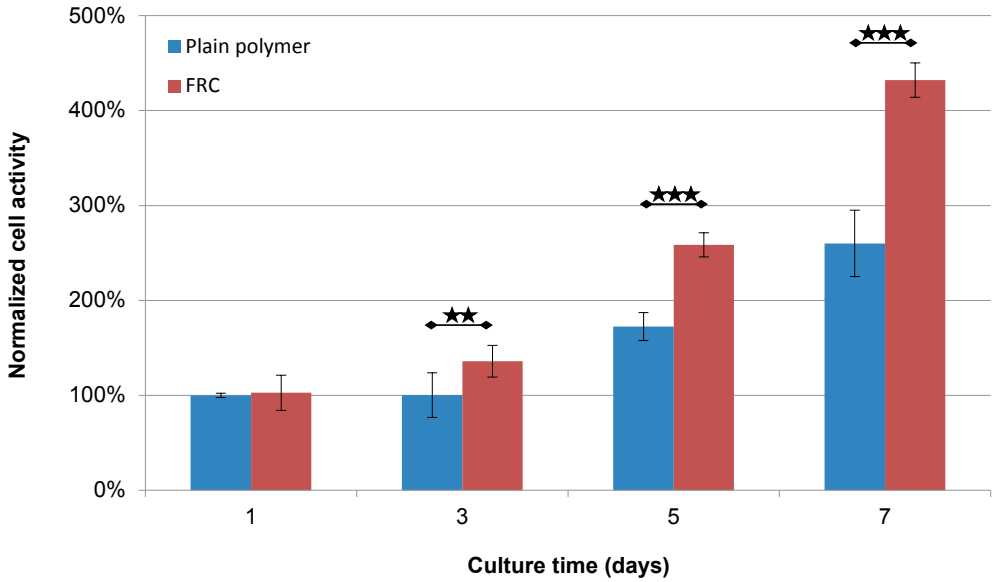

Figure 32 *Proliferation of human gingival fibroblasts on plain polymer and fiber-reinforced composite substrates. The reduction of AlamarBlue™ reagent with plain polymer substrate at 1 d time-point was set to 100%. Data are presented as mean ± standard deviation (n=6). Significant differences (**p<0.01 and ***p<0.001) between the substrate types at same time-point.*

5.6.4. Confocal fluorescence microscopy (III)

Figure 33 displays the confocal fluorescence microscopic image of FRC substrate after 3 d of *in vitro* culture. The fibroblast cells appeared to orient themselves parallel to the direction of E-glass fibers. Unfortunately, no images were taken for the plain polymer substrates due to the high background signals.

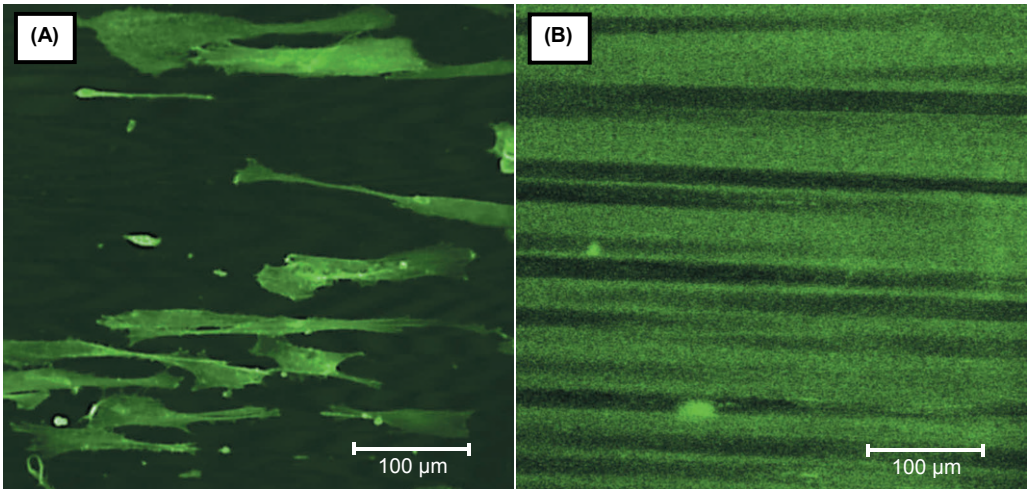

Figure 33 *(A) Confocal fluorescence micrograph of fibroblasts on fiber-reinforced composite (FRC) substrate after 3 days of in vitro culture. (B) FRC surface autofluorescence underneath the fibroblast layer. Position and orientations are identical in (A) and (B). Adopted from original publication III.*

5.7. Tissue culture (IV)

The histologic appearance of porcine gingival explants demonstrated a well-differentiated stratified squamous oral epithelium with fibroblasts cells distributed in the connective tissue layer (Figure 34). Under light-microscopic examination, the overall structure of the gingival tissue was intact and remained so throughout the culture period whereby the epithelial and connective tissue established an immediate close contact with both implants types indicating a good biocompatibility (Figure 35). The epithelial cells migrated and leaned against the implant surface forming a simple nonkeratinized and firm epithelial structure (i.e., lack of gap between the implant and the explant). On FRC implants, the epithelium tended to migrate outward along the FRC surface forming a long epithelial lining. Additionally, connective tissue fibers along the implant-connective tissue attachment seemed to be more pronounced in samples with FRC implant than in samples with plain polymer implants (Figure 36). No signs of infection were detected in tissue cultures over the entire incubation period. The control tissue cultures (i.e., with no implanted biomaterials) remained structurally viable as observed by light-microscope (data not shown). Nevertheless, there were signs of detachment of the keratinized outer layer of the epithelium as well as connective tissue degeneration during the culture period.

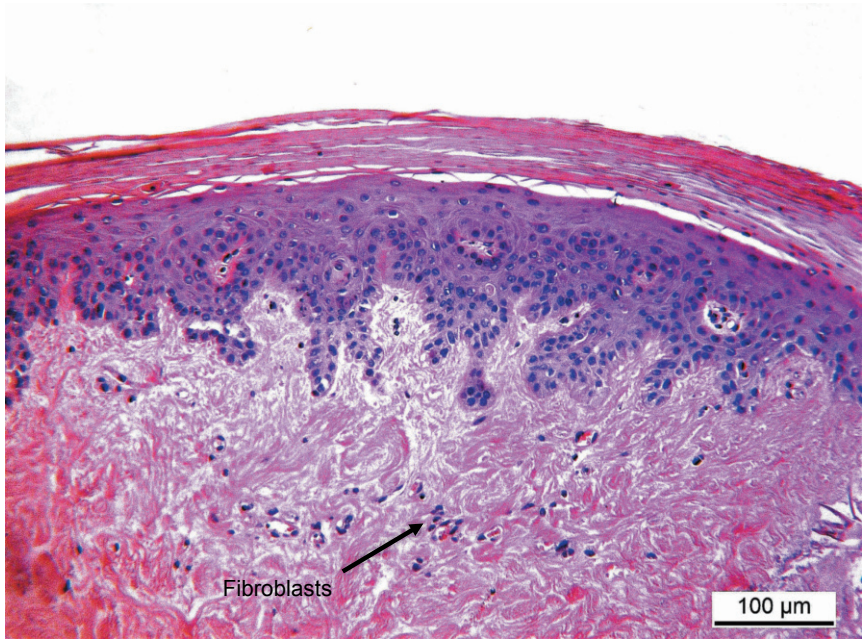

Figure 34 *Hematoxylin and eosin stained porcine gingival mucosa showing a well-defined parakeratinized stratified squamous epithelial layer with fibroblasts scattered in the connective tissue layer.*

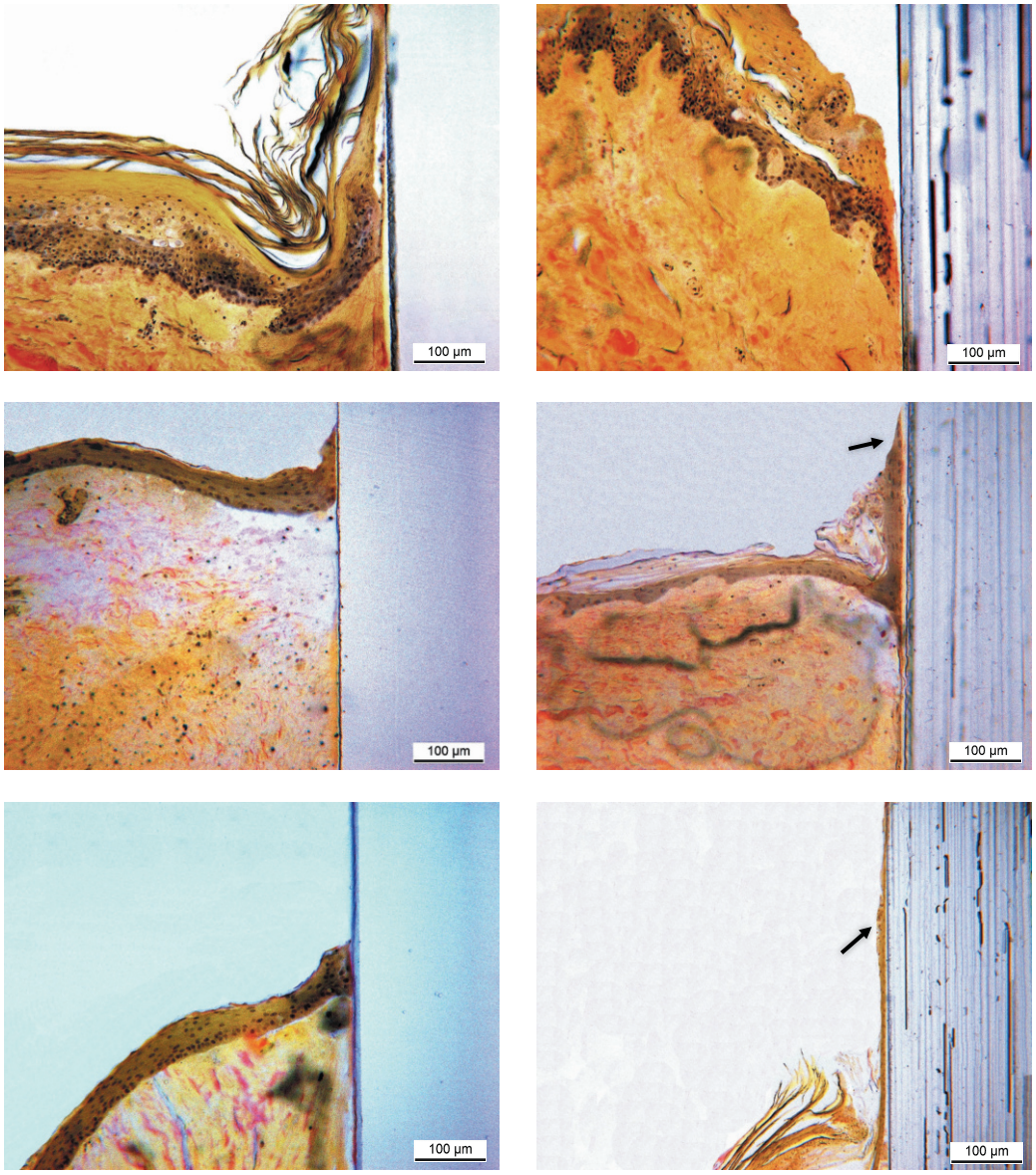

Figure 35 *Van Gieson stained sections of porcine gingival explants attached to plain polymer and fiber-reinforced composite (FRC) implants. Upper row: after 4 days of in vitro culture. Middle row: after 10 days of in vitro culture. Lower row: after 14 days of in vitro culture. Epithelial migration is visible on FRC implants (black arrows).*

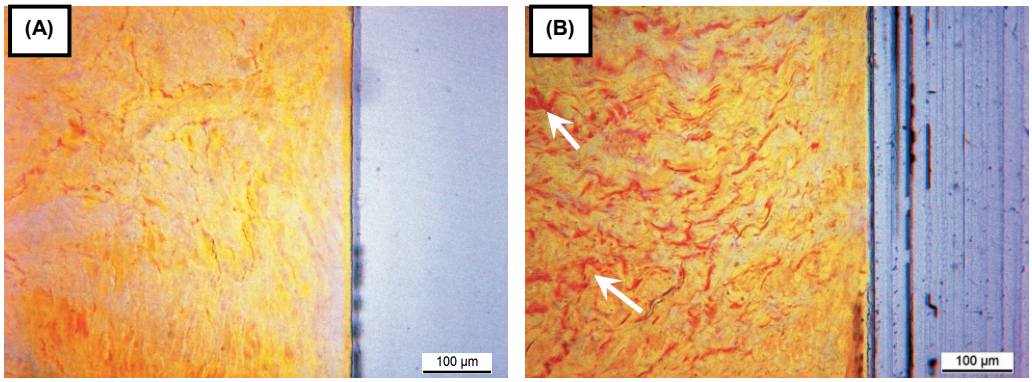

Figure 36 *Van Gieson stained sections of porcine gingival explants attached to: (A) plain polymer and (B) fiber-reinforced composite (FRC) implants after 10 days of in vitro culture. White arrows indicate the noticeable connective tissue fibers along the implant-connective tissue attachment.*

6. DISCUSSION

6.1. General discussion

This series of *in vitro* studies aimed at evaluating BisGMA-TEGDMA based glass fiber-reinforced composites in terms of mechanical properties, surface wettability, hemocompatibility, cytocompatibility, and gingival tissue attachment in an attempt to introduce a new non-metallic oral implant abutment material. The studies presented in this thesis were specifically designed to evaluate the effect of E-glass fibers on the above-mentioned material features. Therefore, the composites were not compared with traditional implant abutment materials, as these would not allow comparable surface modifications. Comparable studies will be done under loaded conditions in our future studies. The aims of the studies presented in this thesis were of interest due to the fact that FRC polymer implants have recently found their way into surgical applications as dental, orthopedic, and especially cranial implants (Ballo, 2008; Mattila, 2009; Tuusa *et al*., 2007; Aitasalo *et al*., 2013). Nevertheless, there is no information available on the soft tissue integration to FRC materials; hence, this series of studies was designed to clarify some aspects on the potential use of FRC in oral implantology.

The mechanical properties of FRCs have been investigated extensively (Vallittu, 1998a; Chong & Chai, 2003; Ballo *et al.*, 2007; Ballo *et al*., 2008a). FRCs exhibit comparable mechanical behaviors with regard to titanium. Study I was conducted to optimize FRCs using high E-glass fiber volume fractions. The fiber content that offered optimal mechanical properties for anchoring devices (i.e., oral implant abutments) was selected and used accordingly in preparing the experimental substrates for the following studies.

The biocompatibility of an oral implant material can be assessed by studying its mechanical, physical, and chemical properties (Wennerberg *et al*., 1995). It is well known that the initial surface events that follow implantation of a biomaterial into a living tissue control later biological reactions, which involve wetting by physiological liquids, adsorption of proteins, and migration and proliferation of cells (Davies, 1998).

Evaluation of the surface wettability of a biomaterial in terms of contact angle measurements is a predictive indicator of its cytocompatibility (Yanagisawa *et al.*, 1989). The surface free energy property of a biomaterial determines its surface wettability (Baier *et al.*, 1968), and subsequently influences the host reactions that occur at tissue/implant interface. Hence, study II was designed to investigate the possible role of exposed E-glass fibers on the surface wettability/energy behavior of BisGMA-TEGDMA polymer surfaces.

In studies II, III, and IV, the FRC and plain polymer surfaces were purposely polished in order to attain comparable smooth surface textures (i.e., $R_a > 0.1$ μm). Roughness alters the wettability characteristics of biomaterials. A smooth surface is recommended

when an implant surface is characterized in terms of surface energy, since the surface free energy is an indication of the surface tension of the solid surface rather than a measurement of surface topographical features (Ponsonnet *et al*., 2003).

The research logic in developing new biomaterials in implant dentistry starts from *in vitro* studies ending into *in vivo* studies. *In vitro* studies include mechanical characterizations, surface wettability evaluations, blood-clotting testing, cell culture experiments, etc. Accordingly in the study III, human gingival fibroblasts response in routine cell culture conditions was used to explore the biological properties and the tentative contact guidance of FRCs under *in vitro* conditions. Human gingival fibroblasts are commonly used in implant materials research. However, monolayer cell-culture models fail to completely replicate the complex three-dimensional native human oral mucosal tissue. Therefore, following the positive cellular response on FRCs in study III, the investigations were taken a step closer to *in vivo* conditions by evaluating FRC implants in a real tissue environment using porcine gingival explants (Study IV). However, *in vivo* soft tissue attachment occurs after complicated biological processes, thus further *in vivo* research is needed before any definitive conclusions can be drawn on the possible benefits of FRCs in implant dentistry.

The release of residual monomers from BisGMA-TEGDMA polymers could challenge the biocompatibility of polymer materials used as medical implants (MacDougall *et al.*, 1998). For this reason, polymer based implants require an optimum degree of monomer conversion. Approximately, a 90% degree of monomer conversion for polymer implants can be reached by following a certain polymerization protocol involving both photopolymerization and heat post-polymerization treatments at 120°C for 24 h (Ballo, 2008), which is near to the glass transition temperature (T_g) of the BisGMA-TEGDMA copolymer. This process creates an adequate thermal energy in the system to generate a free volume, which allows unreacted carbon-carbon bonds to create free radicals and subsequent reactions with each other. Furthermore, water immersion helps in enhancing the biocompatibility of polymer implants through the leaching process of residual monomers (Ferracane & Condon, 1990; Väkiparta *et al.*, 2006; Ballo, 2008). The findings of studies II and III are in agreement with earlier reports, showing that a high degree of monomer conversion results in improved surface wettability/energy and, subsequently, biocompatibility of polymer implants *in vitro*.

6.2. Mechanical properties of high density FRC (I)

Oral implants are mechanical devices designed to transfer occlusal forces through an abutment and implant to the surrounding bone tissue. Under functional conditions, oral implants are exposed to highly complex loads of varying directions, durations, and magnitudes (Brunski, 1988; Rangert *et al*., 1995; Richter, 1998); therefore, optimal mechanical properties are crucial for the long-term success. While the mechanical properties of unidirectional FRC follow the law of ratio of quantity of fibers and volume

of the polymer matrix. Still, little is known if that is valid when high fiber-density FRC is considered. Study I was designed to determine the modulus of elasticity, toughness, load bearing capacity, and strength of unidirectional high fiber-density FRCs using three-point bending test.

The mechanical properties of FRC depend on the fiber vol.% fraction in addition to many other factors such as impregnation of fibers, orientation of fibers, and adhesion of fibers to the polymer matrix (Vallittu & Narva, 1997; Vallittu, 1998b; Isaac, 1999; Behr *et al.*, 2000; Lassila *et al*., 2002). The results of study I showed that the mechanical properties of high fiber-density FRCs are also related to glass fibers vol.% fraction. In spite of that, higher fiber vol.% fractions did not effectively result into significant higher flexural strength values. Moreover, the addition of particulate fillers only improves the load bearing capacity of high fiber-density FRCs, showing no positive effects on other mechanical properties. This is likely due to the dominant effect of high fiber contents. The fiber vol.% fractions in the study I were higher than used by other authors: Mullarky 9.4 vol.% (Mullarky, 1985), Ruyter 13.2 vol.% (Ruyter *et al*., 1986), Yazdanie 14.8 vol.% (Yazdanie & Mahood, 1985), Vallittu 12.4–13.1 vol.% (Vallittu, 1998a; Vallittu & Narva, 1997), Behr 28.1 vol.% (Behr *et al*., 2000), 38.44 (Furtos *et al*., 2012), Goldberg 40 vol.% (Goldberg & Burstone CJ, 1992), or Lassila 45 vol.% (Lassila *et al*., 2002).

The fiber content of FRCs investigated in study I was quantified using combustion and gravimetric analyses. The limitation of these methods is that the findings do not demonstrate whether the fibers are homogenously distributed throughout the matrix or not. The fiber vol.% can also be quantified from a sectional view using optical image analysis. However, this method is considered to be inaccurate and technique-sensitive (Behr *et al*., 2000), since the sectional view of the fibers might look elliptical rather than circular if the fibers are not cut axially during preparation of the substrates. In addition, optical analysis may also show a surface without fibers. For these reasons, this method was not included in the current study.

The three-point bending test on anisotropic materials, such as unidirectional FRCs, is often used to determine the flexural properties of materials. The mode of failure of unidirectional FRCs in flexure is complicated. Craig and Courtney defined three modes of failure that can arise during characterizing FRC under tension (Craig & Courtney, 1975). The three failure modes are: instantaneous, statistical, and stepwise. Instantaneous failure occurs when a load causes a strain accumulation in a restricted area adequate to breakdown the composite structure. A strain concentration spread to a wide area may need additional load or elongation for continued fracture leading to what is termed as stepwise (more bending type) or statistical failure (a series of small intense fractures which recover before complete failure and require more load to progress). Analysis of the mode of failure can assist in better understanding on how and why failure occurs. Hence, accurate reporting should include information on when the fracture starts (initial fracture), how it advances, and when it ends (final fracture) (Herakovich, 1998). In study I, all FRCs investigated demonstrated an initial failure of matrix longitudinal splitting

with some visible signs of matrix transverse splitting as a final failure. The fracture pattern was comparable to that of the diametral tensile strength test through which the fracture occurs along the vertical plane (Anusavice, 2003). The fracture behavior can be explained as such: when the vertical compressive force along the side of the FRC material is applied, a tensile stress that is perpendicular to the vertical plane is developed, thus leading to a longitudinal splitting that passes through the center of the material. The mode of failure of the investigated FRCs was categorized as statistical with no obvious signs of catastrophic failure.

The current findings confirm earlier studies showing that the mechanical properties of FRCs are comparable to those of titanium implants and could be optimized to meet the particular needs of many clinical applications (Ballo, 2008; Mattila, 2009; Hautamäki, 2012). However, the clinical use of FRC in implant dentistry demands further research to consider the behavior of high fiber-density FRCs under cyclic loading conditions since successful oral implants should be capable of bearing not only static load, but also cyclic loads produced by the masticatory system.

6.3. Surface wettability behavior (II)

An important aspect in developing new biomaterials is evaluating the wettability behavior of the surface, in terms of contact angle measurements and surface energy calculations. This strongly influences the physiological events that occur upon implantation (Baier *et al.*, 1984; Mekayarajjananonth & Winkler, 1999; Eriksson *et al.*, 2004; Kennedy *et al.*, 2006; Schwarz *et al.*, 2007). In some animal experiments involving FRC implants, the exposed E-glass fibers on the surface of implants yielded a positive bone response (Ballo *et al.*, 2009; Mattila, 2009). This might be related to the wettability characteristics of FRC surfaces. However, there is lack of information regarding the impact of exposed E-glass fibers on the wettability behavior of polymer surfaces. Hence, study II was designed to investigate the influence of exposed glass fibers on the wettability properties of FRC surfaces.

The effect of surface roughness on the contact angles observations that subsequently reflects on SFE calculations has been reviewed extensively (Busscher *et al*., 1984; Hallab *et al*., 2001; Ponsonnet *et al*., 2001). Surface roughening is possibly counted for the contact angle hysteresis on rough surfaces (R_a > 0.1 μm), whereas the remaining hysteresis on the smooth surfaces (R_a < 0.1 pm) is produced by surface chemical heterogeneity (Busscher *et al*., 1984). In study II, the surfaces exhibited smooth topographies (R_a < 0.1 μm); thus, the influence of surface roughness can be disregarded. Moreover, surface roughness has no effect on the observed contact angles if the static contact angle on the smooth polymer surface (R_a < 0.1 μm) is between 60° and 86° (Busscher *et al*., 1984). Accordingly, most of the unidirectional FRC surfaces in the current study demonstrated water contact angle values within this given range.

A contact angle measurement at the liquid-solid interface is a commonly used approach to study the wettability of solid surfaces. The resultant values are determined by surface energy, topography, and cleanliness of the solid substrate and the surface tension of the liquid (Rame & Garoff, 1996). The SFE results were calculated from contact angle values measured using three different types of liquids: hydrogen bonded (Water); polar (Diiodomethane); and purely non-polar (Formamide). Unidirectional FRCs are considered as moderately hydrophilic polymer surfaces, with water contact angles values within a range of 50°–70°. This, in general, suggests positive cellular responses (Andrade, 1973).

The most striking finding was that the contact angle measurements on smooth FRC surface are dependent on the orientation of E-glass fibers (i.e., perpendicular or parallel to camera's axis). On the FRC surface with fibers running in-plane perpendicular to the axis of the camera, the water contact angles were lower than those on FRC surface with fibers running in-plane parallel to the axis of the camera. This can be related either to the role of surface roughness or surface energy of the substrate. However, since smooth surface topographies were considered in the experiment, this phenomenon can be interpreted to a great extent by the fact that FRC surface is characterized by the presence of different hydrophilic zones represented by E-glass fibers and polymer matrix. Therefore, certain pathways of different surface free energies can be established on the same surface and may cause the water drops to spread along the surface. This multi-hydrophilic principle is of great importance in biomaterial engineering and must be considered in future research because the part of oral implant that comes into contact with soft tissue is recommended to be smoother than that part adjacent to bone tissue. Thus, having a smooth surface with the ability to guide cells' growth would definitely address many current peri-implant problems.

In previous studies, the glass fibers' orientation influences many properties of FRCs - optical, thermal, and mechanical properties (Tezvergil *et al*., 2003; Dyer *et al*., 2004; Antilla *et al*., 2008). Similarly, the current findings show that surface wettability is dependent on the orientation of exposed E-glass fibers. The anisotropic nature of FRC in terms of wettability represents, in fact, an important observation that should be carefully considered when designing FRC devices implanted in living tissues.

In order to investigate the effect of fiber-density on the surface wettability behavior of FRC-implants, three groups of unidirectional FRCs with increasing fiber vol.% fractions from study I were selected and analyzed (groups A, C, and E, respectively). Increasing the fiber vol.% fraction resulted in a linear increase in the polar component (γ^{P}) and a linear decrease in the dispersive component (γ^{D}); this maintained the total component of SFE (γ^{TOT}) at the same order of magnitude for all FRC surfaces.

In the case of FRCs, hydroxyl groups cover the exposed E-glass fibers. Hydroxyl-covered substrate or parts of it in the case of composite is the most likely reason for good surface wettability behavior. Hydroxylated glass surfaces are also used in adhering the glass fibers to the polymer matrix through silane coupling agents (Vallittu, 1997a).

6.4. Blood response (III)

The interactions of the blood system with the implant material are of decisive importance in defining implant's usability (Hong *et al.*, 1999; Park & Davies, 2000; Davies, 2003). The clotting blood represents a natural scaffold, intermediating the living tissue and the foreign implant material (Park *et al*., 2001). This separates the implant surface from the external environment and acts as a barrier to a possible bacterial infection. Simultaneously, fibrin clot functions as a provisional matrix allowing epithelial and fibroblast migration towards the implant surface (Larjava, 2012). Therefore, the hemocompatibility of implant materials or surface treatments should be addressed in the preclinical evaluations of newly developed biomaterials. Hence, study III was intended to evaluate blood response to unidirectional FRC surfaces in terms of blood-clotting ability and platelet adhesion morphology.

The optical density (OD) of hemolyzed blood solution changes with time, a lower OD value implies lower hemoglobin concentration in the whole blood solution that, in turn, indicates more extensive thrombus formation on the substrate surface. In general, the time at which the optical density corresponds to 0.1 can be defined as the clotting time (Sharma, 1984). In the current study, the OD values for FRC substrates declined rapidly upon contact with blood compared to plain polymer substrates. Thus, the clotting time results indicate that the presence of exposed E-glass fibers clearly enhance the blood-clotting ability on a composite surface.

Platelet adhesion, spreading, and aggregation are markers of platelets activation (Heijnen *et al.*, 1999). Platelets activation is essential for the later formation of thrombus. According to the criteria described by Goodman *et al.* (Goodman *et al.*, 1984), the activated patterns of the adherent platelets can be categorized into five different groups: (a) discoid or round; (b) dendritic; (c) early pseudopodial, spread dendritic; (d) intermediate pseudopodial, spreading; and (e) fully spread. Consequently, in study II, the platelets on plain polymer surface were morphologically in a low activated state (i.e., dendritic), whereas the platelets on FRC were in higher activated state (i.e., intermediate pseudopodial, spreading). The main reason behind the superior blood-clotting and higher platelet activity of FRC surfaces is owed to the higher surface wettability characteristics of FRC surfaces, as there is a complex dependence between platelet adhesion and surface wettability/energy. However, further investigation of platelet activation at a molecular level is needed for a detailed understanding.

6.5. Cell response (III)

The process of adhesion and proliferation of cells on a biomaterial surface is crucial for its biocompatibility in living tissues (Hallab *et al*., 1995). This is closely related to the surface properties of biomaterials including surface chemistry, topography, and energy/wettability. Study III was planned to evaluate fibroblasts response to unidirectional FRC surfaces in terms of adhesion kinetics, adhesion strength, and cell proliferation rate.

Incubation times from 1 to 24 h were used to evaluate the initial adhesion of human gingival fibroblasts on plain polymer and FRC substrates. The quantitative DNA measurement revealed higher cell adhesion kinetics on FRC substrates compared to plain polymer already after one hour and the differences were clear over the whole incubation period. In spite of that, the amount of adhered cells was greatly increased on both substrate types by 24 h. The difference after one hour was caused by the higher initial cell adhesion on FRC substrates, while the increase in the cell amount thereafter could be due to the onset of cell proliferation. Blocking the cell proliferation by protein synthesis inhibitor would have given more reliable data on real initial adhesion between the substrates. However, initial adhesion experiment indicated biocompatibility of both materials.

The strength of human gingival fibroblasts attachment was assessed after 6 h of adhesion. In agreement to the adhesion kinetics findings, FRC surfaces exhibited stronger adhesion strength against enzymatic detachment. Similar to the enhanced blood compatibility on FRCs, this could also be related to the higher SFE that is known to have a strong effect on wetting, adsorption, and cell adhesion behaviors (Ponsonnet *et al.*, 2003). In study II, the surface wettability data showed that composites with exposed E-glass fibers generally possess better SFE components than plain polymer surfaces. Specifically, the polar component (γ^P) of SFE was better and is believed to be the most important determinant of cellular adhesion strength (Hallab *et al.*, 2001). Additionally, a relationship between the fractional polarity (FP) [$\gamma^P/(\gamma^P + \gamma^D)$] of biomaterials surfaces and adhesion, spreading, and growth of the cultured cells exists (Schakenraad *et al.*, 1986; Ponsonnet *et al.*, 2003). It was concluded that the peak cytocompatibility of fibroblasts could be achieved when the FP is equivalent to 0.3. In accordance with that, the FP calculated on FRC surfaces was 0.3, however it was 0.2 for the plain polymer surfaces.

The osteoblast response on FRC materials was studied earlier in a cell culture condition (Ballo *et al*., 2008b). In that study, many different kinds of FRC substrates with or without bioactive glass surface modifiers were analyzed and compared with commercial pure titanium. It was found that the cultured cells proliferated on all different FRC surfaces in a similar manner to that of titanium, indicating that BisGMA-TEGDMA FRC polymers are cytocompatible materials with a potential to stimulate osteoblast interactions and promote bone bonding. In the case of oral implants, the creation of a firm and healthy connective tissue cuff around implant abutments depends to a great degree upon the adhesion, proliferation, and colonization of fibroblastic cells. Thus, human gingival fibroblasts were cultured for 7 d on plain polymer and FRC substrates. The cell proliferation rate for both substrate types increased with time throughout the experiment. Within the first day of culture, there was no significant difference between the proliferation rates of both surfaces investigated. However, from day 3 onwards, the proliferation rate was constantly higher on FRC surfaces, and this better fibroblast response may reflect either a higher activity per cell or higher number of cells. Further studies on measuring gene and protein expression profiles are required for a better understanding of cellular metabolic activity on FRC surfaces.

The morphology of fibroblasts cultured on FRC substrates after 3 d of culture was evaluated using confocal fluorescence microscope. The phenomenon through which the cells can adapt and align on a substrate surface microtopography is described in terms of the theory of contact guidance. Study III's findings suggest that fibroblasts on FRC substrates show some degree of contact guidance whereby the cells tended to spread in certain directions on the FRC's anisotropic multi-hydrophilic surface. However, further investigations to confirm this finding are necessary since many factors could play a role in this process (e.g., the glass fiber type and diameter, inter-fiber distance, and type of polymer used, etc.). Accordingly, the anisotropicity of FRC in terms of cell colonization and cell spreading requires critical considerations, which in turn puts demands on the design of FRC appliances for living tissues.

The results of cell culture experiments indicate that FRCs could facilitate wound-healing process of medical devices (e.g., oral implant abutments), which are implanted in direct contact with connective tissues. However, the results obtained in static cell culture conditions cannot be directly extrapolated to clinical conditions.

6.6. Tissue culture (IV)

Soft tissue attachment is emerging as a provocative target for oral implant research (Myshin *et al.*, 2005; Rompen *et al.*, 2005; Cairo *et al.*, 2008; Grusovin *et al.*, 2008; Paldan *et al.*, 2008; Rossi *et al.*, 2008; van Brakel *et al.*, 2011). Inadequate gingival tissue attachment and support to the transmucosal components can worsen the treatment result and even lead to implant failure. One major challenge for peri-implant tissue integration is repeated abutment removals during the restorative phase of the treatment. Initial tissue attachment will be lost upon the first removal of the healing abutment. Replacements of healing abutments and placement of final restorations will consecutively introduce microbial challenge on tissue-implant interface. This has been reported to induce dimensional changes to soft tissue components and marginal bone level in experimental animals (Becker *et al.*, 2012). However, there is still a lack of clinical data about the influence of repeated removal of abutments on the final soft tissue attachment. To the best of knowledge, there is no published method that uses animal gingival explants for evaluating soft tissue/implant interface. Therefore, in study IV, we modified a rafted tissue culture method from a previously introduced skin attachment test model (Fukano *et al.*, 2006) utilizing full thickness porcine gingival explants to study soft tissue attachment on implant surface. Another aim of the study IV was to evaluate soft tissue attachment on unidirectional FRC in terms of gingival attachment and growth.

The pig has similarity to humans in size, organ development, physiology, and disease progression (Lunney, 2007). The porcine model has been acknowledged as the most comparable non-primate to the human with proper suitability for tissue engineering studies (Athanasiou *et al.*, 2009). In fact, porcine gingival tissue relates to that of human in terms of composition and structure more closely than any other animal (Collins *et al.*,

1981; Squier *et al.*, 1991; Wertz & Squier, 1991; de Vries *et al.*, 1991; Wong *et al.*, 2009). Since healthy human gingival tissue is not easily available, in study IV, we decided to use excised attached gingiva obtained from freshly slaughtered pigs to examine the soft tissue/implant interface.

Interestingly, the gingival epithelium did not show apical migration between the explant and implant surface. Instead, on day 10 and 14, the epithelium tended to migrate outward along the FRC surfaces forming a long epithelial lining. This agrees with an earlier study describing epithelial growth on citric acid treated root surface (Larjava *et al.*, 1988), which showed that epithelium tended to migrate outwards of bovine gingival explants in tissue culture conditions. This may be related with the surface properties of the used substrate. One explanation can also be that components of the tissue culture media are readily available on the substrate surface, which is not covered by tissue explant. This creates a nutritional advantage on the uncovered surface making it an easier path for epithelial migration. In our study, the upper parts of the experimental implants were not exposed to culture media at all. However, implant insertion through the gingival explant created a wound with immediate contact with the implant surface. Upon rupturing the gingival tissue, the upper part of the implant had been exposed to blood components creating an ideal surface treatment for epithelial migration. Better blood compatibility of the FRC substrates reported in study III might give one explanation for the pattern of epithelial migration that appeared to be more favorable for the FRC substrates. Thus, the findings of the study IV suggest that gingival tissue attachment and growth can also be dependent on the orientation of exposed E-glass fibers. However, further investigation is still needed. In study IV, implants were placed directly through the gingival explants that resemble flapless surgery conditions where implant diameter on the soft tissue level is larger than the original wound. In the situation, where the wound is not completely closed with the implant, a gap is left between the fresh wound and implant surface. This may allow epithelial migration along the implant surface also in the apical direction.

While transmucosal implants must eventually be examined in *in vivo* conditions, there are definite advantages for the use of tissue culture models for the initial characterization of soft tissue/biomaterials interfaces: (1) Animal tissue is easily available and such culture model can be conducted at a much lower cost, with less labor work, and in a more time-efficient manner when compared to animal models; (2) Tissue culture can be more informative and provide clinically relevant data when compared to conventional monolayer cell-culture system; (3) Study conditions are easy to control and observation of the delicate biological interactions that occur at the tissue/implant interface can be achieved. These processes are not disrupted by animal movement or efforts to mechanically displace the implant; (4) Implant orientation and positioning within the mucosa can be carefully organized; (5) The growth environment of the tissues can be adjusted by adding or removing substances to the culture media; and (6) Variables such as cellular immunity response associated with *in vivo* models are eliminated or reduced. However, with the lack of vascularization, no *in vitro* model can truly mimic

the biological process of the wound healing. The limitations inherent in the current *in vitro* model are: (1) Detachment of tissue from the animal deprives it from the blood flow and the exposure to the host's immune system; (2) Lack of precise knowledge of the general and oral health of the animal; (3) Probable problems related to the cross-species comparisons; and (4) Within prolonged time of tissue culture, mucosal deterioration initiates rendering this model only practical for a limited time frame.

The use of porcine gingival explants in tissue culturing can directly assist in improved understanding and, in turn, engineering of the soft tissue cuff around existing transmucosal implants. Further studies based on this model are necessary to quantitatively assess the soft tissue attachment and to analyze its ultrastructural and molecular features.

6.7. Future perspectives

FRC as an implant material possess many advantages in addition to its favorable mechanical properties such as compatibility with modern diagnostic methods (e.g., CT and MRI), CAD/CAM fabrication process, and has esthetic properties as it can be stained to resemble the color of natural dentin. FRC has a huge potential, especially in one-piece implant designs, since the material allows intraoral preparation without inducing a risk of overheating the underlying bone.

In this thesis, the biological response to BisGMA-TEGDMA based E-glass FRCs was explored under *in vitro* conditions. Thus, studies in real tissue environments under loaded conditions and comparison with other implant abutment materials are necessary to consider the *in vivo* behavior of FRCs before any definitive conclusions can be drawn.

7. CONCLUSIONS

Based on the studies included in this thesis, the following can be concluded:

1. The mechanical properties of unidirectional E-glass FRCs are highly dependent on the fiber volume fraction. However, when high fiber-density is used, the modulus of elasticity, toughness, and load bearing capacity properties of FRCs follow the law of ratio of quantity of fibers and volume of the polymer matrix more precisely than its mechanical strength property.

2. E-glass FRCs are moderately hydrophilic materials showing good wettability characteristics.

3. The presence of exposed E-glass fibers on the surface of FRCs enhances blood-clotting, fibroblast responses, and gingival tissue integration *in vitro*. Thus, FRCs could facilitate wound-healing processes around medical devices (e.g., oral implant abutments), which are implanted in direct contact with connective tissues.

4. The *in vitro* rafted tissue culture model, using porcine gingival explants, preserves gingival tissues' viability and offers a useful and inexpensive test-bed for studies of gingival attachment to different biomaterial surfaces.

5. The anisotropic nature of unidirectional FRC in terms of mechanical properties, surface wettability/energy, cellular responses, and gingival tissue attachment and growth represents important prerequisites that should be carefully considered when designing FRC devices for living tissues.

With special attention to technical design and surgical technique, BisGMA-TEGDMA based E-glass FRC can be considered as a non-metallic oral implant abutment alternative.

ACKNOWLEDGEMENTS

This thesis was carried out at the Department of Prosthetic Dentistry and Turku Clinical Biomaterials Center (TCBC), Institute of Dentistry, University of Turku during the years: 2009–2013.

First and foremost, I offer my sincerest gratitude to my supervisor, Professor Timo Närhi, whom has supported and encouraged me throughout my Ph.D. journey and allowed me to grow as a research scientist. Your advice on research as well as on my career has been invaluable. I simply could not wish for a better supervisor!

I was fortunate to have Professor Pekka Vallittu as my second supervisor. I have been privileged to benefit from his comprehensive expertise in the FRC world. I have constantly been inspired by your professional skills, enthusiasm, and humor.

I am grateful to Professor Ignace Naert (Catholic University of Leuven, Belgium) for accepting the invitation to be my dissertation opponent. In addition, I wish to express my gratitude to Professor Hannu Larjava (University of British Columbia, Canada) and Professor Pentti Tengvall (University of Gothenburg, Sweden) for acting as the official pre-examiners. Their insightful comments have been of great value in improving the academic value of the dissertation. I am deeply honored to have had such a group of esteemed and experienced scholars contributing to my doctoral dissertation.

I wish to thank the members of my Ph.D. steering committee, Professor Eija Könönen and Dr. Eva Söderling, for their helpful career advice and suggestions.

I am thankful to Professor John Jansen and Dr. Frank Walboomers for inviting me to the College of Dental Science at Radboud University Nijmegen Medical Center - Netherlands in the fall of 2010 and our fruitful collaboration there.

I want to give a very special acknowledgment to a person whom, in many ways, I have learnt much from. He has given me some good laughs! Who else could this be than Dr. Lippo Lassila, our lab manager and sauna master. Thanks for inviting me to “FUN-land” where dreams do come true…

A huge thanks to a very unique and dear person to me - Dr. Sufyan Garoushi whom has paved the way for me to come to Finland and helped me greatly in settling down in Turku at the very beginning of my journey. Thank you, now and always! In this regard, I am also indebted to Dr. Hussein Elmasmari (Ajman University of Science and Technology, UAE) for both introducing me to Dr. Sufyan and pointing me to Finland.

In science, you are never on your own! Therefore, I am grateful for the support of all co-authors whom have made contributions to my articles and their stimulating roles in addressing the issues concerning this thesis: Professor Stina Syrjänen; Dr. Lippo Lassila; Dr. Jaana Willberg; Dr. Jonathan Massera; Dr. Frank Walboomers; and Anni Kokkari. I

also highly appreciate all the scientific help and advise offered by Dr. Niko Moritz whom I still wish to have a joint publication. For their skilled technical assistance, I wish to extend a warm thanks to "Katja Sampalahti", Päivi Mäki, Mariia Valkama, and Marja Uola. I had a wonderful time teaching Prosthetic Dentistry to fourth-year dental students, thank you Dr. Marika Doepel for your support and trust in me. For this thesis, Dr. Robert M. Badeau is acknowledged for providing excellent linguistic editing. Dr. Mike Nelson is kindly thanked for advancing my English academic writing and presentation skills.

This dissertation would not have been possible without the financial support of the Finnish Doctoral Program in Oral Sciences (FINDOS). In this regard, I would like to thank Professor Stina Syrjänen (Program's Director) and Dr. Anna Haukioja (Program's Coordinator).

In my daily work, I have been blessed with a friendly and cheerful group of people, including: TCBC trio (Genevieve Alfont, Hanna Mark, and Minttu Vigren); the best ever officemates (Jasmina Bijelic and Dr. Onur Oral, love you both!); the department secretary Mrs. Tarja Peltoniemi (kiitos paljon for everything); Dr. Mervi Puska (thanks for all the nice chats); my best Finnish friend - Dr. Timothy Wilson; Yulia Kulkova (to be Dr. Yulia soon, good luck my dear!); the coolest Japanese on earth - Dr. Kohji Nagata; Dr. Masahiko Kobayashi (the gentleman); Dr. Ulvi Gursoy (I highly appreciate all your help and support); Aaro Turunen (thanks for sharing the wonderful conferences trips); Leila Perea Mosquera; Dr. Arzu Tezvergil-Mutluay; Dr. Jukka Matinlinna; Dr. Jenni Hjerppe; Dr. Riina Mattila; Dr. Anne Aulu; Dr. Sara Nganga; Roda Şeşeoğulları Dirihan; Dr. Timo Heikkinen; Dr. Tomohiro Kawaguchi; Dr. Jingwei He; Krista Vasankari; Ippei Hamanaka; and Misa Iwamoto.

My friends have been a source of positive energy throughout the process. It has been a pleasure and honor to share many of my most memorable moments with you. In particular, Wail Rehan (thanks for your endless support! I will never forget our Hungarian partnership…), Wameed Sulaiman (thanks for showing the real values of a real friend), Jongyun Moon (my real bro!), Dr. Alexander May and Dr. Sigrun Charlotte Denda (who make an energetically wonderful pair! Thanks for being awesome company during IADR congresses), and Hameed Bhai (thanks for the delicious catering service, Delhi Darbar Restaurant was great to me for the past four years). BEST FRIENDS are the siblings God did not give us…

Lastly, and most importantly, I would like to thank my family for all their love and encouragement. To my dear parents, who raised me with a love of science and supported me in all my pursuits (words cannot express my love!). To my elder brother, Dr. Taiseer and his dear family, my lovely and only sister Dr. Sama, and my little brother Awab, who will be a dentist in the near future and complete the family's dental crew! I also want to express my love and appreciation to my aunt (Khalee Raja'a) and her husband (Amo Hashim) for hosting me during my dental education years.

Turku 25.11.2010

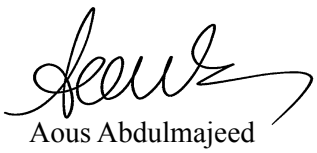

Aous Abdulmajeed

REFERENCES

Abrahamsson I, Berglundh T, Wennstrom J, Lindhe J. (1996) The peri–implant hard and soft tissues at different implant systems. A comparative study in the dog. Clin Oral Implants Res. 7:212–219.

Abrahamsson I, Berglundh T, Lindhe J. (1998) Soft tissue response to plaque formation at different implant systems. A comparative study in the dog. Clin Oral Implants Res. 9:73–79.

Abrahamsson I, Zitzmann NU, Berglundh T, Linder E, Wennerberg A, Lindhe J. (2002) The mucosal attachment to titanium implants with different surface characteristics: an experimental study in dogs. J Clin Periodontol. 29:448–455.

Agerbaek MR, Lang NP, Persson GR. (2006) Comparisons of bacterial patterns present at implant and tooth sites in subjects on supportive periodontal therapy. I. Impact of clinical variables, gender and smoking. Clin Oral Implants Res. 17:18–24.

Aitasalo KMJ, Piitulainen JM, Rekola J, Vallittu PK. (2013) Craniofacial bone reconstruction with bioactive fibre-reinforced composite implant. Accepted Article, doi: 10.1002/hed.23370.

Al–Ahmad A, Wiedmann–Al–Ahmad M, Faust J, Bächle M, Follo M, Wolkewitz M, Hannig C, Hellwig E, Carvalho C, Kohal R. (2010) Biofilm formation and composition on different implant materials in vivo. J Biomed Mater Res B Appl Biomater. 95:101–109.

Albrektsson T, Isidor F. (1994) Consensus report of session IV. In: Lang NP, Karring T, ed., Proceedings of the first European Workshop on Periodontology. London: Quintessence. 365–369.

Andersson B, Taylor A, Lang BR, Scheller H, Schärer P, Sorensen JA, Tarnow D. (2001) Alumina ceramic implant abutments used for single–tooth replacement: a prospective 1– to 3– year multicenter study. Int J Prosthodont. 14:432–438.

Andersson B, Glauser R, Maglione M, Taylor A. (2003) Ceramic implant abutments for shortspan FPDs: a prospective 5–year multicenter study. Int J Prosthodont. 16:640–646.

Andrade JD. (1973) Interfacial phenomena and biomaterials. Med Instrum. 7:110–120.

Antilla EJ, Krintila OH, Laurila TK, Lassila LV, Vallittu PK, Hernberg RGR. (2008) Evaluation of polymerization shrinkage and hygroscopic expansion of fiber–reinforced biocomposites using optical fiber Bragg grating sensors. Dent Mat. 14:1720–1727.

Antonucci JM, Stansbury JW. (1997) Molecular designed dental polymer. In: Arshady R, editor. Desk Reference of Functional Polymers: Synthesis and Application. American Chemical Society Publication. 719–738.

Anusavice KJ. (1996) Phillips' Science of Dental Materials, 10th ed., WB Saunders, Philadelphia. 25–31.

Anusavice KJ. (2003) Phillips' science of Dental Materials. 11th ed., Elsevier, St. Louis. 88–89.

Athanasiou KA, Almarzar A, Detamore M, Kalpakci K. (2009) Tissue engineering of temporomandibular joint cartilage. Morgan & Claypool Publishers.

Baier RE, Shafrin EG, Zisman WA. (1968) Adhesion: mechanisms that assist or impede it. Sci. 162:1360–1368.

Baier RE, Meyer AE, Natiella JR, Natiella RR, Carter JM. (1984) Surface properties determine bioadhesive outcomes: methods and results. J Biomed Mater Res. 18:327–355.

Ballo AM, Lassila LV, Vallittu PK, Närhi TO. (2007) Load bearing capacity of bone anchored fiber-reinforced composite device. J Mat Sci Mat Med. 18:2025–2031.

Ballo AM. Fiber–reinforced composite as oral implant material: Experimental studies of glass fiber and bioactive glass in vitro and in vivo [doctoral thesis]. Turku (Finland): University of Turku; 2008. Available at: http://www.doria.fi/handle/10024/39681

Ballo AM, Lassila LV, Närhi TO, Vallittu PK. (2008a) In vitro mechanical testing of glass fiber–reinforced composite as dental implants. J Contemp Dent Pract. 9:41–48.

Ballo AM, Kokkari AK, Meretoja VV, Lassila LV, Vallittu PK, Närhi TO. (2008b) Osteoblast proliferation and maturation on fiber–reinforced composite surface. J Mat Sci Mat Med. 19:3169–3177.

Ballo AM, Akca EA, Ozen T, Lassila LV, Vallittu PK, Närhi TO. (2009) Bone tissue responses to glass fiber–reinforced composite implants – a histomorphometric study. Clin Oral Implants Res. 20:608–615.

Becker K, Mihatovic I, Golubovic V, Schwarz F. (2012) Impact of abutment material and dis-/re-connection on soft and hard tissue changes at implants with platform-switching. J Clin Periodontol. 39:774–780.

Behr M, Rosentritt M, Lang R, Handel G. (2000) Flexural properties of fiber reinforced composite using a vacuum/pressure or a manual adaptation manufacturing process. J Dent. 28:509–514.

Berglundh T, Lindhe J, Ericsson I, Marinello CP, Liljenberg B, Thomsen P. (1991) The soft tissue barrier at implants and teeth. Clin Oral Implants Res. 2:81–90.

Berglundh T, Lindhe J, Jonsson K, Ericsson I. (1994) The topography of the vascular systems in the periodontal and peri–implant tissues in the dog. J Clin Periodontol. 21:189–193.

Berglundh T, Lindhe J. (1996) Dimension of the periimplant mucosa. Biological width revisited. J Clin Periodontol. 23:971–973.

Berglundh T, Abrahamsson I, Welander M, Lang NP, Lindhe J. (2007) Morphogenesis of the peri–implant mucosa: an experimental study in dogs. Clin Oral Implants Res. 18:1–8.

Berglundh T, Zitzmann NU, Donati M. (2011) Are peri-implantitis lesions different from periodontitis lesions? J Clin Periodontol. 38:188–202.

Black J, Hastings GW. (1998) Handbook of Biomaterials Properties, Chapman & Hall, London, UK.

Blue DS, Griggs JA, Woody RD, Miller RH. (2003) Effects of bur abrasive particle size and abutment composition on preparation of ceramic implant abutments. J Prosthet Dent. 90:247–254.

Bollen CM, Papaioanno W, Van Eldere J, Schepers E, Quirynen M, van Steenberghe D. (1996) The influence of abutment surface roughness on plaque accumulation and peri–implant mucositis. Clin Oral Implants Res. 7:201–211.

Bouillaguet S, Schutt A, Alander P, Schwaller P, Buerki G, Michler J, Cattani–Lorente M, Vallittu PK, Krejci I. (2006) Hydrothermal and mechanical stresses degrade fiber–matrix interfacial bond strength in dental fiber–reinforced composites. J Biomed Mater Res B Appl Biomater. 76:98–105.

Bowen RL. (1963) Properties of a silica–reinforced polymer for dental restoration. J Am Dent Assoc. 66:57–64.

Brunette DM. (2001) Principles of cell behavior on titanium surfaces and their application to implanted devices. In: Brunette DM, Tengvall P, Textor M, Thomsen P, editors. Titanium in medicine. Berlin and Heidelberg, Springer. 485–512.

Brunski JB. (1988) Biomechanics of oral implants: future research directions. J Dent Educ. 52:775–787.

Buser D, Weber HP, Donath K, Fiorellini JP, Paquette DW, Williams RC. (1992) Soft tissue reactions to non–submerged unloaded titanium implants in beagle dogs. J Periodontol. 63:225–235.

Busscher HJ. (1992) Wettability of surfaces in the oral cavity. In: Schrader ME, Loeb GI, editors, Modern Approaches to Wettability, New York, 249–261.

Busscher HJ, van Pelt AWJ, de Boer P, de Jong HP, Arends J. (1984) The effect of surface roughening of polymers on measured contact angles of liquids. Coll Surf. 9:319–331.

Bürgers R, Gerlach T, Hahnel S, Schwarz F, Handel G, Gosau M. (2010) In vivo and in vitro biofilm formation on two different titanium implant surfaces. Clin Oral Implants Res. 21:156–164.

Cairo F, Pagliaro U, Nieri M. (2008) Soft tissue management at implant sites. J Clin Periodontol. 35:163–167.

Cate T, Nanci A. (2008) Oral histology (7th edition ed.). St Louis, Missouri 63146: Elsevier Mosby.

Chavrier C, Couble ML, Magloire H, Grimaud JA. (1984) Connective tissue organization of healthy human gingiva. Ultrastructural localization of collagen types I-111-IV. J Periodont Res. 19:221–229.

Cheal EJ, Spector M, Hayes WC. (1992) Role of loads and prosthesis material properties on the mechanics of the proximal femur after total hip arthroplasty J Orthop Res. 10:405–422.

Chehroudi B, Gould TR, Brunette DM. (1988) Effects of a grooved epoxy substratum on epithelial cell behavior in vitro and in vivo. J Biomed Mater Res. 22:459–473.

Chong KH, Chai J. (2003) Strength and mode of failure of unidirectional and bidirectional glass fiber-

reinforced composite materials. Int J Prosthodont. 16:161–166.

Cochran DL, Hermann JS, Schenk RK, Higginbottom FL, Buser D. (1997) Biologic width around titanium implants. A histometric analysis of the implant gingival junction around unloaded and loaded nonsubmerged implants in the canine mandible. J Periodontol. 68:186–198.

Cochran DL. (1999) A comparison of endosseous dental implant surfaces. J Periodontol. 70:1523–1539.

Collins P, Laffoon J, Squier CA. (1981) Comparative study of porcine oral epithelium. J Dent Res. 60:543.

Combe EC, Owen BA, Hodges JS. (2004) A protocol for determining the surface free energy of dental materials. Dent Mat. 20:262–268.

Costanzo PM, Giese RF, van Oss CJ. (1990) Determination of the acid–base characteristics of clay mineral surfaces by contact angle measurements implications for the adsorption of organic solutes from aqueous media. J Adhes Sci Tech. 4:267–275.

Craig WH, Courtney TH. (1975) On the tension test as a means of characterizing fiber composite failure mode. J Mater Sci. 10:1119–1126.

Dahlén G, Charalampakis G, Abrahamsson I, Bengtsson L, Falsen E. (2012) Predominant bacterial species in subgingival plaque in dogs. J Periodontal Res. 47:354–364.

Dale BA. (2002). Periodontal epithelium: a newly recognized role in health and disease. Periodontol 2000. 30:70–78.

Darvell BW. (2006) Materials science for dentistry, 8th ed., Darvell BW, Pokfulam.

Davies JE. (1998) The importance and measurement of surface charge species in cell behavior at the biomaterial interface," In: Ratner, editor. Surface characterisation of biomaterials, Progress in Biomedical Engineering, Elsevier, Amsterdam. 219–230.

Davy KW, Kalachandra S, Pandain MS, Braden M. (1998) Relationship between composite matrix molecular structure and properties. Biomat. 19:2007–2014.

Degidi M, Artese L, Scarano A, Perrotti V, Gehrke P, Piattelli A. (2006) Inflammatory infiltrate, microvessel density, nitric oxide synthase expression, vascular endothelial growth factor expression, and proliferative activity in peri–implant soft tissues around titanium and zirconium oxide healing caps. J Periodontol. 77:73–80.

de Jong HP, van Pelt AWJ, Arends J. (1982) Contact angle measurements on human enamel. J Dent Res. 61:11–13.

de Vries ME, Bodde HE, Verhoef JC, Junginger HE. (1991) Developments in buccal drug delivery. Crit Rev Ther Drug Carrier Syst. 8:271–303.

do Nascimento C, Pita MS, Fernandes FHNC, Pedrazzi V, de Albuquerque Junior RF, Ribeiro RF. (2013) Bacterial adhesion on the titanium and zirconia abutment surfaces. Clin Oral Impl Res. 00:1–7.

Duarte PM, de Mendonça AC, Máximo MB, Santos VR, Bastos MF, Nociti Júnior FH. (2009) Differential cytokine expressions affect the severity of peri-implant disease. Clin Oral Implants Res. 20:514–520.

Duncan JP, Freilich MA, Latvis CJ. (2000) Fiber–reinforced composite framework for implant–supported overdentures. J Prosthet Dent. 84:200–204.

Dyer SR, Lassila LV, Jokinen M, Vallittu PK. (2004) Effect of fiber position and orientation on fracture load of fiber reinforced composite. Dent Mat. 20:947–955.

Egelberg J. (1966) The blood vessels of the dento–gingival junction. J Periodontal Res. 1:163–179.

Eggers G, Rieker M, Kress B, Fiebach J, Dickhaus H, Hassfeld S. (2005) Artefacts in magnetic resonance imaging caused by dental material. MAGMA. 18:103–111.

Ellingsen JE, Lyngstadaas SP. (2003) In: Bio–implant interface: improving biomaterials and tissue reactions. Boca Raton, FL, CRC Press.

Emecen-Huja P, Eubank TD, Shapiro V, Yildiz V, Tatakis DN, Leblebicioglu B. (2013) Peri-implant versus periodontal wound healing. J Clin Periodontol. 40:816–824.

Ericsson I, Berglundh T, Marinello C, Liljenberg B, Lindhe J. (1992) Long-standing plaque and gingivitis at implants and teeth in the dog. Clin Oral Implants Res. 3:99–103.

Eriksson C, Nygren H, Ohlson K. (2004) Implantation of hydrophilic and hydrophobic titanium discs in rat tibia: Cellular reactions on the surfaces during the first 3 weeks in bone. Biomat. 25:4759–4766.

Ferracane JL, Condon JR. (1990) Rate of elution of leachable components from composites. Dent Mater. 6:282–287.

Freilich MA, Goldberg AJ. (1997) The use of a pre–impregnated, fiber reinforced composite in the fabrication of a periodontal splint: a preliminary report. Pract Periodontics Aesthet Dent. 9:873–876.

Freilich MA, Karmaker AC, Burstone CJ, Goldberg AJ. (1998) Development and clinical applications of a light–polymerized fiber–reinforced composite. Prosthet Dent. 80:311–318.

Freudenthaler JW, Tischler GK, Burstone CJ. (2001) Bond strength of fiber–reinforced composite bars for orthodontic attachment. Am J Orthod Dentofacial Orthop. 120:648–653.

Fujiseki M, Matsuzaka K, Yoshinari M, Shimono M, Inoue T. (2003) An experimental study on the features of peri-implant epithelium: immunohistochemical and electron-microscopic observations. Bull Tokyo Dent Coll. 44:185–199.

Fukano Y, Knowles NG, Usui ML, Underwood RA, Hauch KD, Marshall AJ, Ratner BD, Giachelli C, Carter WG, Fleckman P, Olerud JE. (2006) Characterization of an in vitro model for evaluating the interface between skin and percutaneous biomaterials. Wound Repair Regen. 14:484–491.

Furtos G, Silaghi-Dumitrescu L, Moldovan M, Baldea B, Trusca R, Prejmerean C. (2012) Influence of filler/reinforcing agent and post-curing on the flexural properties of woven and unidirectional glass fiber-reinforced composites. J Mater Sci. 47:3305–3314.

Gargiulo AW, Wentz FM, Orban B. (1961a) Mitotic activity of human oral epithelium exposed to 30 per cent hydrogen peroxide. Oral Surg Oral Med Oral Pathol. 14:474–492.

Gargiulo AW, Wentz FM, Orban B. (1961b) Dimensions and relations of the dentogingival junction in humans. J Periodontol. 32:261–267.

Goldberg AJ, Burstone CJ. (1992) The use of continuous fiber reinforcement in dentistry. Dent Mater. 8:197–202.

Goodman SL, Lelah MD, Lambrecht LK, Cooper SL, Albrecht RM. (1984) In vitro vs. ex vivo platelet deposition on polymer surfaces. Scan Electron Microsc. 1:279–290.

Grossner–Schreiber B, Griepentrog M, Haustein I, Müller, WD, Lange K P, Briedigkeit H, Göbel UB. (2001) Plaque formation on surface modified dental implants. An in vitro study. Clin Oral Implants Res. 12:543–551.

Grusovin MG, Coulthard P, Worthington HV, Esposito M. (2008) Maintaining and recovering soft tissue health around dental implants: a Cochrane systematic review of randomised controlled clinical trials. Eur J Oral Implantol. 1:11–22.

Hallab N, Bundy K, O'Connor K, Clark R, Moses RL. (1995) Cell adhesion to biomaterials: correlations between surface charge, surface roughness, adsorbed protein, and cell morphology. J Long Term Eff Med Implants. 5:209–231.

Hallab N, Bundy K, O'Connor K, Moses RL, Jacobs JJ. (2001) Evaluation of metallic and polymeric biomaterial surface energy and surface roughness characteristics for directed cell adhesion. Tissue Eng. 7:55–71.

Hamdan M, Blanco L, Khraisat A, Tresguerres IF. (2006) Influence of titanium surface charge on fibroblast adhesion. Clin Implant Dent Relat Res. 8:32–38.

Hautamäki M. Repair of segmental bone defects with Fiber-reinforced composite: a study of material development and an animal model on rabbits [doctoral thesis]. Turku (Finland): University of Turku; 2012. Available at: http://www.doria.fi/handle/10024/86184

Heijnen HF, Schiel AE, Fijnheer R, Geuze HJ, Sixma JJ. (1999) Activated platelets release two types of membrane vesicles: microvesicles by surface shedding and exosomes derived from exocytosis of multivesicular bodies and alpha–granules. Blood. 94:3791–3799.

Heitz-Mayfield LJ, Lang NP. (2010) Comparative biology of chronic and aggressive periodontitis vs. peri-implantitis. Periodontol 2000. 53:167–181.

Henriksson K, Jemt T. (2003) Evaluation of custom–made procera ceramic abutments for single–implant tooth replacement: A prospective 1–year follow–up study. Int J Prosthodont. 16:626–630.

Hensten–Pettersen A. (1998) Skin and mucosa reactions associated with dental materials. Euro J Oral Sci. 106:707–712.

Herakovich C. (1998) Mechanics of fiber composites, 305. New York: Wiley. 322–359.

Hermann JS, Buser D, Schenk RK, Higginbottom FL, Cochran DL. (2000) Biologic width around

titanium implants. A physiologically formed and stable dimension over time. Clin Oral Implants Res. 11:1–11.

Hisbergues M, Vendeville S, Vendeville P. (2009) Zirconia: established facts and perspectives for a biomaterial in dental implantology. J Biomed Mater Res B Appl Biomater. 88:519–529.

Hormia M, Sahlberg C, Thesleff I, Airenne T. (1998) The epithelium-tooth interface--a basal lamina rich in laminin-5 and lacking other known laminin isoforms. J Dent Res. 77:1479–1485.

Huang N, Yang P, Leng YX, Chen JY, Sun H, Wang J, Wang GJ, Ding, PD, Xi TF, Leng Y. (2003) Hemocompatibility of titanium oxide films. Biomat. 24:2177–2187.

Hull D, Clyne TW. (1996) An Introduction to Composite Materials, 2nd ed., Cambridge University Press, Cambridge, UK.

Imai Y, Nose Y. (1972) A new method for evaluation of antithrombogenicity of materials. J Biomed Mat Res. 6:165–172.

Isaac DH. (1999) Engineering aspects of the structure and properties of polymer– fiber composites. In: Vallittu PK, editor. The First International Symposium on Fiber–Reinforced Plastics in Dentistry, 27–29 August 1998, Turku, Finland. University of Turku, Institute of Dentistry & Biomaterials Project.

Javed F, Al-Hezaimi K, Almas K, Romanos GE. (2011a) Is titanium sensitivity associated with allergic reactions in patients with dental implants? A systematic review. Clin Implant Dent Relat Res. 17:1–6.

Javed F, Al-Hezaimi K, Salameh Z, Almas K, Romanos GE. (2011b) Proinflammatory cytokines in the crevicular fluid of patients with peri-implantitis. Cytokine. 53:8–12.

Kamel EM, Burger C, Buck A, von Schulthess GK, Goerres GW. (2003) Impact of metallic dental implants on CT–based attenuation correction in a combined PET/CT scanner. Eur Radiol. 13:724–728.

Kasemo B. (1983) Biocompatibility of titanium implants: surface science aspects. J Prosth Dent. 49:832–837.

Kasemo B. (2002) Biological surface science. Surf Sci. 500:656–677.

Kennedy SB, Washburn NR, Simon CG Jr, Amis EJ. (2006) Combinatorial screen of the effect of surface energy on fibronectinmediated osteoblast adhesion, spreading and proliferation. Biomat. 27:3817–3824.

Kunzler TP, Drobek T, Schuler M, Spencer ND. (2007) Systematic study of osteoblast and fibroblast response to roughness by means of surfacemorphology gradients. Biomat. 28:2175–2182.

Lang NP, Berglundh T. (2011) Periimplant diseases: where are we now? Consensus of the Seventh European Workshop on Periodontology. J Clin Periodontol. 38:178–181.

Larjava H, Salonen J, Häkkinen L, Närhi T. (1988) Effect of citric acid treatment on the migration of epithelium on root surfaces in vitro. J Periodontol. 59:95–99.

Larjava H, Koivisto L, Häkkinen L, Heino J. (2011) Epithelial integrins with special reference to oral epithelia. J Dent Res. 90:1367–1376.

Larjava H. (2012) Oral Wound Healing: Cell Biology and Clinical Management, 1st ed., John Wiley & Sons, New York.

Lassila LV, Nohrstrom T, Vallittu PK. (2002) The influence of short–term water storage on the flexural properties of unidirectional glass fiber–reinforced composites. Biomat. 23:2221–2229.

Lassila LV, Tanner J, Le Bell AM, Narva K, Vallittu PK. (2004) Flexural properties of fiber reinforced root canal posts. Dent Mater. 20:29–36.

Lassila LV, Tezvergil A, Lahdenperä M, Alander P, Shinya A, Shinya A, Vallittu PK. (2005) Evaluation of some properties of two fiber-reinforced composite materials. Acta Odontol Scand. 63:196–204.

Le Bell A–M, Tanner J, Lassila LVJ, Kangasniemi I, Vallittu PK. (2004) Bonding of composite resin luting cement to fibre reinforced composite root canal post. J Adh Dent. 6:319–325.

Lekholm U, Grondahl K, Jemt T. (2002) Outcome of oral implant treatment in partially edentulous jaws followed 20 years in clinical function. Clin Implant Dent Relat Res. 8:178–186.

Lemons JE. (1998) Unanticipated outcomes: dental implants. Implant Dent. 7:351–353.

Lindhe J, Berglundh T, Ericsson I, Liljenberg B, Marinello C. (1992) Experimental breakdown of peri-implant and periodontal tissues. A study in the beagle dog. Clin Oral Implants Res. 3:9–16.

Linkevicius T, Apse P. (2008) Influence of abutment material on stability of peri–implant tissues: a systematic review. Int J Oral Maxillofac Implants. 23:449–456.

Listgarten MA, Lai CH. (1975) Ultrastructure of the intact interface between an endosseous epoxy resin dental implant and the host tissues. J Biol Buccale. 3:13–28.

Listgarten MA, Lang NP, Schroeder HE, Schroeder A. (1991) Periodontal tissues and their counterparts around endosseous implants. Clin Oral Implants Res. 2:1–19.

Loe H, Karring T. (1969) Mitotic activity and renewal time of the gingival epithelium of young and old rats. J Periodontal Res Suppl. 18–19.

Loza–Herrer MA, Rueggeberg FA. (1998) Time temperature profiles of post–cure composite oven. Gen Dent. 46:79–83.

Loza–Herrero MA, Rueggeberg FA, Caughman WF, Schuster GS, Lefebvre CA, Gardner FM. (1998) Effect of heating delay on conversion and strength of a post–cured resin composite. J Dent Res. 77:426–431.

Lum LB, Osier JF. (1992) Load transfer from endosteal implants to supporting bone: an analysis using statics Part two: Axial loading. J Oral Implantol. 18:349–353.

Lunney JK. (2007) Advances in swine biomedical model genomics. Int J Biol Sci. 3:179–184.

MacDougall M, Selden JK, Nydegger JR, Carnes DL. (1998) Immortalized mouse odontoblast cell line MO6–G3 application for in vitro biocompatibility testing. Am J Dent. 11:11–16.

Mallick PK. (1997) Fiber Reinforced Composites. Materials, Manufacturing and Design, Marcel Dekker Inc., New York, NY, USA.

Mallick PK. (2008) Fiber–reinforced composites: materials, manufacturing, and design, 3rd edn. CRC Press, Taylor & Francis Group, Boca Raton, FL.

Mannocci F, Sherriff M, Watson TF, Vallittu PK. (2005) Penetration of bonding resins into fibre–reinforced composite posts: a confocal microscopic study. Int Endod J. 38:46–51.

Matinlinna JP, Areva S, Lassila LVJ, Vallittu PK. (2004) Characterization of siloxane films on titanium substrate derived from three aminosilane. Surf Interface Anal. 36:1314–1322.

Mattila R. Non–resorbable glass fiber–reinforced composite with porous surface as bone substitute material: Experimental studies in vitro and in vivo focused on bone-implant interface [doctoral thesis]. Turku (Finland): University of Turku; 2009. Available at: http://www.doria.fi/handle/10024/47317

Mekayarajjananonth T, Winkler S. (1999) Contact angle measurement on dental implant biomaterials. J Oral Implantol. 25:230–236.

Meretoja VV, Rossi S, Peltola T, Pelliniemi LJ, Närhi TO. (2010) Adhesion and proliferation of human fibroblasts on sol-gel coated titania. J Biomed Mater Res A. 95:269–275.

Miettinen VM, Vallittu PK. (1997) Water sorption and solubility of glass fiber–reinforced denture polymethyl methacrylate resin. J Prosthet Dent. 77:531–534.

Mombelli A, Lang NP. (1998) The diagnosis and treatment of peri-implantitis. Periodontol 2000. 17:63–76.

Moon IS, Berglundh T, Abrahamsson I, Linder E, Lindhe J. (1999) The barrier between the keratinized mucosa and the dental implant. An experimental study in the dog. J Clin Periodontol. 26:658–663.

Mullarky RH. (1985) Aramid fiber reinforcement of acrylic appliances. J Clin Orthod. 19:655–658.

Myshin HL, Wiens JP. (2005) Factors affecting soft tissue around dental implants: a review of the literature. J Prosthet Dent. 94:440–444.

Narva KK, Vallittu PK, Helenius H, Yli–Urpo A. (2001) Clinical survey of acrylic resin removable denture repairs with glass–fiber reinforcement. Int J Prosthodont. 14:219–224.

Nevins M, Kim DM, Jun SH, Guze K, Schupbach P, Nevins ML. (2010) Histologic evidence of a connective tissue attachment to laser microgrooved abutments: A canine study. Int J Periodontics Restorative Dent. 30:245–255.

Nevins M, Camelo M, Nevins ML, Schupbach P, Kim DM. (2012) Connective tissue attachment to laser-micro grooved abutments: A human histologic case report. Int J Periodontics Restorative Dent. 32:385–392.

Norström A, Watson H, Engström B, Rosenholm J. (2001) Treatment of E–glass fibres with acid, base and silanes. Colloids Surf A. 194:143–157.

Nowzari H, Botero JE, DeGiacomo M, Villacres MC, Rich SK. (2008) Microbiology and cytokine levels around healthy dental implants and teeth. Clin Implant Dent Relat Res. 10:166–173.

Nowzari H, Phamduong S, Botero JE, Villacres MC, Rich SK. (2012) The profile of inflammatory cytokines in gingival crevicular fluid around healthy osseointegrated implants. Clin Implant Dent Relat Res. 14:546–552.

Owens DK, Wendt RC. (1969) Estimation of the surface free energy of polymers. J Appl Poly Sci. 13:1741–1747.

Page RC, Offenbacher S, Schroeder HE, Seymour GJ, Kornman KS. (1997) Advances in the pathogenesis of periodontitis: summary of developments, clinical implications and future directions. Periodontol 2000. 14:216–248.

Paldan H, Areva S, Tirri T, Peltola T, Lindholm TC, Lassila L, Pelliniemi LJ, Happonen RP, Närhi TO. (2008) Soft tissue attachment on sol-gel-treated titanium implants in vivo. J Mater Sci Mater Med. 19:1283–1290.

Paquette DW, Brodala N, Williams RC. (2006) Risk factors for dental implant failure. Dent Clin North Am. 50:361.

Park JY, Davies JE. (2000) Red blood cell and platelet interactions with titanium implant surfaces. Clin Oral Implants Res. 11:530–539.

Park JY, Gemmell CH, Davies JE. (2001) Platelet interactions with titanium: modulation of platelet activity by surface topography. Biomat. 22:2671–2682.

Prestipino V, Ingber A. (1993a) Esthetic high-strength implant abutments. Part I. J Esthet Dent. 5:29–36.

Prestipino V, Ingber A. (1993b) Esthetic high-strength implant abutments. Part II. J Esthet Dent. 5:63–68.

Ponsonnet L, Comte V, Othmane A, Lagneau C, Charbonnier M, Lissac M, Jaffrezic N. (2002) Effect of surface topography and chemistry on adhesion, orientation and growth of fibroblasts on nickel–titanium substrates. Mater Sci Eng C. 21:157–165.

Ponsonnet L, Reybier K, Jaffezic N, Comte V, Lagneau C, Lissac M. (2003) Relationship between surface properties (roughness, wettability) of titanium and titanium alloys and cell behavior. Mater Sci Eng C. 23:551–560.

Pöllänen MT, Salonen JI, Uitto VJ. (2003) Structure and function of the tooth-epithelial interface in health and disease. Periodontol. 31:12–31.

Quirynen M, Van der Mei HC, Bollen CM, Van den Bossche LH, Doornbusch GI, van Steenberghe D, Busscher HJ. (1994) The influence of surface–free energy on supra and subgingival plaque microbiology. An in vivo study on implants. J Periodontol 65:162–167.

Quirynen M, De Soete M, van Steenberghe D. (2002) Infectious risks for oral implants: a review of the literature. Clin Oral Implant Res. 13:1–19.

Ramakrishna S, Mayer J, Wintermantel E, Leong KW. (2001) Biomedical applications of polymer-composite materials: A review. Compos Sci Technol. 61:1189–1224.

Rame E, Garoff S. (1996) Microscopic and macroscopic dynamic interface shapes and the interpretation of dynamic contact angles. J Col and Interface Sci. 177:234–244.

Rangert B, Krogh PH, Langer B, Van Roekel N. (1995) Bending overload and implant fracture. Int J Oralmaxillofac Implants. 10: 326–334.

Reed BB, Choi K, Dickens SH, Stansbury JW. (1997) Effect of resin composition of kinetics of dimethacrylate photopolymerization. Poly Preprints. 38:108–109.

Richter EJ. (1998) In vivo horizontal bending moments on implants. Int J Oral Maxillofac Implants. 13:232–244.

Rompen E, Domken O, Degidi M, Farias Pontes AE, Piattelli A. (2006) The effect of material characteristics, of surface topography and of implant components and connections on soft tissue integration: a literature review. Clin Oral Implants Res. 17:55–67.

Rossi S, Tirri T, Paldan H, Tulamo R-M, Kuntsi-Vaattovaara H, Närhi T. (2008) Peri-implant tissue response to TiO_2 modified implants. Clin Oral Implants Res. 19:348–355.

Ruyter IE, Ekstrand K, Bjork N. (1986) Developement of carbon/graphite fiber reinforced poly (methyl methacrylate) suitable for implant-fixed dental bridges. Dent Mater. 2:6–9.

Scacchi M. (2000) The development of the ITI dental implant system. Part 1: A review of the literature. Clin Oral Implants Res. 11:8–21.

Scarano A, Piattelli M, Caputi S, Favero GA, Piattelli A. (2004) Bacterial adhesion on commercially

pure titanium and zirconium oxide discs: an in vivo human study. J Periodontol. 75:292–296.

Schakenraad JM, Busscher HJ, Wildevuur CR, Arends J. (1986) The influence of substratum free energy on growth and spreading of human fibroblasts in the presence and absence of serum proteins. J Biomed Mat Res. 20:773–784.

Schakenraad JM, Busscher HJ, Wildevuur CHRH, Arends J. (1988) Thermodynamic aspects of cell spreading on solid substrata. Cell Biophy. 13:75–91.

Schierano G, Ramieri G, Cortese M, Aimetti M, Preti G. (2002) Organization of the connective tissue barrier around long–term loaded implant abutments in man. Clin Oral Implants Res. 13:460–464.

Schiott CR, Loe H. (1970) The origin and variation in number of leukocytes in the human saliva. J Periodontal Res. 5:36–41.

Schou S, Holmstrup P, Reibel J, Juhl M, Hjørting-Hansen E, Kornman KS. (1993) Ligature-induced marginal inflammation around osseointegrated implants and ankylosed teeth: stereologic and histologic observations in cynomolgus monkeys (Macaca fascicularis). J Periodontol. 64:529–537.

Schroeder HE. (1973) Transmigration and infiltration of leukocytes in human junctional epithelium gingival tissue. Helv Odontol Acta. 17:6–18.

Schroeder HE, Listgarten MA. (1997) The gingival tissues: the architecture of periodontal protection. Periodontol 2000. 13:91–120.

Schwarz F, Ferrari D, Herten M, Mihatovic I, Wieland M, Sager M, Becker J. (2007) Effects of surface hydrophilicity and microtopography on early stages of soft and hard tissue integration at non-submerged titanium implants: an immunohistochemical study in dogs. J Periodontol. 78:2171–2184.

Scott HG. (1975) Phase relationships in zirconia–yttria system. J Mater Sci. 10:1527–1535

Schupbach P, Glauser R. (2007) The defense architecture of the human periimplant mucosa: a histological study. J Prosthet Dent. 97:15–25.

Sharma CP. (1984) LTI carbons: bloodcompatibility. J Col and Interface Sci. 97:585–586.

Siar CH, Toh CG, Romanos G, Swaminathan D, Ong AH, Yaacob H, Nentwig GH. (2003) Peri–implant soft tissue integration of immediately loaded implants in the posterior macaque mandible: a histomorphometric study. J Periodontol. 74:571–578.

Sicilia A, Cuesta S, Coma G, Arregui I, Guisasola C, Ruiz E, Maestro A. (2008) Titanium allergy in dental implant patients: a clinical study on 1500 consecutive patients. Clin Oral Implants Res. 19:823–835.

Siddiqi A, Payne AG, De Silva RK, Duncan WJ. (2011) Titanium allergy: could it affect dental implant integration? Clin Oral Implants Res. 7:673–680.

Smith DC. (1961) The acrylic denture: mechanical evaluation of midline fracture. Br Dent J. 110:257–267.

Squier CA, Cox P, Wertz PW. (1991) Lipid content and water permeability of skin and oral mucosa. J Invest Dermatol. 96:123–126.

Stern IB. (1981) Current concepts of the dentogingival junction: the epithelial and connective tissue attachments to the tooth. J Periodontol. 52:465–476.

Teughels W, Van Assche N, Sliepen I, Quirynen M. (2006) Effect of material characteristics and/or surface topography on biofilm development. Clin Oral Implants Res. 17:68–81.

Tezvergil A, Lassila LV, Vallittu PK. (2003) The effect of fiber orientation on the thermal expansion coefficient of fiber reinforced composites. Dent Mat. 19:471–477.

Travan A, Donati I, Marsich E, Bellomo F, Achanta S, Toppazzini M, Semeraro S, Scarpa, T, Spreafico V, Paoletti S. (2010) Surface modification and polysaccharide deposition on BisGMA/TEGDMA thermoset. Biomacromol. 11:583–592.

Tuusa SM, Peltola MJ, Tirri T, Lassila LV, Vallittu PK. (2007) Frontal bone defect repair with experimental glass–fiber–reinforced composite with bioactive glass granule coating. J Biomed Mater Res B Appl Biomater. 82:149–155.

Tuusa SM, Peltola MJ, Tirri T, Puska MA, Röyttä M, Aho H, Sandholm J., Lassila LV, Vallittu PK. (2008) Reconstruction of critical size calvarial bone defects in rabbits with glass–fiber–reinforced composite with bioactive glass granule coating. J Biomed Mater Res B Appl Biomater. 84:510–519.

Vallittu PK. (1994) Acrylic resin-fiber composite-Part II: The effect of polymerization shrinkage of polymethyl methacrylate applied to fiber roving on transverse strength. J Prosthet Dent. 71:613–617.

Vallittu PK. (1995a) The effect of void space and polymerization time on transverse strength of acrylic–glass fiber composite. J Oral Rehabil. 22:257–261.

Vallittu PK. (1995b) Impregnation of glass fibers with polymethylmethacrylate using a powder–coating method. Appl Composite Mater. 2:51–58.

Vallittu PK. (1997a) Glass fiber reinforcement in repaired acrylic resin removable dentures: preliminary results of a clinical study. Quintessence Int. 28:39–44.

Vallittu PK. (1998a) Some aspects of the tensile strength of unidirectional glass fiber–polymethyl–methacrylate composite used in dentures. J Oral Rehabil. 25:100–105.

Vallittu PK. (1998b) The effect of glass fiber reinforcement on the fracture resistance of a provisional fixed partial denture. J Prosthet Dent. 79:125–130.

Vallittu PK. (1999a) Flexural properties of acrylic polymers reinforced with unidirectional and woven glass fibers. J Prosthet Dent. 81:18–26.

Vallittu PK. (1999b) Prosthodontic treatment with a glass fiber–reinforced resin–bonded fixed partial denture: a clinical report. Prosthet Dent. 82:132–135.

Vallittu PK. (2009) Interpenetrating polymer networks (IPNs) in dental polymers and composites. J Adhes Sci and Technol. 23:961–972.

Vallittu PK, Narva K. (1997) Impact strength of a modified continuous glass fiber–poly (methyl methacrylate). Int J Prosthodont. 10:142–148.

van Brakel R, Cune MS, van Winkelhoff AJ, de Putter C, Verhoeven, JW, van der Reijden W. (2011) Early bacterial colonization and soft tissue health around zirconia and titanium abutments: An in vivo study in man. Clin Oral Implants Res. 22:571–577.

van Brakel R, Meijer GJ, Verhoeven JW, Jansen J, de Putter C, Cune MS. (2012) Soft tissue response to zirconia and titanium implant abutments: an in vivo within-subject comparison. J Clin Periodontol. 39:995–1001.

Van Oss CJ, Chaudhury MK, Good RC. (1998) Interfacial Lifshitz–van der Waals and polar interactions in macroscopic systems. Chem Rev. 88:927–941.

Vigolo P, Givani A, Majzoub Z, Cordioli G. (2006) A 4–year prospective study to assess peri–implant hard and soft tissues adjacent to titanium versus gold–alloy abutments in cemented single implant crowns. J Prosthodont. 15:250–256.

Väkiparta M, Puska M, Vallittu PK. (2006) Residual monomers and degree of conversion of partially bioresorbable fiber-reinforced composite. Acta Biomater. 2:29-37.

Wennerberg A. On surface roughness and implant incorporation [doctoral thesis]. Gothenburg (Sweden): University of Gothenburg; 1996.

Wennerberg A, Albrektsson T, Andersson B, Krol JJ. (1995) A histomorphometric and removal torque study of screwshaped titanium implants with three different surface topographies. Clin Oral Implants Res. 6:24–30.

Wertz PW, Squier CA. (1991) Cellular and molecular basis of barrier function in oral epithelium. Crit Rev Ther Drug Carrier Syst. 8:237–269.

Winkler S, Ortman HR, Ryczek MT. (1975) Improving the retention of complete dentures. J Prosth Dent. 34:11–15.

Wirth C, Comte V, Lagneau C, Exbrayat P, Lissac M, Jaffrezic-Renault N, Ponsonnet L. (2005) Nitinol surface roughness modulates in vitro cell response: a comparison between fibroblasts and osteoblasts. Mater Sci Eng C. 25:51–60.

Wolff D, Schach C, Kraus T, Ding P, Pritsch M, Mente J, Joerss D, Staehle HJ. (2010) Fiber–reinforced composite fixed dental prostheses: a retrospective clinical examination. J Adhes Dent. 13:187–194.

Wong JW, Gallant-Behm C, Wiebe C, Mak K, Hart DA, Larjava H, Häkkinen L. (2009) Wound healing in oral mucosa results in reduced scar formation as compared with skin: evidence from the red Duroc pig model and humans. Wound Repair Regen. 17:717–729.

Yanagisawa I, Sakuma H, Shimura M, Wakamatsu Y, Yanagisawa S, Sairenji E. (1989) Effects of "wettability" of biomaterials on culture cells. J Oral Implantol. 15:168–177.

Yazdanie N, Mahood M. (1985) Carbon fiber acrylic resin composite: an investigation of transverse strength. J Prosthet Dent. 54:543–547.

Zhao DS, Moritz N, Laurila P, Mattila R, Lassila LV, Strandberg N, Mäntylä T, Vallittu PK, Aro HT. (2009) Development of a multicomponent fiber–reinforced composite implant for load–sharing conditions. Med Eng Phys. 31:461–469.

Zitzmann NU, Berglundh T, Ericsson I, Lindhe J. (2004) Spontaneous progression of experimentally induced periimplantitis. J Clin Periodontol. 31:845–849.

Zitzmann NU, Berglundh T. (2008) Definition and prevalence of peri–implant diseases. J Clin Periodontol. 35:286–291.